The Role of Non-Neuronal Acetylcholine Production in Immune Cells

by

Maryse Lachapelle

A thesis submitted in partial fulfillment of the requirements for the degree of Master of Science (MSc) in Chemical Sciences

The Faculty of Graduate Studies
Laurentian University
Sudbury, Ontario, Canada

THESIS DEFENCE COMMITTEE/COMITÉ DE SOUTENANCE DE THÈSE
Laurentian Université/Université Laurentienne
Office of Graduate Studies/Bureau des études supérieures

Title of Thesis
Titre de la thèse: The Role of Non-Neuronal Acetylcholine Production in Immune Cells

Name of Candidate
Nom du candidat: Lachapelle, Maryse

Degree
Diplôme: Master of Science

Department/Program
Département/Programme: Chemical Sciences

Date of Defence
Date de la soutenance: October 01, 2021

APPROVED/APPROUVÉ

Thesis Examiners/Examinateurs de thèse:

Dr. Alain Simard
(Supervisor/Directeur(trice) de thèse)

Dr. Aseem Kimar
(Committee member/Membre du comité)

Dr. TC Tai
(Committee member/Membre du comité)

Dr. Philippe-Pierre Robichaud
(External Examiner/Examinateur externe)

Approved for the Office of Graduate Studies
Approuvé pour le Bureau des études supérieures
Tammy Eger, PhD
Vice-President Research (Office of Graduate Studies)
Vice-rectrice à la recherche (Bureau des études supérieures)
Laurentian University / Université Laurentienne

ACCESSIBILITY CLAUSE AND PERMISSION TO USE

Abstract

The cholinergic system deals with the production, function, transport, and degradation of acetylcholine (ACh), a molecule commonly known as a neurotransmitter. This system has been shown to regulate inflammation via its resolution. Although increasing evidence suggests the importance of ACh in immune regulation, its role within specific immune cells remains inconclusive. Assessing the presence of cholinergic markers in immune cells in conjunction with their pharmacological inhibition will thus help to clarify the functional roles of the cholinergic system in the immune response. The aim of this study was to evaluate the role of non-neuronal ACh production in immune regulation. Expression studies using qPCR, western blots, mass spectrometry, and immunocytochemistry revealed the presence of ACh and choline acetyltransferase in immune tissues and within immune cells of such tissues. In addition, the effect of cholinergic inhibitors on immune function was examined on M1/M2 murine bone marrow derived macrophages (BMDMs) by examining their cytokine profile. Overall, inhibiting the synthesis of ACh seemed to significantly cause cell death in M1 BMDMs and non-significantly cause cell death in M2 BMDMs; yet other treatment conditions did not seem to cause cell death. However, due to pharmacological and statistical limitations, cytokine secretion profiles were generally inconclusive. These data further shed light on the role cholinergic system within immune cells, but further research would be necessary to validate these findings.

Key Words

Cholinergic system, immune cells, acetylcholine, choline acetyltransferase, bone marrow derived macrophages, inflammation

Abbreviations

ACh – Acetylcholine

AChE – Acetylcholinesterase

AD- Alzheimer's disease

APC – Antigen presenting cells

BCA- Bicinchoninic acid assay

BChE – Butyrylcholinesterase

BM – Bone marrow

BMDM- Bone Marrow Derived Macrophages

CAP- Cholinergic Anti-inflammatory Pathway

CBA- Cytometric Bead Array

ChAT – Choline acetyltransferase

ChT – Choline transporter

CNS – Central nervous system

CTL2- Choline Transporter Like Protein 2

DC – Dendritic cell

DICE- Database of Immune Cell Expression

DNA – Deoxyribonucleic acid

EAE – Experimental Autoimmune Encephalomyelitis

FBS – Fetal bovine serum

IL – Interleukin

LDH- Lactate Dehydrogenase

mAChR – Muscarinic acetylcholine receptor

MHC – Major histocompatibility complex

MNC – Mononuclear cells

MSCs- Mesenchymal Stem Cells

mRNA - Messenger ribonucleic acid

MRM- Multiple Reaction Monitoring

MS – Mass Spectrometry

nAChR – Nicotinic acetylcholine receptor

no-RT – no-Reverse Transcription

NTC – No template control

OCTN1- Organic Cation Novel Type 1

PBMC – Peripheral blood mononuclear cell

PBS – Phosphate buffered saline

PCR – Polymerase chain reaction

PMA- Positive Allosteric Modulator

PVDF – Polyvinylidene fluoride or polyvinylidene difluoride

qPCR – Quantitative polymerase chain reaction

RBC – Red blood cell

RIPA – Radioimmunoprecipitation assay

RNA – Ribonucleic acid

RPMI – Roswell Park Memorial Institute Medium

RT – Reverse transcription

SEM- Standard Error's Mean

SDS-PAGE – Sodium dodecyl sulfate polyacrylamide gel electrophoresis

siRNA – Small interfering ribonucleic acid

TBE – Tris/Borate/ Ethylenediaminetetraacetic acid

Tbp – Tata Binding Protein

TBS – Tris buffered saline

TBST – Tris buffered saline with tween

TNF – Tumor Necrosis Factor

VAChT- Vesicular acetylcholine transporter

VNS – Vagus nerve stimulation

WT – Wild type

Acknowledgements

First, I would like to acknowledge the help and guidance of my supervisor, Dr. Alain Simard. Dr. Simard has always been there to lend a helping hand with my project and is a source of much encouragement. He was always there to give me feedback when I needed it, and from that, I have learned so much. He also always supported and helped me when I applied for bursaries and encouraged me to go to conferences. Dr. Simard trained me in many of the techniques, such as animal work, bone marrow extraction, reverse transcription, qPCR, and western blotting. He also taught me how to properly work in a bio safety cabinet and how to analyze my qPCR results. Overall, I am very grateful to have been under the guidance of such a great supervisor.

To this end, I would like to thank my committee members Dr. Aseem Kumar and Dr. T.C. Tai for their support, their time, as well as their help. They have been important to ensure proper progress throughout my MSc, to review my MSc thesis, and to provide valuable feedback.

I would also like to thank Dr. Natalie Lefort for helping me with western blots and equipment use at the Northern Ontario School of Medicine. I would like to thank Maxime Lefebvre for training me in BCA assays. Furthermore, I would like to thank my former lab partner, Eduardo Soto Espinosa and our former laboratory assistant, Dr. Ramya Narendrula, for their help in some of the earlier experiments in my master's. Danika Roy, a fellow MSc student in my lab has been incredibly helpful with her insight and support on tissue culturing, PCRs, and cytokine studies. Additionally, I would like to thank the licensed

phlebotomists, Sara Walsh and Natalie Desanti, in conjunction with the participants who volunteered for this study.

I would like to thank Heather Dufour for establishing my mass spectrometry experiments and running my mass spectrometry samples. She has been very helpful and integral to gathering all the mass spectrometry data herein.

In conducting the semi-quantitative analysis of immunocytochemistry slides on the Cytation 5, the help and support from Dr. Reema Vazirani and Jeremy Gagne from BioTek was instrumental in generating a non-biased protocol.

In addition, I would like to thank Nicole Paquette and Chris Blomme for taking care of our mice at the animal facility as well as for their support with the animal work.

Finally, I would like to thank Dr. T.C. Tai's lab for lending us some of their reagents and equipment needed to complete this study. In addition, I want to thank the Natural Sciences and Engineering Research Council of Canada (NSERC) for funding my research and awarding me with a scholarship for the second year of my MSc.

Principally, it was great working in Dr. Alain Simard's lab, I could not have asked for a better environment to work in. Working in this lab had a meaningful impact on my life as I believe the lessons I have learned throughout my MSc made me a more resilient, critical thinking, and resourceful person. Hence, I am grateful that I did research in Dr. Simard's lab.

Table of Contents

List of Figures

List of Tables

Introduction

1.0 A Brief Background on the Cholinergic System, the Immune System, and Autoimmune Diseases

The cholinergic system deals with the production, function, and degradation of acetylcholine (ACh). This system is traditionally known to play a role in the autonomic nervous system. More specifically, the cholinergic system is mostly parasympathetic. It is known to play a role in memory, digestion, breathing, control of the heartbeat, blood pressure, movement, and several other functions.[1]

In terms of evolution, ACh as well as ACh synthesizing activity has been found in evolutionary primitive life and in complex multicellular organisms.[2] With that being said, the presence of these cholinergic components in these simple, primitive life forms suggests that the cholinergic system plays an essential role in organisms, with or without a nervous system. Furthermore, the presence of non-neuronal ACh in mammalians suggests the expression of this molecule as a local mediator as well as a neurotransmitter since the beginning of life.[2]

Through time, it is becoming increasingly clear that the immune system and the cholinergic system work together. In fact, the nervous system and the immune system constantly communicate with each other by utilizing neurotransmitters like ACh.[3] In addition, the parasympathetic and the sympathetic nervous systems act directly by innervating lymphoid organs; thus, the nervous system has implications in immune functions.[3]

The immune system is composed mainly of the cells and molecules that mediate immunity. The collective and coordinated response towards antigens is called an immune response. In a healthy host, the immune system usually acts against infectious foreign substances; however, it can also have a response towards non-infectious foreign substances.

Moreover, the immune response can be classified into two types: proinflammatory and anti-inflammatory.[4] These responses are mediated by a certain group of cytokines which are endogenous chemical substances that control immune responses in the host. [4] Some cytokines are proinflammatory while others are anti-inflammatory. [4] Those who are proinflammatory are important to fight against exogenous antigens and they can cause harm against healthy cells, especially when they are not properly regulated. In contrast, anti-inflammatory cytokines are important for resolving inflammation. [4] This regulatory role of anti-inflammatory cytokines is important to prevent inflammation from causing harm to healthy cells and tissues.[4] In fact, ACh has been shown to have an anti-inflammatory effect.[5–10] Therefore, the cholinergic system seems to play a role in immune regulation.

When an individual has an immune system that is not properly regulated, they might have an autoimmune disease and/or an inflammatory disease. An inflammatory disease is when inflammation is not properly resolved by the anti-inflammatory immune response. In turn, this dysregulation causes an exaggerated proinflammatory immune response which damages healthy cells and tissues. Autoimmune diseases may also be defined as inflammatory diseases however not all inflammatory diseases are autoimmune.

Autoimmune diseases are the result of an immune system that mistakenly reacts to self-antigens instead of only reacting to foreign antigens.[11] Autoimmune diseases are said to

be caused by the inability of the immune system to distinguish between these two types of antigens. [11] As a result of the defense of the immune system against self-molecules, there are damaging consequences that vary depending on the type of autoimmune disease.[11] In addition, autoimmune diseases generally result in tissue damage due to a surplus in inflammation that is not completely resolved by the anti-inflammatory immune response. For instance, in multiple sclerosis, the myelinated axons of the central nervous system (CNS) are targeted.[12] The dysregulated inflammation and demyelination in patients with multiple sclerosis thus leads to debilitating symptoms.

Often, the treatments of inflammatory diseases are anti-inflammatory drugs to suppress the deleterious effects of the dysregulated immune response. As previously mentioned, the cholinergic system and the immune system have been shown to work together and ACh has been shown to have an anti-inflammatory effect. Therefore, the cholinergic system's ability to resolve inflammation by stimulating an anti-inflammatory immune response makes it an interesting target for treating autoimmune diseases.

Further studies on the interplay between ACh production and immune regulation is thus necessary to find better targets for drugs against autoimmune diseases. Hence, studying this important relationship will be the focus of this thesis. The following sections of this introduction will provide a more in-depth background on many topics briefly covered in this section.

1.1 Markers and Receptors of The Neuronal Cholinergic System

The functioning of the cholinergic system depends on several proteins that work together to perform a particular function. Herein, these cholinergic proteins will be referred to as *cholinergic markers*. The well-known neuronal markers of the cholinergic systems that will be observed in this study are choline acetyltransferase (ChAT), acetylcholinesterase (AChE), vesicular acetylcholine transporter (VAChT), choline transporter (ChT) and butyrylcholinesterase (BChE). ChAT is an enzyme that synthesizes ACh from choline (Ch) and acetylcoenzyme A. BChE as well as AChE degrade ACh into Ch and acetate. VAChT is responsible for ACh transport by synaptic vesicles to allow for exocytosis of ACh.[13] Moreover, ChT maintains ACh synthesis by transporting the surrounding Ch molecules resulting from ACh degradation back into the neuron.[14] Altogether, these proteins are responsible for the complete life cycle of ACh, from its production and function to degradation.

In the neuromuscular junction, the newly synthesized ACh from ChAT in the corpuscula nerve endings is transported to the synaptic vesicles, where they are released during synapsis (Figure 1).[4–7] In the synapse, the ACh attaches itself to the postsynaptic receptors, namely ACh receptors (AChRs) (Figure 1).[4–7] To cease the stimulation of the postsynaptic neurons, ACh is recaptured by transporter proteins or it is degraded by AChE to Ch and acetate (Figure 1).[4–7] Similar mechanisms are used for the function of ACh in the rest of the nervous system.[4–7]

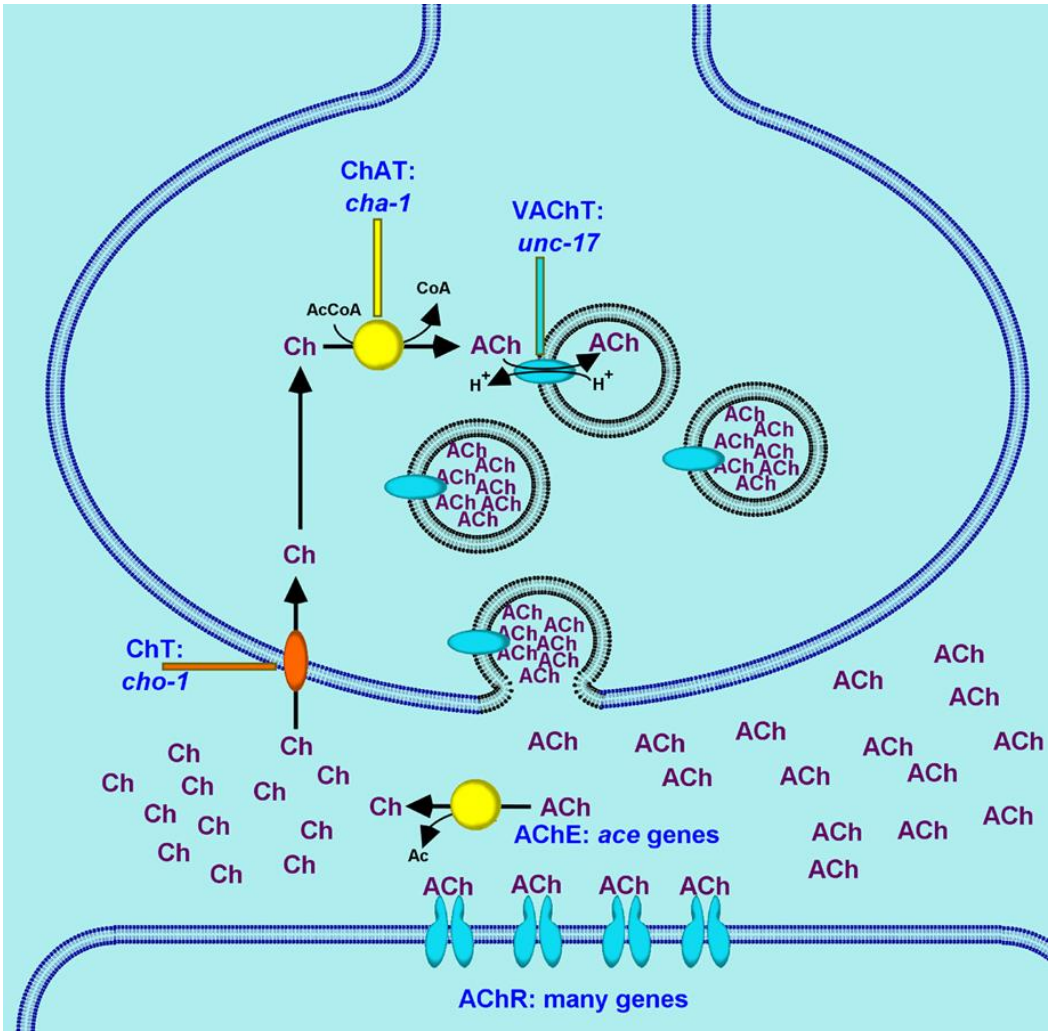

Figure 1: The Roles of the Cholinergic Markers in the Neuromuscular Junctions

Taken from: Rand, J.B. (2007) WormBook the Online Review of *C. elegans* BIOLOGY. URL: http://www.wormbook.org/chapters/www_acetylcholine/acetylcholine.html[15]

There are also two main types of AChRs: the muscarinic acetylcholine receptor (mAChR) and the nicotinic acetylcholine receptor (nAChR). The nAChRs are isotropic (a receptor forming an ion pore that can open or close) and contain five subunits.[1] In contrast, the mAChRs are metabotropic (meaning they do not have a channel that opens or closes since they are associated with a G-protein).[1] nAChRs are pentameric ligand gated ion channels.[1] This receptor modulates the postsynaptic neurotransmission at the neuromuscular

junction and at the peripheral autonomic ganglia.[1] In the CNS, it mostly mediates the release of neurotransmitters from presynaptic sites.[1] The nAChRs` subunits in humans are encoded by 9 genes for the alpha subunits and 4 genes for the beta subunits.[1] The α_2- α_6 subunits assemble with β_2-β_4 subunits to form heteropentamers.[1] The α_7 and α_9 can form homopentamers but there is some evidence suggesting that α_7 β_2 and α_9 α_{10} heteropentamers exist.[1] Conversely, mAChRs are G-protein coupled receptors subdivided into two categories: inhibitory receptors and excitatory receptors.[1] Both nAChRs and mAChRs have been found in mammalian non-neuronal cells.[16]

1.2 Constituents of the Immune System

Immunity is the ability of the immune system to protect the host against antigens. There are two types of immunity: innate immunity, which is immediate and non-specific, and adaptive immunity, which is specific, effective, very robust, and takes time to develop.[4] For adaptive immunity, there are two sub-categories: humoral, which involves the use of antibodies, and cell-mediated immunity, which involves antigen presentation from an antigen presenting cell (APC), T cell recognition, and subsequent release of cytokines.[4]

Furthermore, as previously discussed, the immune response can be classified into two types: proinflammatory and anti-inflammatory.[4] These responses are mediated by proinflammatory and anti-inflammatory cytokines. [4] Those who are proinflammatory are important to fight against antigens capable of causing harm.[4] Such proinflammatory cytokines include interleukin (IL-6) and tumor necrosis factor α (TNF-α).

IL-6 is an important proinflammatory cytokine. IL-6 binds to the IL-6 receptor on target cells which can subsequently induce important downstream signaling to eradicate

antigens.[17] First, IL-6 can increase the expression of proteins in the plasma that play important roles in acute immunity such as C reactive proteins, serum amyloid A, fibrinogen, and hepcidin in hepatocytes (liver cells).[18] It also plays important roles in adaptive immunity. For instance, it helps with T cell differentiation (excluding Treg cell differentiation) and with B cell antibody production.[18] IL-6 also plays an important role in hematopoiesis by being required and sufficient for hematopoietic stem cell production.[19] This cytokine can therefore play an important role in many autoimmune and/or inflammatory diseases like rheumatoid arthritis, lupus, ankylosing spondylitis, psoriasis, colitis, renal diseases, Crohn's disease, and many more.[17–21] Hence, despite the important role of IL-6 in host defense against pathogens, the unregulated release of this proinflammatory cytokine can result in a strong immune response causing harm to the host.[4] Overall, IL-6 is a proinflammatory cytokines that might contribute to pathologies if dysregulated.

TNF-α, like IL-6 is a proinflammatory cytokine. In fact, TNF-α is one the main proinflammatory cytokines. The proinflammatory cytokine TNF-α binds to a TNF receptor.[22] This interaction regulates many essential cell functions including cell proliferation, survival, differentiation, and apoptosis.[22] Immune cells that generate high levels of TNF-α are macrophages and these cells are also very responsive to this cytokine.[22] Dysregulated TNF-α production and TNF receptor signaling has been associated with many inflammatory or autoimmune diseases including rheumatoid arthritis, Crohn’s disease, atherosclerosis, psoriasis, sepsis, diabetes, and obesity.[22] Therefore, modulating the release of this cytokine may circumvent the pathophysiology of several inflammatory or autoimmune diseases.

Conversely, anti-inflammatory cytokines are important to reduce the heightened proinflammatory response to maintain homeostasis in the host by preventing unnecessary tissue damage. [4] IL-10 is one of the key anti-inflammatory cytokines. IL-10's ability to prevent inflammation takes place by binding to heterodimeric IL-10 receptors (namely, IL-10R1, IL-10R2).[23] When IL-10 binds to its IL-10 receptor, the JAK/STAT signaling pathway is activated which in turn leads to changes in expression profile and immunomodulatory genes.[23,24] As a result, there is a decrease in the release of proinflammatory cytokines, a decrease in antigen presentation, and phagocytosis.[23,24] These reductions allow for immune cells with IL-10 receptors (many cells but mostly monocytes and macrophages) to have enhanced inhibitory, tolerance, and scavenger functions.[23,24] Taken together, IL-10's main feature is thus its ability to resolve inflammation.

Cytokines are often produced by immune cells and released from them to mediate the immune response. Therefore, immune cells are an important constituent of the immune system. The principle immune cells of innate immunity include monocyte/macrophages, basophils, mast cells, eosinophils, natural killer cells (NK cells), and neutrophils.[4] Dendritic cells fall within the category of adaptive and innate immunity as they make great APCs and can phagocytose microbes.[4] Furthermore, the main immune cells for cell-mediated and humoral adaptive immunity are T lymphocytes and B lymphocytes, respectively.[4] The way these immune cells function within innate and adaptive immunity will be outlined herein.

In addition to playing a role in the different types of immunity, immune cells come from two different lineages: either myeloid or lymphoid.[10] Immune cells from the myeloid lineage include granulocytes/macrophage progenitors such as neutrophils, eosinophils, basophils, mast cells, dendritic cells, and monocytes (a precursor for macrophages).[10] Other

cells from the myeloid lineage are the megakaryocytes and erythrocytes.[10] Conversely, immune cells from the lymphoid lineage include T lymphocytes and B lymphocytes in conjunction with natural killer cells.[10] The functions of the immune cells from these lineages will be briefly discussed.

Firstly, myeloid cells are mainly composed of phagocytes which include macrophages and neutrophils.[4] Their roles are to ingest and obliterate microbes as well as to remove damaged tissues.[4] Neutrophils only live for one to two days and their main function is to phagocytose microbes, especially products of necrotic cells.[4] Other functions of neutrophils include the opsonization (the process of recognizing and targeting for phagocytosis) of microbes.[4] This short-lived immune cell eliminates these microbes in phagolysosomes (the fusion of a phagosome with a lysosome in a cell to perform phagocytosis).[4] In fact, they synthesize antimicrobial substances that kill extracellular microbes but this substance can also cause damage to healthy tissues.[4] Taken together, phagocytes play an important role in immunity through eradicating foreign substances and performing regulatory functions.

In the bone marrow (BM), there are precursor cells that differentiate into monocytes in the blood stream upon the release of macrophage colony-stimulating factor (M-CSF).[4] Then, monocytes migrate to a target tissue in which they become macrophages.[4] Therefore, monocytes are essentially precursors of macrophages.[4] Macrophages phagocytose microbes and necrotic host cells to eliminate the effects of toxins, trauma or interrupted blood supply.[4] They also annihilate neutrophils that die after accumulating at sites of infection.[4] These cells are also activated by microbial substances to release cytokines that favor the recruitment of more monocytes and leukocytes (white blood cells) by lining the endothelial surface of

blood vessels.[4] Some of these cytokines even encourage the migration to the target sites.[4] Macrophages can also repair tissues by stimulating new blood vessel growth and by generating collagen-rich extracellular matrix (fibrosis).[4] In the process of the phagocytosis of necrotic cells, pathogens, or exogenous debris, these cells secrete either proinflammatory or anti-inflammatory cytokines to induce a certain immune response.[25] Therefore, macrophages can behave by promoting or regulating inflammation.

These cells from the myeloid lineage can have two polarities: the proinflammatory M1 or the anti-inflammatory M2. These polarities may be determined by assessing proinflammatory markers in conjunction with the cytokines secreted from these cells. There are many characteristic markers and cytokines that may altogether characterize the M1 and M2 cell populations. The cell surface marker panel used to target M1/M2 populations may depend on the experiments and the environments in which these cells are found.

In vivo, the extreme polarization of M1/M2 cells might exist. However, these cells may also reside within a spectrum where they contain certain cell surface markers allowing them to be characterized as behaving in a more M1 or M2 fashion. M1 cells may be characterized by expressing high levels of MHC II, Ly-6C (Lymphocyte antigen 6 complex locus G6D), and CCR2 (C-C chemokine receptor type 2).[26,27] These proinflammatory macrophages/monocytes may also secrete higher levels of IL-6 and TNF-α which are both proinflammatory cytokines and a lower level of IL-10, an anti-inflammatory cytokine.[28,29] Conversely, M2 cells may contain CX3CR1 (Chemokine (C-X3-C motif) receptor 1) and CD206 (macrophage mannose receptor) and negative or low levels of M1 cell surface markers.[30–32] These anti-inflammatory macrophages/monocytes may additionally release lower levels of IL-6 and TNF-α in conjunction with higher levels of IL-10, an anti-

inflammatory cytokine.[28] Altogether, M1/M2 cells may be characterized through their cytokine profile and their cell surface marker.

In research, it is important to characterize the balance of M1/M2 cells since dysregulation in M1/M2 cells may lead to deleterious consequences. Hence, M1/M2 cells play an important role in pathologies. For example, M1 cells are commonly known to promote inflammatory diseases, while M2 cells are essential to repair mechanisms.[28] Thus, when M1 monocytes/macrophages cause a destructive proinflammatory immune response, the M2 monocytes/macrophages are recruited to stimulate an anti-inflammatory immune response to restore balance and resolve inflammation. However, M2 cells can also promote tumor growth as they support their survival.[30] Therefore, a disbalance in favor of either M1 or M2 cells can cause harm.

In the host, M1 cells also can change their polarization into M2 cells and vice versa. This switch in polarization depends on the environment of the cells. For instance, in an environment filled with pathogens and with monocytes/macrophages who behave in a proinflammatory manner, M1 polarization will be in favor to eradicate the infection. The ability for these cells to respond to their environment is thus an important feature in allowing them to behave appropriately within the host.

Furthermore, other myeloid cells include mast cells, basophils, and eosinophils. These three types of cells play an important role in allergy and immunity against parasites. Mast cells come from the BM and can be found in the skin and mucosal epithelia. Once activated, they release many inflammatory mediators that fight against parasite infections and cause allergic reactions.[4] Basophils are blood granulocytes that are structurally and

functionally similar to mast cells.[4] Eosinophils, another granulocyte, contain capsules in their cytoplasm with enzymes that are deleterious to cell walls of parasites and that can also destroy host tissues.[4] Eosinophils have also been shown to play a role in the pathology of allergies.[33,34] Altogether these cells are similar in terms of function.

Unlike the previously discussed immune cells who mostly play a role in innate immunity, DC's play an important role in bridging innate and adaptive immunity. DCs reside in tissues and are also circulating; they can detect the presence of microbes in their environments, capture them, and present them to T lymphocytes (or T cells).[4] In fact, these are sometimes known as professional APCs as their properties are tailored to detect antigens and initiate an adaptive immune response by presenting antigens to naïve T lymphocytes, a cell from the lymphoid lineage.

Most cells of the lymphoid lineage play a role in adaptive immunity. Cells from the lymphoid lineage consist of lymphocytes and natural killer cells. There are two types of lymphocytes: T lymphocytes and B lymphocytes.[4] B lymphocytes are important for humoral immunity since they produce and secrete antibodies that will bind to antigens, neutralize them and destroy them.[4] B lymphocytes (B cells) mature in the BM whereas T lymphocytes mature in the thymus. [4] T lymphocytes (T cells) are the mediators of cell-mediated immunity. [4] There are two subtypes of T cells: $CD4^+$ T helper cells and $CD8^+$ killer T cells.[4] Upon the recognition of a peptide bound to a major histocompatibility complex (MHC) II of an APC, CD4+ T helper cells secrete cytokines to activate B cells, to instruct the macrophage on how to destroy the extracellular microbe and stimulate inflammation.[4] $CD8^+$ killer T cells, bind to the MHC I of APC via the T cell receptor, prompting the destruction of cells containing intracellular microbes.[4] APCs can present both self and foreign antigens.

However, the T and B cells should not recognize self-antigens. The presence and survival of lymphocytes recognizing self-antigens is a hallmark of autoimmune diseases. Finally, natural killer cells are the only type of lymphoid cell from the innate immune system. They recognize damaged or stressed cells and help to kill these cells. These processes provide early defense against pathogens and influence the nature of the following adaptive immune response.[4] Therefore, B cells and T cells predominantly play a role in adaptive immunity whereas NK cells mostly play a role in innate immunity.

The scope of this thesis will cover certain immune cells of interest such as CD4+ T cells, CD8+ T cells, macrophages/monocytes, and B cells found within selected immune tissues. Such immune tissues include the murine spleen, thymus, and BM in conjunction with human peripheral blood mononuclear cells (PBMCs). The spleen is a secondary lymphoid organ through which the blood is filtered.[4] Therefore, this immune organ eliminates pathogens that may be found in the blood with their immune cells.[4] The spleen is also the organ that initiates the adaptive immune response against blood-borne antigens.[4] Hence, the spleen is important for the activation of T and B cells by APCs.[4] The thymus is the site of T cell maturation, while the BM is the site of maturation for all other immune cell types and hematopoiesis.[4] Therefore, in the BM, all the blood cells, which include the immune cells are produced.[4] Finally, PBMCs are a group of cells found within the blood which include lymphocytes and monocytes.[4] Altogether, this research project will only focus on selected immune cells and tissues, a first step in providing a complete understanding on the entire immune system.

1.3 The Relationship Between the Cholinergic System and the Immune System

As stated earlier, multiple evidence shows that ACh is found in non-neuronal cells/tissues, the first sample of ACh to be isolated by Dale and Dudley in 1929 was from the spleen, a tissue that does not contain any cholinergic innervation .[16,35] In 1933, Chang and Gaddum found ACh in several organs and tissues that do not contain cholinergic innervation, including the human placenta, rabbit skin, and horse and ox spleen, in conjunction with organs and tissues with cholinergic innervation, including dog brain and rabbit intestines.[16,36] However, most of the research regarding ACh has been focused on its function as a neurotransmitter ever since Sir Henry Dale and Otto Loewi won the Nobel Prize in Physiology of Medicine in 1936 for discovering the chemical transmission of nerve action.[16] Then, in 2000, Borovikova *et al.* demonstrated that electrical stimulation of the vagal nerve inhibits proinflammatory cytokine without changing the production of anti-inflammatory cytokines in endotoxemic mice.[37,38] This was the first piece of evidence that showed a relationship between the cholinergic system and the immune system.[37,38]

Borovikova et al.'s discovery played a significant role in the field of neuroimmunology. With their finding, they discovered the cholinergic anti-inflammatory pathway (CAP).[37,38] As the name suggests, this pathway elicits an anti-inflammatory immune response by utilizing the cholinergic system.[37] Initially, this response mainly occurred through vagus nerve stimulation (VNS) in order to restore balance after a proinflammatory immune response.[37] This proinflammatory immune response can be stimulated by pathogens, ischemia, or other injuries.[37] The vagus nerve is one of the

principle nerves of the parasympathetic autonomic nervous system which mediates metabolic homeostasis.[39] Furthermore, the vagus nerve is a main constituent of the neural reflex mechanism of inflammation.[39] VNS sends afferent signals to the brain which is where the signal will be processed.[37,38] After processing, the brain sends efferent signals which results in ACh release that will predominantly interact with the α7 subunit of the nAChR on macrophages and other immune cells.[37,38] Hence, the brain sends efferent signals to balance the proinflammatory immune response through the CAP.[16] Although the CAP has been shown to modulate inflammation by preventing the synthesis of proinflammatory cytokines, the exact mechanisms remain unclear.[16] Taken together, when the cholinergic system was first discovered for its immunomodulatory role, VNS was being used to stimulate the CAP for which its mechanism to this day is unclear.

Not only can VNS activate the CAP, but it may also have other effects on the body. Because of the multiple effects VNS might stimulate, it can be used to treat many types of diseases. For instance, VNS is currently approved by the Food and Drug Administration to treat drug-resistant epilepsy and treatment-resistant depression in patients.[40–42] Physical stimulation of such a nerve through the application of an electrical current can potentially treat many other diseases such as Type 2 diabetes, rheumatoid arthritis, irritable bowel diseases, sepsis, lung injury, and stroke/traumatic brain injury.[40,43,44] Hence, in many studies, VNS has been shown to potential treat these diseases and their key findings are outlined below.

To begin, type 2 diabetes is a disease where the individual can produce insulin, but glucose cannot enter the cell, rendering the patient with a high glucose level. In a type 2 diabetic rodent model induced with a high-fat diet and streptozotocin, VNS has been shown

to reduce blood glucose in diabetic rats by enhancing vagal efferent activity and the release of GLP-1.[45] Interestingly, GLP-1 has also been associated with a reduction in inflammation.[46,47] Overall, this study suggests that VNS may potentially be used to treat type 2 diabetes.

Furthermore, rheumatoid arthritis is both an inflammatory and autoimmune disease commonly characterized by an inflamed synovial membrane. VNS has improved rheumatoid arthritis disease in both humans and animal models of the disease.[48] In an experimental collagen-induced arthritis, vagotomy & selective disruption of α7nAChR lead to a worsened disease state.[48–50] VNS delivered once daily in humans with rheumatoid arthritis has also lead to a reduction in joint swelling, cytokine production, disease score and protection against synovitis and periarticular bone erosions.[48] These findings suggest that VNS may treat rheumatoid arthritis and α7nAChR seem to be a key element in preventing disease exacerbation.

Moreover, inflammatory bowel disease includes inflammatory diseases such as Crohn's disease and colitis. VNS has been shown to improve the disease state of a rat model of colitis and vagal tone has been shown to be blunted in individuals with colitis. [5,43,51,5239,47–49] Thus, in a pilot study with seven Crohn's disease patients by Bonaz *et al.*, VNS has been shown to be a feasible and well-tolerated treatment in most patient as five of them evolved toward clinical, biological, and endoscopic remission with a restored vagal tone.[43] Therefore, it seems that VNS holds some potential in treating inflammatory bowel disease.

Also, stroke and traumatic brain injuries involve widespread neural inflammation in their pathophysiology.[40,53] Such inflammation may be treated through VNS as it leads to the

reduction of TNFα, a cytokine marker used as an indicator for trauma and ischemic injuries.[40,53] These findings suggest that VNS might be a good treatment option to control neural inflammation in patients with traumatic brain injury.

In the case of lung injury, inflammation may encourage the manifestation of ventilator induced lung injury (VILI).[40] Ceasing the CAP through vagotomy (which is the surgical removal of certain vagus nerve branches) worsened VILI.[40,54] Vagotomized animals with mechanical ventilation resulted in higher alveolar damage and higher levels of IL-6 as well as more hemorrhage compared to control animals.[40,54] Hence, it seems that the vagus nerve plays an important role in preventing aggravated VILI. This finding would suggest that using VNS could help patients recover from this type of lung injury.

Like VILI, inflammation plays a big role in the pathology of sepsis. Sepsis is a major inflammatory disease induced by an infection which leads to chronic proinflammatory signaling. In turn, such events may lead to organ dysfunction and death if not treated appropriately. Treating sepsis is also extremely expensive as it is estimated to cost $22,000 per patient and 18 million individuals are estimated to be affected by this disease each year.[40,55] However, VNS has been proposed to treat sepsis by restoring the balance between the sympathetic and parasympathetic tone which consequently halts the progression of sepsis.[40] Endotoxemia is an event which often occurs in septic patient. Accordingly, it has been shown that in LPS induced endotoxemia, VNS reduced mortality.[6,40] Interestingly, this finding is thought to be due to ACh release.[6,40] VNS can also reduce proinflammatory cytokine levels, prevent tissue injury, and improve outcome in septic animal models.[56] Overall, it seems that VNS might be used to treat sepsis as it seems to improve disease outcome.

Altogether, VNS can be used to treat many inflammatory and autoimmune diseases through the CAP. However, this anti-inflammatory immune response might be stimulated without needing the surgical intervention that would be required for VNS. In fact, as discussed in the next section, modulating the cholinergic system within immune cells might be a better option as it avoids the risk of surgery.

1.4 The Cholinergic System in Non-Neuronal Cells and Tissues

As the CAP induced by VNS demonstrates the relationship between the cholinergic system and the immune system, it does not however show the complete role of cholinergic markers within non-neuronal cells. The first evidence of cholinergic components in non-neuronal tissues was obtained by using techniques such as radioimmunoassays and high performance liquid chromatography with electrochemical detection.[16] With these techniques, ACh has been found in many different types of cells/tissues like immune cells, epithelial cells of the skin, respiratory tissues as well as in alimentary tracts of almost all forms of life on earth.[2,16,57–59] The progress of research in molecular biology has increased our knowledge of non-neuronal ACh and its implications in immunity, inflammation, and wound healing, in addition to cancer and cardiovascular, respiratory, digestive, and orthopedic diseases.[16] These findings suggest the presence of the cholinergic system in numerous tissues throughout the body and suggest ACh's importance as a mediator.

Within the immune system, it is known that T and B cells express most cholinergic components such as ACh, AChE, and ChAT and T cell activation lead to an increase in ChAT. The expression of such markers suggests a role of the cholinergic system in restoring balance following a proinflammatory immune response.[60] More specifically, CD4 T cells in

the spleen[9,10] have been confirmed to produce ACh, and human PBMCs have previously been shown to contain ACh.[8] One study showed that in T cells, antigen activation is necessary for ChAT expression, however, not all T cells that have experienced antigens express ChAT.[7] ChAT expression was additionally shown in many human lymphoma cell lines such as MOLT-3, MOLT-4, HSB-2, and CEM. [7,61,62] In an *in vitro* culture of the human MOLT-3 T cell line, phorbol myristate acetate and phytohemagglutinin (which both induce a T cell immune response), induced the release of ACh, suggesting that ACh release by CD4+ T cells can be stimulated by T cell receptor activation.[7] Similarly to T cells, B cells do express ChAT but must be activated to induce ChAT expression.[7,9] Taken together, T and B cells seem to express many cholinergic components and the production of ACh seems to upregulate upon immunological activation.

Other immune cells have been shown to express ACh and/or cholinergic markers. Indeed, BM-derived DCs and spleen-derived mononuclear leukocytes in mice have been shown to express AChE transcripts in a resting state and ChAT transcripts when immunologically stimulated.[63] In the same study, macrophages from murine peritoneal cavity also express AChE in the resting state. [63] However, the authors did not verify if these transcripts were translated into proteins. [63] In addition, NK cells from the murine spleen and from human PBMCs have been shown to express ChAT, VAChT, and AChE at the transcript and protein level.[64] In the same study ACh and ChAT were upregulated upon LPS and IL-2 stimulation, suggesting that ChAT and ACh likely play a role in immune regulation to maintain inflammatory homeostasis. [64] Thus, the cholinergic system within these immune cells seem to overall play a role in maintaining homeostasis which may explain why immunological stimulation increases the level of ACh production.

Within the spleen, different stimuli seem to induce the release of ACh depending on the immune cell from which the ACh is released. For instance, norepinephrine, the neurotransmitter released in the spleen (as this organ is adrenergically innervated), induces ACh release from CD4+ T cells but not in B cells.[7] To date, the stimulus that has been found to stimulate the release of ACh from B cells is the gut peptide hormone cholecystokinin.[7] In NK cells however, the signals that stimulate the release of ACh is unknown.[7] Altogether, ACh released from T cells, B cells, and NK cells seems to be induced by different stimuli which might reflect potential functional differences in the endogenous cholinergic systems within each of these immune cells.

Within immune tissues, ACh synthesizing activity has been documented in the rat spleen, thymus and blood.[60] Although ACh synthesizing activity suggests the presence of ChAT in these tissues, this finding does not confirm that the synthesis of this molecule comes from ChAT activity.

Cholinergic receptors have also been shown to be expressed in immune cells. In fact, α9 nAChRs have been shown to be highly expressed in immune cells.[65,66] Furthermore, T cells and B cells express nAChRs in conjunction with mAChRs.[60] To this end, non-neuronal ACh acts like an autocrine or paracrine agent on mAChRs and nAChRs of effector cells. Therefore, the proper functioning of the cholinergic system plays an important role in biological and physiological processes by acting through these cholinergic receptors.

By utilizing exogenous ligands, the cholinergic system has been shown to act on immune cells by stimulating an anti-inflammatory immune response. For instance, it has been shown that the administration of nicotine, an exogeneous ligand to α7nAChRs has an

anti-inflammatory immune response. The anti-inflammatory response from ACh may be due to the inhibition of the release of TNF-α by blocking the NF-κB pathway.[67] There are different subtypes of nAChRs but the main one that was found to have an anti-inflammatory effect was the one with the α7 subtype. The importance of this subtype has been identified by knocking down the α7 receptor with siRNA, which prevented NF-κB signaling and TNFα secretion.[67,68] Thus, with the evidence available to date, it seems that the cholinergic system's ability to regulate inflammation is primarily through the α7nAChRs.

Another cell that seems to play an important role in immunomodulation are Mesenchymal stem cells (MSCs). MSCs are multipotent stem cells which can differentiate into adipocytes, osteoblasts, chondrocytes, myocytes, β-pancreatic islets cells and, neuronal cells.[69] Although they are not known as immune cells, increasing evidence suggest that these cells play an important role in immunomodulation through various means. More specifically, MSCs can prevent T-cell proliferation, cytokine secretion and cytotoxicity as well as regulate the balance of Th1/Th2.[69–72] MSCs can also regulate the functions regulatory T cells.[69,73] For B cells, they can increase their viability yet inhibit their proliferation and cease the cell cycle.[69,74] To this end, MSCs modulate the release of antibodies and production of co-stimulatory molecules of B cells. [69,74] MSCs have been shown to inhibit the maturation, activation, and antigen presentation of dendritic cells.[69,75,76] MSCs can additionally inhibit NK cell activation induced by IL-2.[69,77] Therefore, MSCs to modulate inflammation by changing the way immune cells behave.

Interestingly, recent evidence has shown a link between MSC's immunomodulatory function and the cholinergic system.[78] In fact, MSCs have been shown to be able to produce ACh through ChAT activity and release this molecule which then binds to nAChRs on

activated immune cells. [78] This binding of ACh to nAChR consequently lead to immunosuppression. [78] Indeed, the addition of MSCs to mixed lymphocyte reaction and phytohemagglutinin activated PBMCs lead to a suppression in lymphocytes proliferation, IFNγ release, and TNFα release. [78] These effects were mostly reversed with α-bungarotoxin, an antagonist of ACh.[78] It thus seems that MSCs play an important immunomodulatory role through a cholinergic mechanism. These studies make MSCs an attractive target for further investigation of the immune implications of the cholinergic system.

As previously stated, some cholinergic components such as ACh, ChAT, AChE, nAChRs, and mAChRs seem to be expressed in both neuronal and non-neuronal cells. However, non-neuronal cells seem to have a distinction regarding the cholinergic marker involved in the transportation of Ch. In fact, choline transporter like protein 2 (CTL2) seems to be the most probable protein mediating the transport of Ch into the cell rather than ChT since CTL2 has been found in the tongue, muscle, kidney, liver, spleen, lung, inner ear, and neutrophil whereas ChT has only been found in the spinal cord and the brain.[79] CTL2 exists in two isoforms: CTL2-P1 and CTL2-P2.[79] Human CTL2-P1 does not transport Ch whereas CTL2-P2 does contain Ch transport activity.[79] In addition, an autoimmune disease has been associated with a blockade in CTL2 which results in altered hair cells causing hearing loss.[79,80] CTL2 transports Ch which can then either be used for phosphocholine synthesis or ACh synthesis.[79] Therefore, it seems more likely for Ch to be transported through CTL2 rather than ChT.

Another distinction in non-neuronal cells involves the transporter protein mediating the transport of ACh outside of the cell. Organic Cation Transporter Novel Type 1 (OCTN1) is a membrane protein that has been proposed to transport ACh outside of non-neuronal cells

such as immune cells rather than VAChT.[81–84] It has been shown with the expression of OCTN1 and medianoche in immune cells that ACh release from such cells is likely not associated with vesicles.[81–84] It thus seems that OCTN1 might be a more suitable candidate for the transport of ACh outside of the cell.

Regarding infectious diseases, the cholinergic system may also play a role in response to viral and bacterial infections. In fact, one study evaluated ChAT expression in response to viral infection.[7,85] They showed that the levels of ChAT increased as a response to lymphocytic choriomeningitis virus and vesicular stomatitis virus in CD4+ T cells and CD8+ T cells. [7,85] The induction of such ChAT expression was dependent on IL-21 (a cytokine important for viral immunity) signaling.[7,85,86] Moreover, in the cultures of CD8+ T cells from lymphocytic choriomeningitis virus-infected mice, ACh was released without further stimulation.[7] Such findings are not restricted to viruses. In fact, cholinergic activity was detected in infected lesions by positron emission tomography in pigs with postoperative abscesses and in mice with *Staphylococcus aureus*.[56,59] To this end, high levels of cholinergic activity take place within lesions of humans suffering from pneumonia or non-small-cell lung carcinoma. [56,59] Taken together, the cholinergic system seems to play a role in lymphocytic choriomeningitis virus, vesicular stomatitis virus, *Staphylococcus aureus,* pneumonia, and non-small-cell lung carcinoma. Perhaps the increased level in ACh production is due to its reported ability to protect healthy cells and tissues during inflammation.

In an animal model of multiple sclerosis, it has been previously shown in Dr. Simard's lab that nicotine can act as an exogeneous ligand to α7nAChRs and attenuate the symptoms of experimental autoimmune encephalomyelitis (EAE), a mouse model for

multiple sclerosis.[66] They showed, that nicotine partially retained the ability to reduce lymphocyte infiltration into the CNS, prevented auto-reactive T cell proliferation and helper T cell cytokine production. [66] Nicotine also down-regulated co-stimulatory protein expression on myeloid cells, and increased the differentiation and recruitment of regulatory T cells, even without α7-nAChRs.[66] Overall, this suggests that nicotine was able to attenuate EAE.

Interestingly, a study showed that synapses between ChAT+ NK cells and CCR2+Ly6Chi monocytes occurred through the α7-nAChR.[64] The authors also showed that there were more ChAT+ NK cells in mice with EAE than their healthy counterparts.[64] Moreover, the non-neuronal cholinergic activity of human NK cells has been shown to be upregulated as a response to CNS autoimmune disease. [64] These findings suggest that the non-neuronal cholinergic activity within NK cells plays a role in immune regulation of multiple sclerosis.

In another study on multiple sclerosis, the progression of this disease has been tracked by assessing the expression of certain cholinergic markers such as AChE, BChE, ChAT and α7nAChR.[87] Therefore, the cholinergic system is not only important in terms of developing new drugs but it may also be used as a tool to further understand the pathophysiology of autoimmune or inflammatory diseases like multiple sclerosis.

Overall, all these interesting findings suggest that the cholinergic system in immune cells may play a role in immune regulation by stimulating an anti-inflammatory immune response. However, the exact role of the cholinergic system in immune cells is mostly unknown and assessing the presence of the cholinergic markers in immune tissues or cell

groups in conjunction with their endogenous immune cells would be the first step in revealing its functionality. Accordingly, assessing the role of ACh production in BM derived macrophages (BMDM) would be a first step in understanding the role of the cholinergic system within immune cells and tissues.

Objectives and Hypothesis

Our study seeks to elucidate the role of ACh production in immune regulation. The first aim of the project herein investigates the expression cholinergic components in immune tissues and immune cells. More specifically, we will first assess the expression of all cholinergic markers within immune tissues at the transcript level. Then, the presence of ACh, ChAT, AChE, and ChT proteins will be assessed in immune tissues. Moreover, the expression of ChAT within immune cells of interest from these tissues will be investigated as well. The goal of this study is not to perform a comparative analysis of each marker amongst different tissues or cell types: rather, the objective is to assess whether each cholinergic protein is present within a given tissue or cell type. Therefore, the first aim of this study is to evaluate whether the cholinergic markers in conjunction to ACh are present in the bone marrow, thymus, spleen, and blood tissues, and in cell subsets within these tissues. The second aim of this study will be to investigate the role of ACh production in immune processes with a pharmacological approach. The second aim will be completed on BMDMs and it will assess its role through assessing the cytokine profiles of each pharmacological condition. Given the information above, it is hypothesized that immune tissues and cells will express the machinery required for ACh synthesis. Moreover, inhibitors of ChAT and ChT are hypothesized to increase inflammation while inhibitors of AChE will reduce inflammation in immune cells. This finding would suggest that the cholinergic system plays a crucial role in immune regulation. Assessing the role of ACh production in immune regulation within immune cells would further our understanding on the cholinergic system's role in inflammation. These findings could then provide novel targets for more effective treatments against autoimmune and inflammatory diseases.

Materials and Methods

2.0 Collection of Murine Tissues

C57BL/6J WT mice were bought from Jackson Laboratories (catalog# 000664) and were held at the animal facility at Laurentian University. They were housed in groups of up to 5 mice with a 12-hour lights on and lights off cycle whereby the lights were on from 7:00 am until 7:00 pm. The mice were also supplied regular chow ad libitum. Our experiments regarding animal work with the mice were reviewed, approved, and conducted following the policies outlined by the Laurentian University Animal Care Committee.

To harvest the tissues, the mice were anesthetized with isoflurane and were sacrificed via neck dislocation. Ethanol was sprayed on the mice and with the surgical kit (Fine Science Tools, Item No. 20830-01), they were dissected to extract the femur and tibia that were then put in sterile 1× PBS (Phosphate Buffered Saline, prepared from 10× PBS solution from Bio-Rad, catalog # 1610780 or PBS, Phosphate Buffered Saline, 10× Solution, Fisher BioReagents, catalog # BP399-1). The mouse's brain, spleen and thymus were also collected and were either placed in 1× PBS for subsequent cell isolation, placed in RNA Later for RNA isolation (ref# AM7024) or placed in an empty test tube in dry ice to be subsequently stored at -80 °C for mass spectrometry (MS) sample preparation .

2.1 BM Cell Extraction

The protocol followed herein was adapted from a previous protocol by St-Pierre et al.[65] The BM was flushed with a 25- or 26-gauge needle that was attached to a 5 mL syringe containing 1× PBS or complete media (1% penicillin/streptomycin and 10% fetal bovine

serum (FBS) in 1640 RPMI media) if cells were cultured downstream. The bones were held with a pair of forceps in one hand and the needle containing the 1× PBS or complete media was used to flush the bones by performing an up and down motion on top of a cell strainer with 40 μm holes placed on the opening of a 50 mL conical tube. The bone was continuously being flushed until it had a pink/white color. Afterwards, the plunger end of the syringe was used to gently press on the clumped cell debris left on the cell strainer. Then, the cell strainer was rinsed with more 1× PBS or complete media. The tube was centrifuged at 520 × g for 13 minutes at 4°C and the supernatant was removed.

For BM cells that were used for downstream tissue culturing and immunocytochemistry (ICC) experiments, red blood cells (RBCs) were lysed by adding 5 mL of 1 × RBC lysis buffer, resuspending the cells, and incubating them for 5 minutes. After the 5 minutes, 25 mL of 1× PBS was added, the content of the tube was mixed by inversion. Then these tubes were centrifuged at 520 × g for 10 minutes at 4°C and the supernatant was removed.

The cells were then suspended in a new volume of 5 mL of 1× PBS or complete media and counted with a hemocytometer (Phase counting chamber from Hausser Scientific, Catalog No. 3200). BM cells were then used for ICC or BMDM tissue culturing, as detailed in section 2.10 or 2.13 of the materials and methods, respectively. For other downstream applications, once the cells were counted, the 5 mL cell suspension was centrifuged at 450 × g for 5 minutes at 4°C to form a pellet. For western blots and MS, the supernatant was removed, and the cells were stored at -80°C until cell lysis. For qPCR, the supernatant was removed and 500 μL of RNA Later was added and the cells were suspended by using a pipette. The cell suspension in Invitrogen RNA Later Stabilization Solution (ref# AM7024)

was stored for at least 24 hours at 4°C (cannot store the cells at 4°C for longer than a month) to allow the RNA Later to be taken up by the cells. After 24 hours, the cells were stored indefinitely at -20 °C until ready for use.

2.2 Splenocyte Extraction

This protocol was adapted from Stem Cell Technologies' splenocyte single cell suspension protocol. Spleens were harvested from the mice and placed in 1× PBS. Then each spleen was sliced in small pieced in a small volume of 1× PBS in a petri dish. The small pieces of spleen were then placed on a cell strainer with 40 μm holes placed on top of a 50 mL conical tube. With the plunger end of a syringe the pieces of spleens were gently crushed to allow for the cells to go through the cell strainer. Once there are no remaining pieces of the spleen intact in the cell strainer, the plunger end of the syringe and the cell strainer were both rinsed with 1× PBS. The conical tubes containing the cells were then centrifuged at 520 × g for 13 minutes at 4 °C and the supernatant was discarded. Afterwards, 5 mL of 1× RBC lysis buffer was added and incubated for 4 minutes at room temperature. Then, the cells were centrifuged at 520 × g for 10 minutes at 4 °C and the supernatant was discarded. After the supernatant was discarded, 5 mL of 1× PBS was added to the cells which were then counted on a hemocytometer. Then, the volume of cell suspension was adjusted to a concentration of 5 million cells/mL for ICC.

2.3 Human PBMC Isolation

Human whole blood samples from healthy volunteers over the age of 18 was drawn by a licensed phlebotomist. The participants used in this study do not smoke nicotine and do not regularly take anti-inflammatory medication. To reduce variability in the data, the

participants were asked to fast 10 hours prior to donating blood. The experiments using human samples were reviewed, approved, and conducted following the policies outlined by the Laurentian University Research Ethics Board for Research Involving Human Participants. The blood was collected in BD Vacutainer™ glass blood collection tubes with sodium heparin (BD, catalog # B366480) to prevent the blood from coagulating.

Peripheral blood mononuclear cells were isolated following SepMate's protocols. Fresh solutions of PBS + 2% FBS (Gibco, Cat#10082147) and complete medium (RPMI-1640 + L-glutamine medium, 10% FBS) were prepared prior to starting. Prior to isolating the PBMCs, the sample, the 1× PBS + 2% FBS, the density gradient medium, and the centrifuge were all at room temperature. First, the total blood volume was noted and combined into 50 mL conical tubes. The sample was then diluted with an equal volume of 1× PBS + 2% FBS. This was done by preparing a 34 mL solution of blood (17 mL of blood with 17 mL of 1× PBS + 2% FBS) in 50 mL conical tubes. The tubes were then gently mixed. By using a 2 mL or a 5 mL serological pipette, 15 mL of density gradient (Corning`s Lymphocyte Separation Medium, Fisher scientific, catalog # MT25072CV) medium was added to the SepMate tube (Stem Cell Technologies, ref # 85450) by carefully pipetting it through the central hole of the SepMate insert. The top of the density gradient medium resulted in being above the insert. By keeping the SepMate tube vertical, 34 mL of diluted sample was added to separate SepMate tubes by pipetting down the side of the tubes very slowly. The SepMate tube was then centrifuged at 1200 × g for 10 minutes at room temperature with the brake on. After the centrifugation, the top layer containing the enriched MNCs was quickly poured into a new 50 mL conical tube for each SepMate tube and 1× PBS + 2 % FBS was added to the 50 mL mark of each tube. Once the volume in the tube

was adjusted to 50 mL, they were centrifuged at 300 × g for 8 minutes at room temperature, with the brake on. After centrifugation, most of the supernatant was removed without disturbing the pellet (~ 3 mL was left to re-suspend). The pellet was re-suspended, and the re-suspensions were combined into one 50 mL conical tube and 1× PBS + 2% FBS was added to the 50 mL mark. This tube was centrifuged at 300 × g for 8 minutes at room temperature, with the brake on and the supernatant was removed without disturbing the pellet.

To lyse RBCs, the pellet was re-suspended in 3-10 mL of prepared 1 × RBC Lysis buffer and incubated for 4-5 minutes at room temperature. Immediately after this short incubation, the tube was centrifuged at 500 × g for 5 minutes at room temperature and the supernatant was removed. To the cells, 1× PBS + 2% FBS was added up to the 50 mL mark and centrifuged at 300 × g for 8 minutes at room temperature. The supernatant was then removed and 5 mL of complete medium (HyClone™ RPMI 1640 + L-glutamine, Fisher Scientific, catalog # SH300270, 10% FBS, 1% penicillin) was added to re-suspend the cells. The cells were then counted on a hemocytometer and the cells were stored the same way as the BM cells for their respective downstream applications (western blot or qPCR).

2.4 RNA Extraction

The kit used for the RNA extraction was the Invitrogen PureLink RNA MiniKit (catalog # 12183025). The manufacturer's "Using TRIzol® Reagent with the PureLink® RNA Mini Kit" protocol was followed for the RNA isolation and the "On-column PureLink® DNase Treatment Protocol" was followed for the DNAse treatment. A rotor-stator was used to homogenize the spleen and the thymus.

The isolated RNA suspended in 50 to 70 μL of RNase free water was immediately assessed for its concentration (measured in ng/μL), A260/A280 and A260/A230 with a nanodrop (Nanodrop One, Thermo Scientific, serial #: AZY1708333). The blank solution used was RNase free water. The samples were then stored at -80°C.

2.5 RNA Integrity

To verify the RNA integrity, a 1% agarose gel was made in 1× Tris/Borate/EDTA (TBE) buffer (Bio Basic's TBE buffer (Tris-Borate-EDTA), Premix powder, catalog # A0024). The mixture of TBE and agarose (Froggarose LE, Molecular Biology Grade Agarose from FroggaBio, catalog # A87500G) was heated in the microwave until the mixture started boiling. At that moment, the mixture was stirred and put in the microwave again until the next time the mixture boiled. Once the mixture was clear and cooled, ethidium bromide was added to make a solution containing a 0.5 μg/mL final concentration. This solution was then poured into the casting tray containing the comb. After 45 minutes at room temperature, the gel had solidified. The samples containing 500 ng of RNA, some RNase free water, as well as loading dye (Agarose Gel 6X Loading Dye, Ficoll based from Alfa Aesar by Thermo Fisher Scientific, catalog # AAJ62800AB) were added to each well. Each well contained 10 μL of sample and the wells of the gels were loaded only after the electrophoresis tank had been filled with 1× TBE buffer and the gel had been put in place. Note that there should be a layer of 1× TBE buffer on top of the gel. After the gel box had been covered and the electrodes were engaged, the voltage was set at 90 V and run for one hour. The gel was then examined with trans UV by using a ChemiDoc XRS system (serial # 765/03422) with the Quantity One Software (v4).

2.6 Reverse Transcription

For reverse transcription, the SensiFast cDNA synthesis kit from BIOLINE was used (catalog # BIO-65054). The reverse transcription was done by following the manufacturer's protocol. Once each sample was prepared, they were inserted in the Thermo Cycler (Bio-Rad's MJ Mini Personal Thermal Cycler, Model PTC1148). For the no-RT control samples, the only difference was that the mixture contained an additional volume of RNase free water instead of reverse transcriptase. A no-RT control was made for each RNA sample to verify for the presence of genomic DNA.

2.7 PCRs

Since the goal of this study was to assess the presence of cholinergic genes, we could have used a standard PCR technique. However, we decided to use a qPCR thermal cycler and subsequently run the PCR product on a gel. We decided to use a qPCR thermal cycler because future studies may assess the differences in expression levels during different inflammatory disease states, after treatment with various immune stimulants or anti-inflammatory drugs. The current study therefore provided the ideal opportunity to optimize the qPCR conditions that would be later used for comparative analysis. Nonetheless, it is important to highlight that no comparative analysis was done on the qPCR results for the current study.

For the SYBR green qPCR, the SensiFAST SYBR Lo-ROX kit from BIOLINE (catalog # CSA-01195) was used by following the manufacturer's protocol. The quantity of cDNA in each qPCR reaction was optimized since higher concentrations of cDNA seemed

to have a lower C_q value. In fact, this was probably due to contaminants from the RT that inhibited the PCR reaction. Briefly, in each well of the 96-well plate, a mixture containing 2 μL of a 250 ng/20μL sample, 0.80 μL of primers from Integrated DNA Technology (Table 1 for information on the primers used), 7.2 μL of RNase free water and 10 μL of 2X SensiFast SYBR Lo-ROX Mix was added. The sample can either be cDNA, a no-RT control or RNAse free water (for the no template control (NTC)). The housekeeping gene that was used was Tata Binding Protein (tbp). Also, a NTC was prepared by adding 2 μL of water and the no-RT control was also added in another PCR tube to make sure that there were no false positives and genomic DNA contamination in the samples. The no-RT control was only assessed with the housekeeping gene, tbp. All the results from the qPCR had negative results for the no-RT control and the NTC as well as positive results for tbp. The temperature programming used was the protocol`s 2-step cycling program for all genes except for human BChE and ChAT. For the latter genes, the temperature programming that was used was the protocol's 3-step cycling program since the primers for these genes generated larger PCR products. For most primers, the optimal annealing temperature was 57.0°C but for human BChE and ChAT primers, the optimal annealing temperature was 60.0°C. A melt curve was always completed to ensure the amplification of only one PCR product. The 96-well plate was analyzed on the Bio-Rad CFX Connect Real-Time PCR thermal cycler (optical module serial # 788BR07960 and thermal cycler serial # BR008028) using the CFX Maestro Software (v4.1.2433.1219).

For one spleen sample and for one human PBMC sample, the PCR product size was confirmed by completing the exact same protocol on the CFX Connect Thermal Cycler except that the melt curve was removed from the protocol. In addition, for the murine

spleen, the protocol to confirm the PCR product size for tbp, murine BChE, CTL2, and OCTN1 was set to 35 cycles whereas for ChAT, human BChE, AChE, ChT, and VAChT, the protocol was set to 40 cycles. For the human PBMCs, the protocol to confirm the PCR product size for tbp, CTL2, and OCTN1 was set to 35 cycles whereas for ChAT, BChE, AChE, ChT, and VAChT, the protocol was set to 40 cycles. After completion of the PCR, 4 µL of 6× agarose loading dye (the same used in section 2.4) was added to the 20 µL PCR product and loaded on a 1% agarose gel with ethidium bromide as described in section 2.4 of the Materials and Methods. The gel ran at 120 V for 1 hour for the large gels and 100 V for 1 hour for the mini gels.

Table 1: Information on the Primers Used for SYBR Green qPCR

Gene	Primer 1	Primer 2	Predicted Product Size	Reference Sequence Number	Species
AChE	5'-GTCCAGACTAACGTACTGCT-3'	5'-ATGCGATACTGGGCCAAC-3'	AChE: 114 bp	Table 2M_015831	Human
AChE	5'-AGGTTCAGGCTCACATATTGC-3'	5'-GCTCAGCGACTTATGAAATACTG-3'	AChE: 128 bp	NM_009599	Mouse
ChAT	5'-GCTTTTGTGAGAGCCGTGAC -3'	5'-CCGGTTGCTCATCAGGTAGG -3'	ChAT: 222 bp	NM_020986.4, NM_001142934.2, NM_020984.4, NM_020549.5, and NM_020985.4	Human
ChAT	5'-AGGGCAGCCTCTCTGTATGA -3'	5'-ATCCTCGTTGGACGCCATTT -3'	ChAT: 241 bp	NM_009891.2	Mouse
BChE	5'-ATCCTCCAAACTTCCGTGGC -3'	5'-GAATCCTGCTTTCCACTCCCA -3'	BChE: 370 bp	NM_000055.4	Human
BChE	5'-GATTTTGCCAGTCCATCATGT-3'	5'-CTAAACTTCGTGCTCCCCAA-3'	BChE: 116 bp	NM_009738	Mouse

VAChT	5’-GACTGTAGAGGCGAACATGAC-3’	5’-CTGCTAGTGAACCCCTTGAG-3’	VAChT: 96 bp	NM_003055	Human
VAChT	5’-GACACTGCCATAGACTGATACG-3’	5’-CTTAGTGGTCTCGCTCTGC-3’	VAChT: 96 bp	NM_021712	Mouse
ChT	5’-CATGTCTGCCTCTTCTGTAGTC-3’	5’-CCATCCCAGCCATACTCAT-3’	ChT: 101 bp	NM_021815	Human
ChT	5’-ACCAGAGCCCATACACAGT-3’	5’-CTACCAGCTTTCCTTCAGACA-3’	ChT: 131 bp	NM_022025	Mouse
Tbp	5’-CAGCAACTTCCTCAATTCCTTG-3’	5’-GCTGTTTAACTTCGCTTCCG-3’	Tbp: 104 bp	NM_003194	Human
Tbp	5’-CCAGAACTGAAAATCAACGCAG-3’	5’-TGTATCTACCGTGAATCTTGGC-3’	Tbp: 147 bp	NM_013684	Mouse
OCTN1	5’-GCCACTGTTTGCTTACTTCATC-3’	5-CTTCAGCCTCTCTAAATCTTCTCT-3’	OCTN1: 146 bp	NM_003059	Human
OCTN1	5’-TCTTCCTGTCCACCATCGT-3’	5’-CTTCCTGCCAAACCTGTCT-3’	OCTN1: 143 bp	NM_019687	Mouse

CTL2	5’-GCACCACCCCTCAATTATTACTG-3’	5-ACATGCCATAGACGCTGAA-3’	CTL2: 94 bp	NM_020428	Human
CTL2	5’-GATCAGAATTGTGCAAGATACAGC-3’	5’-CATGCCATAGACGCTGAAGA-3’	CTL2: 115 bp	NM_152808	Mouse

The primers in this table were designed and made by Integrated DNA Technology (IDT). IDT tested and validated these primers as well. However, we still evaluated the primer efficiency.

2.8 Protein Extraction

The protocol for protein extraction was adapted from Thermo Fisher's protocol that came with their RIPA Lysis and Extraction buffer (catalog # 89900). The tissues (thymus, spleen, and brain that was used as a positive control) were first rinsed 3 times with cold 1× PBS and transferred to a tube containing 1 mL of RIPA buffer (150 mM NaCl, 1% Triton X-100, 0.1% SDS, 0.5% Na Deoxycholate, 50 mM Tris and 1 Roche cOmplete Protease Inhibitor Cocktail Tablet (LOT 19987900) per 10 mL) was added and the tissue was homogenized by using a rotor stator. For the cells, 1 mL of 1× PBS was added to the pellet and the cells were subsequently centrifuged at 450 × g for 5 minutes at 4 °C. The supernatant was decanted and approximately 300 µL of RIPA buffer was added. The cells were lysed by pipetting up and down multiple times. The cell or tissue homogenate were kept on ice for 10 minutes while shaking the tube frequently. To isolate the proteins in the supernatant, the tissue homogenate was centrifuged at 12,000 rpm at 4°C for 20 min and the cell homogenate was centrifuged at 10,000 rpm for 10 min at 4°C. After the centrifugation, the supernatant was transferred to a new 1.5 mL tube and was stored at -80°C until ready to quantify the protein concentration.

2.9 BCA Assay

For the BCA assay, the Pierce™ BCA Protein Assay Kit (Thermo Scientific, catalog # PI23225) was utilized and the manufacturer's microplate protocol was followed. The diluent used was 1× PBS and RIPA buffer was used for the protein blanks since it was the buffer in which the proteins were stored and extracted. The plate was analyzed in the plate

reader (BioTek PowerWave XS, serial # 198303) which measured the absorbance at a 562 nm wavelength for each well of the plate by using the Gen5 (v2.00) software.

2.10 Western Blots

Since this study does not include a comparative analysis, no reference gene was used. The scope of this study was only to detect the presence of the cholinergic proteins and not to compare expression levels between the different tissues.

The western blot protocol was adapted from Bio-Rad's protocol. First, the protein samples were prepared by adding a certain amount of protein (Table 2), a volume of loading buffer required to make a sample of 1× loading buffer (Bio-Rad's 2× Laemmli sample buffer, catalog #1610737 or Alfa Aesar's Laemmli SDS Sample Buffer, reducing (4×)) and some RIPA buffer to the desired final volume (if necessary). However, before the loading buffer was added, a fresh solution containing 50 µL of β-mercaptoethanol for every 950 µL of 2× Laemmli sample buffer was freshly made (this step was only necessary if the Bio-Rad's 2× Laemmli sample buffer was used as the 4× Laemmli buffer already contained a reducing agent). Once each protein sample was made, they were heated at 95°C for 5 to 10 minutes. The protein samples were then quickly centrifuged to capture the condensed vapors at the bottom of the tube. Once the protein gel electrophoresis apparatus was set up, the comb was removed from the gel so that 10 µL of each sample could be loaded into each well. The gels that were used were the precast Bio-Rad protein gels (4–15% Mini-PROTEAN® TGX Stain-Free™ Protein Gels, 12 well, 20 µl, catalog # 4568085) and the running buffer used was a 1× solution diluted from the 10× Tris/Glycine/SDS, catalog # 1610732 from Bio-Rad or the Pierce™ 10× Tris-Glycine SDS Buffer, catalog# 28362. The

gel was run at 110 V for approximately one hour or until the ladder (Precision Plus Protein™ All Blue Prestained Protein Standards from Bio-Rad, catalog # 1610373 or BLUeye Prestained Protein ladder from FroggaBio, catalog # PM007-0500) was clearly separated. After the gel finished running, the protein separation was verified by exposing the gel to UV transillumination on Bio-Rad's ChemiDoc MP Imaging System (serial # 733BR 2507) which interacts with Bio-Rad's stain free gel to allow visualization (Figure 2).

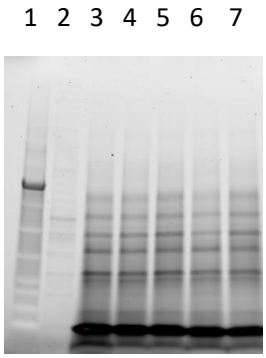

Figure 2: Protein Separation after SDS-PAGE Electrophoresis

This figure is an image of successfully separated proteins captured on the ChemiDoc MP using the Stain Free Gel imaging option. Lane number one contains the ladder, lane number two contains a brain lysate, and the rest of the lane contains BM samples. Should the proteins demonstrate unsuccessful separation, the experiment would be ceased.

Once the gels have been visualized, the PVDF (Polyvinylidene fluoride or polyvinylidene difluoride) membrane (Bio-Rad's Immun-Blot LF PVDF Membrane Roll, catalog # 1620264) can be activated for the wet transfer with pure methanol and the gel, the filter papers as well as the sponges were soaked in 1× transfer buffer (25 mM Tris, 192 mM glycine and 20% methanol). After presoaking all these elements of the wet transfer system (including the activated membrane) in the 1× transfer buffer, the sandwich in the cassette was assembled by placing the presoaked sponge on the black side of the cassette followed by two filter papers, the gel, the activated membrane, two filter papers, and a sponge. At this

point, the cassette was closed and properly placed into the wet transfer tank. This wet transfer tank was placed in an ice bucket on top of a stir plate. There was also an ice pack inside the tank to prevent overheating. Once the apparatus was properly set up and connected to the power pack, the transfer was powered at 100V for 1 hour.

Following the transfer, the membranes were visualized to assess transfer efficiency by exposing the membrane to UV transillumination on the Bio-Rad's ChemiDoc MP (serial # 733BR 2507) Imaging System (Figure 3). If the transfer was successful, the membrane was placed in a blocking buffer (5% Blotting-grade Blocker from Bio-Rad, catalog # 170-6404 diluted in TBST) for one hour to one hour and a half on a belly dancer at room temperature. During the incubation, the primary antibody solution was prepared in a blocking buffer (see Table 2 for concentrations of the primary antibody used). Once the membrane was blocked in the blocking buffer, it was incubated overnight at 4°C on a rocker.

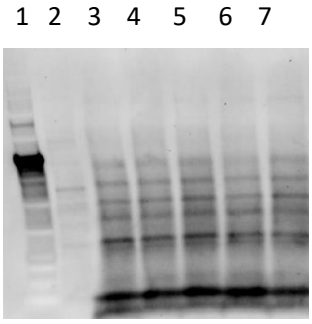

Figure 3: Proteins Transferred on the PVDF Membrane after Wet Transfer

This figure is an image of the transferred proteins from the gel in Figure 2. The image was captured on the ChemiDoc MP using the Stain Free Blot option. If the proteins were not successfully transferred, the experiment would have been ceased. Lane number one contains the ladder, lane number two contains a brain lysate, and the rest of the lanes contain BM lysates.

The next day, the membranes were washed three times in TBST (0.1% of Tween added to 1× Tris buffered saline (TBS) solution prepared from Fisher BioReagents 10× TBS solution from Fisher Scientific, catalog # BP24711) for five minutes and once in 1× TBS (prepared from Fisher BioReagents 10× TBS solution from Fisher Scientific, catalog # BP24711) for 10 minutes. Then,1/30,000 of secondary antibody (abcam, Goat Anti-Rabbit IgG H&L (HRP), code: ab97051) solution for the primary antibodies with a rabbit host was used or 1/3000 of secondary antibody (abcam, Rabbit Anti-Chicken IgY H&L (HRP), code: ab6753) solution for the primary antibody with a chicken host was used. These secondary antibody solutions were diluted in blocking buffer. Once the secondary antibody solution was made, the membrane incubated in this solution for one hour at room temperature on the belly dancer. After the hour had passed, three additional five-minute washes in TBST and one ten-minute wash in 1× TBS was completed. Finally, the enhanced chemiluminescence (ECL from Bio-Rad, Clarity Western ECL Substrate, 500 mL, catalog # 1705061 or Thermo Scientific's SuperSignal™ West Femto Maximum Sensitivity Substrate, catalog # 34094) reagent was added by adding equal portions of each solution, which reacts with the HRP that was conjugated to the secondary antibody. After this step, the membrane was visualized on the Bio-Rad's ChemiDoc MP Imaging System under the Chemiluminescent blot option with the auto-rapid or auto-optimal exposure.

Table 2: Quantity of Protein Used per Well and Information on the Antibodies Used for Western Blots

Protein	**Quantity of Protein in (µg) per 10 µL well**	**Target Species in Western Blot**	**Concentration of Primary Antibody**	**Description**	**Code on abcam/Catalog Number on Fisher Scientific**
AChE	10	Mouse and human	1/1000	Rabbit polyclonal to Acetylcholinesterase	Ab93487
ChAT	15	Mouse	1/1000	Rabbit monoclonal [EPR16590] to Choline Acetyltransferase	Ab178850
ChAT	20	Mouse	1/250	Chicken Polyclonal Anti-Choline Acetyltransferase antibody (ab34419)	Ab34419
ChAT	20	Human	1/2000	Rabbit Polyclonal Anti-Choline Acetyltransferase antibody (ab223346)	Ab223346
ChAT	15	Human	1/1000	Rabbit Polyclonal Anti-Choline Acetyltransferase antibody (ab137349)	Ab137349
BChE	10	Mouse	1/3000	Rabbit polyclonal to Butyrylcholinesterase	Ab154763
VAChT	Maximum quantity of protein (9-46 µg)		2.4 µg/mL	VAChT Rabbit anti-Human, Mouse, Rat, Polyclonal, Invitrogen™	OSV00002G
ChT	Maximum quantity	Mouse and Human	1.0 µg/mL	Rabbit polyclonal to SLC5A7	Ab56074

	of protein (9-46 μg)				

2.10 Preparation of ICC Slides

The slides were prepared by following an adapted version of BD Biosciences' ICC protocol. More specifically, we adapted their Adhesion Method of preparing slides. After counting the freshly isolated cells, the cells were diluted with 1 × PBS to a concentration of 5 million cells per mL. All Superfrost positively charged slides were labeled and wells were made with a white wax pen and an Immedge pen (Vector Laboratories' ImmEdge^{TM} Pen, Hydrophobic Barrier Pen, catalog # VECTH4000). These wells encourage the liquid to stay in a specific spot on the slide. The slides were then washed with 1 × PBS for 5 minutes. Afterwards, the slides were placed in a humidified chamber. With a repeater pipette, 50 µL of the 5 million per mL cell solution was added to each well of the slides. Once the cell suspension was added to each well, they were incubated at room temperature for 20 minutes to allow cells to adhere to the slide. Then, a 4% PFA solution in PBS (Alfa Aesar's Agarose Gel Loading Dye (6×, Alkaline), catalog # J62157) was added. These slides incubated for 15-20 minutes to fix cells. The slides were washed 3 times with 1 × PBS in a staining tray for 5 minutes at room temperature for each wash and the staining tray was placed on belly dancer during these washes. Finally, the slides were rinsed in a staining tray containing tap water and air dried for approximately 45 minutes at room temperature. The slides were then stored at -80°C until needed for downstream ICC staining.

2.11 ICC Staining, Imaging, and Analysis

The manufacturer's protocol of the TSA kit from Biotium (catalog #33001) was adapted. To begin, the slides were equilibrated at RT and observed under the microscope to make sure cells are present. Cells adhered to the slides were then permeabilized with permeabilization buffer (0.3% saponin in 1 × PBS) at room temperature for 15 minutes. Then, the slides were rinsed 3 times with 1 × PBS. In addition, the activity of endogenous peroxidases (which may cause high background) were quenched by incubating the sample with peroxidase quenching buffer (0.3% (w/w) H_2O_2 and 0.1% (w/w) NaN_3 in 1 × PBS) for 20 minutes at room temperature. The slides were then rinsed 3 times with 1 × PBS followed by an incubation with blocking buffer (5mL of Goat Serum Albumin in 100 mL of 1 × PBS with 0.3% saponin) for 1 hour at room temperature. The primary antibody was then added (Table 3) to each sample on the slides and incubated for 1 hour or 4°C overnight in a humidified chamber. After the incubation, the samples were washed 3 times with 1 × PBSS (0.1% of saponin in 1× PBS) and each wash was incubated at room temperature for 5 minutes. A secondary antibody cocktail solution (Table 4) was made with blocking buffer and the samples were incubated with this solution at room temperature for 1 hour. Following the incubation, the samples were washed 3 times with 1 × PBSS and each wash was incubated at room temperature for 5 minutes. Then, the samples were washed 3 times with 1 × PBS and each wash was incubated at room temperature for 5 minutes. After the washes, the staining solution was prepared by diluting the CF® Dye or biotinXX tyramide stock solution 1:500 in the Tyramide Amplification buffer (components found in TSA kit from Biotium catalog #33001) according to the manufacturer's protocol (see protocol of TSA kit from Biotium catalog #33001). These samples were then incubated for 10 minutes at room

temperature. After the incubation, the samples were washed 3 times with 1 × PBS for 5 minutes at room temperature for each wash. Finally, the mounting media containing DAPI (Invitrogen™ ProLong™ Diamond Antifade Mountant with DAPI from ThermoFisher Scientific, catalog # P36962) was added and the coverslips were mounted. The mounting media was cured for up to 24 hours before imaging on BioTek's Cytation 5 Imager (serial # 190 509A). Images were taken at a magnification of 40X on the imager of the Gen5 Software (v3.06).

Semi-quantitative analysis was performed on the Gen5 Prime Software (v3.10) by taking montaged images in each well to prevent biases. For each sample, a total of 40 images were taken at a 20X magnification for each filter (GFP, Texas Red, DAPI, and phase contrast). Each image within the montage was spaced anywhere from 150 µm to 400 µm (depending on the size of the well that was drawn). Images only containing artifacts were masked and therefore excluded in the analysis. Once, the montaged images were obtained, an automated cell count was completed by first stitching the montage images, followed by using many sets of conditions containing fluorescence thresholds in conjunction with a cell area maximum. As a result, many sets of conditions were created to count for cells that do not fluoresce in green nor red, cells only fluorescing in green (ChAT only), cells only fluorescing in red/orange (cell surface marker only), and cells expressing colocalization (cell surface marker and ChAT). For each experimental well, prior to setting up the conditions for the cell count of the entire montage, an analysis on one of the images was conducted to determine the optimal fluorescence thresholds. Therefore, each well had slightly different fluorescence threshold values for each filter in every set of conditions. This preliminary analysis was important to control for experimental and sample differences. Prior to

automatically counting the cells, it was also important to make sure that the automated count was reliable by initially counting the cells manually for approximately 4 images and comparing this count with its automated count for every set of conditions. Since the counts were nearly the same, the software's automated count was deemed reliable after that initial comparative analysis.

Table 3: Information on the Primary Antibodies Used for ICC on Murine and Human Samples

Name	Target Protein	Target Specie	Host and Isotype	Concentration of Antibody Used	Clonality	Catalog Number
Anti-Choline Acetyltransferase antibody	ChAT	Human	Rabbit, IgG	1/500	Polyclonal	Ab137349
Recombinant Anti-Choline Acetyltransferase antibody	ChAT	Mouse	Rabbit, IgG	1/500	Monoclonal (clone: EPR16590)	Ab178850
Purified anti-mouse/human CD11b Antibody	CD11b	Human/ Mouse	Rat, IgG2b, κ	1/100	Monoclonal (clone: M1/70)	101202 (BLG)
Purified anti-mouse CD19 Antibody	CD19	Mouse	Rat, IgG2a, κ	1/200	Monoclonal (clone: 6D5)	115501 (BLG)
Purified anti-human CD19 Antibody	CD19	Human	Mouse, IgG1, κ	1/100	Monoclonal (clone: HIB19)	302201 (BLG)
Purified anti-mouse CD4 Antibody	CD4	Mouse	Rat, IgG2b, κ	1/100	Monoclonal (clone: GK1.5)	100401 (BLG)
Purified anti-human CD4 Antibody	CD4	Human	Mouse, IgG1, κ	1/67	Monoclonal (clone: RPA-T4)	300501 (BLG)
Purified anti-mouse CD8b Antibody	CD8b	Mouse	Rat IgG2b, κ	1/200	Monoclonal (clone: YTS156.7.7)	126602 (BLG)

Purified anti-human CD8a Antibody	CD8a	Human	Mouse IgG1, κ	1/67	Monoclonal (clone: C8/144B)	372902 (BLG)
Purified anti-mouse CD105 Antibody	CD105	Mouse	Mouse IgG2a, κ	1/100	Monoclonal (clone: MJ7/18)	120401 (BLG)

Table 4: Information on the Secondary Antibodies Used for ICC on Murine and Human Samples

Name	**Target Specie**	**Concentration of Antibody Used**	**Host and Isotype**	**Clonality**	**Catalog Number**
Alexa Fluor® 594 Goat anti-mouse IgG (minimal x-reactivity) Antibody	Mouse	1/250	Goat, IgG	Polyclonal (clone: Poly4053)	405326 (BLG)
Alexa Fluor® 594 Goat anti-rat IgG (minimal x-reactivity) Antibody	Rat	1/100	Goat, IgG	Polyclonal (clone: Poly4054)	405422 (BLG)
HRP Goat Anti-Rabbit IgG (H+L), Highly Cross-Adsorbed	Rabbit	1/200	Goat, IgG	Polyclonal	20403 (biotium)

2.12 Liquid Chromatography/Mass Spectrometry

All reagents used for Liquid Chromatography/MS were LC/MS grade. For MS sample preparation on cells, the protocol was adapted from a paper written by Zhang et al.[88] To prepare cells for MS analysis the cells were first collected through centrifugation and 100 µL of 0.1% Formic acid in water was added to the isolated cells. Then, the cells were vortexed for 30 seconds and homogenized with a rotor stator for 30 seconds. Afterwards, 300 µL of Acetonitrile was added and vortexed for 30 seconds. The homogenate was then centrifuged at 16100 × g, 4°C for 10 minutes. Subsequently, the supernatant was collected and centrifuge again at 16100 × g, 4°C for 10 minutes. This final supernatant was then added to a clean microcentrifuge tube and placed in an insert at Perdu Central Analytical Facility (PCAF).

For MS sample preparation on tissues, the protocol was adapted from a paper written by Wang et al.[89] To prepare tissues for MS, every 30 mg of tissue was homogenized in 300 µL of 2% Formic Acid in water with a rotor stator and vortexed for 30 seconds. Then, 2 mL 75:25 acetonitrile:methanol was added, vortexed for 30 seconds, and centrifuged at 16100 × g, at 4°C for 10 minutes. This supernatant collected from this centrifugation was centrifuged again at 16100 × g, at 4°C for 10 minutes. The tissue was subsequently dried with a SpeedVac Vacuum Concentrator attached to a cold trap and then re-dissolved in 300 µL of Acetonitrile. Then the sample was vortexed for 30 seconds centrifuged at 16100 × g, at 4°C for 10 minutes. Supernatant collected was centrifuged again at 16100 × g, at 4°C for 10 minutes and the resulting supernatant was transferred to a clean microcentrifuge tube. This liquid was then placed in an insert at the Perdu Central Analytical Facility (PCAF).

At the PCAF, a 10 ppb ACh standard solution was made as the positive control and Acetonitrile was used as a negative control. An Ultra-High-Pressure Liquid Chromatography coupled with Triple-Quadrupole MS system was used.

As for the liquid chromatographic conditions of the Water's H Class Plus Ultra-high pressure liquid chromatography system with a flow through needle autosampler and quaternary pump modules, a Water's ACQUITY UPLC BEH Amide Column was used at a flow rate of 0.5 mL/min and a column temperature of 45°C. The sample temperature was at 4°C and the injection volume was 5 µL. The aqueous mobile phase that was used was 100 mM Ammonium Formate solution and the organic mobile phase that was used was Acetonitrile. To elute the molecules with similar chemical properties as ACh, a gradient elution system was used (Table 5).

Table 5: Gradient Elution Information

Time	**Flow Rate (mL/min)**	**% of 100 mM Ammonium Formate**	**% of Acetonitrile**
Initial	0.5	1	99
1	0.5	1	99
1.5	0.5	10	90
3	0.5	40	60
3.5	0.5	70	30
4	0.5	70	30
4.25	0.5	1	99
5	0.5	1	99

As for the mass spectrometric conditions, a Water's Xevo TQ-S micro was the triple-quadrupole mass spectrometer used for these experiments. A cone voltage of 25 V and a capillary voltage of 2 kV was used. The collision gas used was argon for an ES+ ionization mode and the acquisition mode used was Multiple Reaction Monitoring (MRM). The desolvation temperature was 550 °C and the desolvation gas flow was 900 L/hr. The cone

gas flow was 150 L/hour and the source temperature was 150 °C. Finally, the collision voltage was 12 V and a transition of 146.0-87.05 m/z was used. Waters MassLynx™ Software (v4.2) was used to acquire the MS and UPLC data.

2.13 Bone Marrow Derived Macrophage (BMDM) Isolation and Culture

The BM cells were isolated as described in section 2.1 of the Materials and Methods using RPMI media with 10% FBS in conjunction with 1% penicillin/streptomycin (complete media) to flush the tibia and femur and to resuspend the cells for the cell count.

After the cell count, the cells were resuspended in complete media to have 1.0×10^6 cells/mL solution supplemented with 10 ng/mL of recombinant human macrophage colony-stimulating factor (M-CSF) (Sigma-Aldrich, catalog # SRP3110). Then, the cells were seeded by adding 1 mL of the cell suspension solution to each required well of the non-tissue culture treated 12-well plate. For each n value, one plate was required for the M1 polarization of BMDMs and one plate was required for the M2 polarization of BMDMs. Cells were cultured with complete RPMI supplemented with 10 ng/ml M CSF for 3 days in a humidified incubator at 37°C and 5% CO_2. On day 3, the cells were polarized into M1 and M2 cells by supplementing each well with media containing the appropriate polarizing reagents. The BMDMs were polarized into M1 with 50 pg/mL of lipopolysaccharide (LPS), 10 ng/mL of IFNγ and 10 ng/mL of M-CSF. M2 cells however were polarized with 20 ng/mL of IL-4, 20 ng/mL of IL-13, and 10 ng/mL of M-CSF. The cells were then placed into a humidified incubator at 37°C and 5% CO_2 for another 3 days. On day 6 of culture, 1

mL of the cell culture supernatant was discarded by pipetting. Then, the cells were treated with appropriate agonist and/or inhibitor (Table 6) and 100 ng/ml LPS for 5 hours in a humidified incubator at 37°C and 5% CO_2. After the incubation, the plates were centrifuged at 500 × g for 8 minutes at 4 °C and the supernatant was harvested for cytometric bead array (CBA) assay.

Table 6: BMDM Culture Conditions

Name of Condition	Constituent(s)
No Treatment	• Nothing was added to this well on day 6
LPS Only	• 100 ng/mL of LPS
LPS + Ch	• 100 ng/mL of LPS • 100 µM of Ch[90,91]
LPS + ACh	• 100 ng/mL of LPS • 100 µM of ACh[92–96]
LPS + ACh + Galantamine (AChE Inhibitor)	• 100 ng/mL of LPS • 100 µM of ACh[92–96] • 10 µM of Galantamine[97]
LPS + Galantamine (AChE Inhibitor)	• 100 ng/mL of LPS • 10 µM of Galantamine[97]
LPS + BrACh (ChAT Inhibitor)	• 100 ng/mL of LPS • 100 µM of BrACh[16,98]
LPS + α-Neta (ChAT Inhibitor)	• 100 ng/mL of LPS • 5 µM of α-Neta[99]
LPS + ML 352 (Ch transporter inhibitor)	• 100 ng/mL of LPS • 10 µM of ML 352[100]
Total Release	• Nothing was added to this well on day 6.
Culture Media	• Nothing was added to this well on day 6.

2.14 Cytometric Bead Array (CBA)

The CBA Flex Set for IL-6, IL-10, and TNF were used herein (Table 7) and the manufacturer's protocol from BD's CBA Flex Sets was adapted. To begin, the standards were made by first reconstituting and serially diluting the standards 2 times in assay diluent. To prepare these standards, vials of lyophilized standards (TNF, IL-6, and IL-10) from each BD CBA Mouse Flex Set were added to 4 mL of assay diluent in a 15 mL polypropylene tube to make the top standard. The top standard was then serially diluted 2 times in the following order: 1:2, 1:4, 1:8, 1:16, 1:32, 1:64, 1:128, and 1:256 with assay diluent. One standard containing only the assay diluent was used as a blank. A volume of 25 µL samples or standard to each well of 96-well v-bottom plate. For samples used to assess IL-6 and TNF levels, the samples were diluted 10 times in 1× PBS within each well whereas samples were not diluted 10 times for IL-10. Then, 25 µL of 1× PBS + Cytokine beads Master Mix (for each well, 0.5 µL of each cytokine bead was added and diluted 1× PBS to be able to add 25 µL to each well) was added to each sample and standard. The plate was shortly placed on a plate shaker and then incubated for 1 hour at room temperature in the dark. Then, 25 µL of Detection Reagents with 1× PBS (for each well, 0.5 µL of each Detection Reagent was added and diluted in 1× PBS to be able to add 25 µL to each well) was added to each well. The plate was shortly placed on a plate shaker and then incubated for 1 hour at room temperature in the dark. Then, 100 µL of 1× PBS was added to each well to wash and centrifuged at 230 × g for 5 minutes at 4°C (acceleration & deceleration: 5). The supernatant was subsequently removed by inverting the plate and another 100 µL of 1× PBS was added to each well to resuspend the pellet. Each resuspended pellet was transferred to a FACS tube and ran on the BD FACSCanto II flow cytometer with the BD FACS Diva

Software (v6.13) whereby approximately 1500 events were recorded per tube. The voltages used were 400 V for FSC, 385 V for SSC, 475 V for PE, 490 V for APC, and 470 V for APC-Cy7. The data from the flow cytometer was extrapolated using the FCAP Array Software (v3.0).

Table 7: CBA Flex Set Information

Cytokine of Mouse CBA Flex Set	**Catalog Number on BD Biosciences**
TNF	558299
IL-6	558301
IL-10	558300

2.15 Cytotoxicity Test

The Invitrogen™ CyQUANT™ LDH Cytotoxicity Assay, fluorescence from Thermo Fisher Scientific (catalog # C20302) was used to assess, the cytotoxicity of the BMDM supernatant samples from section 2.14. The manufacturer's protocol was used whereby complete media from day 6 of culture was used as a negative control and a total release control (where the cells in a no treatment well were put through a freeze/thaw cycle to purposely lyse the cells) was used as a positive control. BioTek's Cytation 5 plate reader (serial # 190 509A) was used and the data was acquired on the Gen5 Software (v3.10).

2.16 Statistical Analysis

As the PCRs, the western blots, MS, and the ICC experiments were not used to compare expression levels between the different tissues, no statistical tests were necessary for this study. Therefore, the standard error's mean (SEM) will suffice for MS results and the data from the qPCR thermal cycler will be presented akin to standard PCR results.

The data from the LDH assay and the CBAs of IL-10 for M1 polarized BMDMs was analyzed with a repeated measures one-way ANOVA against the LPS Only group. Dunnett's multiple comparisons test was used and $p \leq 0.05$ was considered statistically significant. The statistical analysis was conducted on GraphPad Prism 8.4.1 software.

Results

3.0 Expression of Cholinergic Genes in Immune Tissues

The first step in determining the role of ACh production within immune cells entails assessing the expression of cholinergic genes in immune tissues. To assess the expression of these genes, SYBR Green qPCR was used whereby this technique was not optimized for quantification but was only used to determine whether the transcripts of interest were present. A no-RT and NTC was used to control for genomic DNA and environmental DNA contaminations, respectively. These controls had Cq values of more than 35 cycles or had a Cq value that was 10 cycles or higher than positive samples. Tbp was used as a positive control to make sure the PCR technique was working properly. As neuronal tissues are commonly known to express cholinergic machinery, the brain was used as a positive control for murine tissues. According to the PCR data in Figure 4A, each murine primer generated a band specific to the PCR product of interest. Therefore, each set of murine primers seem to work properly as they appear to be specific to its target gene. Among murine immune tissues, it seems that for some cholinergic genes such as ChAT, ChT, and VAChT, the Cq values were around or above 30 cycles. Within the BM (Figure 4E), BChE also had a Cq value slightly above 30 cycles suggesting faint expression. To verify the specificity of the PCR products, we ran the PCR products on a gel and found that when the Cq values were around or above 30 cycles, the PCR product became increasingly non-specific. In fact, for ChAT, ChT, and VAChT the presence of a smear or of multiple bands suggest non-specific amplification (Figures 4C-E). Moreover, for BChE within the BM, there are multiple bands present which suggest non-specific amplification. However, in the spleen and thymus, BChE

had a Cq value lower than 30 cycles in conjunction with one clear band at the predicted band size, suggesting specific amplification. Among murine tissues (the spleen, thymus, and BM) in Figure 4, it seems that AChE, Tbp, CTL2, and OCTN1 were specifically expressed in all murine tissues. Collectively, our data therefore show that some cholinergic genes (OCTN1, CTL2, BChE and AChE) were specifically expressed in most immune tissues while the expression of ChAT, ChT, and VAChT in these tissues, was negative or inconclusive.

In regard to human PBMCs, we did not have a human neuronal tissue as a positive control. Therefore, we were unable to validate whether the human primers were specific for most human sets of primers. However, we used M0 differentiated U937 cell lines, a human monocytic cell line as a positive control sample for the human ChAT primers. These cell lines were cultured, differentiated, and its RNA was isolated by Danika Roy, another master's student in the Simard lab. According to Figure 4B, the presence of a single band at the expected molecular weight suggests that the human ChAT primers specifically amplified ChAT cDNA. Within human PBMCs, the Cq values of ChAT, AChE, ChT, VAChT, and BChE were above 30 cycles, suggesting little to no expression of these genes whereas OCTN1 and CTL2 had Cq values below 30 cycles suggesting higher expression of these transcripts. Accordingly, we ran the PCR product on a gel to assess the specificity of the PCR product and it seems that when the Cq values were above 30 cycles, the bands were either fainter or the specificity of the PCR product diminished, rendering some of these results less clear. More specifically, BChE and ChAT did not seem to be expressed. However, even though ChT and VAChT had Cq values above 30 cycles, they expressed a faint band at the expected band size suggesting that VAChT and ChT were expressed in human PBMCs. As for AChE, according to the Cq value in Figure 4F, it seems that AChE

was expressed in human PBMCs. Although, according to image of the gel in Figure 4F, it seems that such amplification was non-specific which renders the expression of AChE in human PBMCs unclear at the transcript level. Conversely, for CTL2, OCTN1, and tbp, who had Cq values were below 30 cycles, the PCR product seemed to be specific as a single clear band at the predicted molecular weight was present. Overall, in human PBMCs, it seems that CTL2, OCTN1, ChT, and VAChT were expressed whereas, the expression for ChAT, AChE, and BChE is either negative or inconclusive.

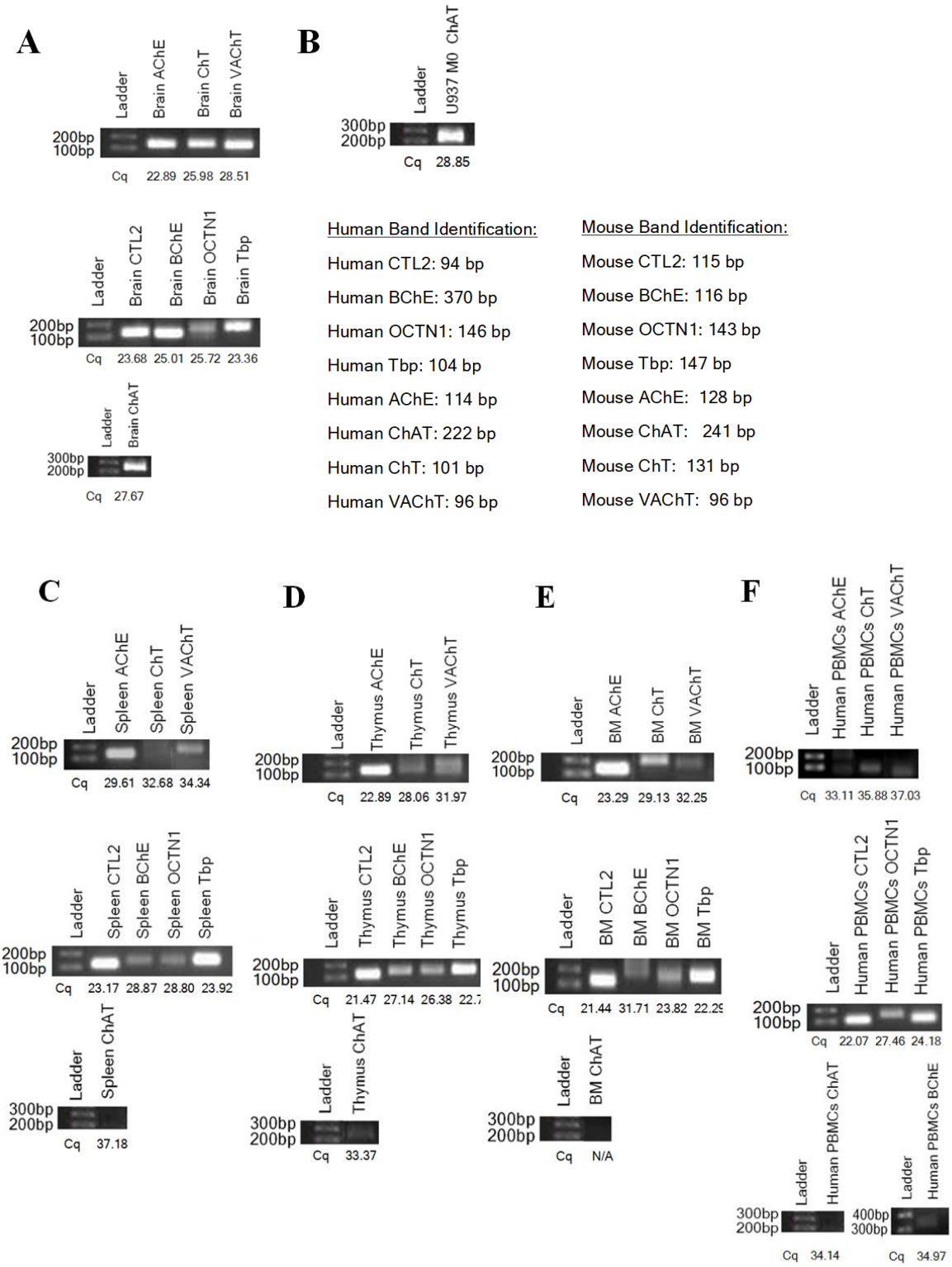

Figure 4: Data from PCRs of Cholinergic Genes

The expression of cholinergic genes (ChAT, AChE, BChE, ChT, VAChT, CTL2, and OCTN1) in murine spleen, bone marrow and thymus, and in human PBMCs, were assessed by PCR. The cholinergic genes were first assessed in each immune tissue (n = 6-8) on a qPCR thermal cycler and then one representative sample from each immune tissue was run on a 1% agarose gel for every gene of interest. All the data in this figure was acquired from Bio-Rad's CFX Connect thermal cycler (a qPCR thermal cycler) whereby the PCR product was visualized on the gel with the ChemiDoc XRS. Images of these gels are shown in Figure 4A-4F. Overall, it seems that some key cholinergic genes such as ChAT were being expressed at a Cq value above or around 27 cycles and the specificity of their PCR product seemed to diminish as the Cq value surpassed 30 cycles, rendering some of the PCR data inconclusive. Tbp was used as a positive control to ensure that the PCR reaction worked properly. Figure 4A shows some PCR data (n = 1) of the cholinergic genes in the murine brain, a positive control for mouse tissues. Figure 4B contains PCR results for M0 differentiated U937 human monocytic cell lines whereby the RNA was obtained from Danika Roy, a master's student in our lab. This sample was used to demonstrate that the human ChAT primers do specifically amplify ChAT. A no-RT and NTC was used to control for genomic DNA and environmental DNA contaminations, respectively. These controls had Cq values of more than 35 cycles or had a Cq value that was approximately 10 cycles or higher than its positive control. Taken together, in the mouse tissues (the thymus, spleen, and BM), AChE, CTL2, ChT, VAChT, and OCTN1 were expressed but the expression of ChAT was only shown in the thymus. In human PBMCs, CTL2, OCTN1, ChT, and VAChT were expressed whereas, the expression for ChAT, AChE, and BChE were unclear or negative.

3.1 Expression of Cholinergic Proteins in Immune Tissues

Western blot experiments were completed to assess the presence of cholinergic proteins such as ChAT, ChT, and AChE. First, we assessed the expression of ChAT proteins in murine immune tissues (the murine spleen, thymus, and BM) by western blot (Figure 5). The arrows in Figure 5 show where the theoretical molecular weight would be located on the blot. The theoretical molecular weight of ChAT in murine tissues is 72 kDa which was determined by the protein sequence of ChAT (UniProt accession accession number: Q03059). This molecular weight does not account for any protein modifications such as post-translational modifications. To better assess the presence of ChAT (which is the cholinergic protein of most interest since it synthesizes ACh), two primary antibodies targeting ChAT were used. According to figure 5A, the bands suggested the presence of ChAT in the murine thymus, BM, and spleen. According to Figure 5A, the bands in the murine spleen and Thymus were detected at around 48 kDa and in the murine BM, the band was detected at approximately 100 kDa. For the spleen sample, there was an additional band detected at around 180 kDa. The band in the brain (the positive control) was detected at around 75 kDa which is near the theoretical molecular weight. Altogether, the bands in the immune tissues were of a different molecular weight than the band in the murine brain. Figure 5B depicts the expression of ChAT using a separate primary antibody. According to this figure, the presence of ChAT was further shown for the murine spleen and thymus. However, we were unable to confirm the band for the murine BM as we lacked murine BM sample with a sufficiently high protein concentration for western blots and we suffered many limitations regarding obtaining additional mice. In Figure 5B, it seems that another darker band in the spleen sample was detected at around 60 kDa. With the second primary

antibody depicted in Figure 5B, there were three bands detected for the positive control (the brain), one slightly above 75 kDa, one at 48 kDa and the second at 35 kDa. Overall, it seems that a different molecular weight than the theoretical molecular weight of ChAT was expressed within the murine spleen, thymus, and BM. However, for the murine BM, the results were not as conclusive as for the murine spleen and thymus.

We also evaluated the expression of ChAT in human PBMCs via western blot (Figure 6). In human tissues, the theoretical molecular weight for ChAT is approximately 82.5 kDa according to the sequence of the human ChAT protein (UniProt accession number: P28329). The arrows in Figure 6 indicate where the theoretical molecular weight would be located on the blot. IMR-32, a neuronal cell line was used as a positive control. Figure 6A shows the results for the first primary antibody targeting ChAT and Figure 6B shows the results for the second primary antibody. According to Figure 6A, it seems that the band for human PBMCs and IMR-32 was detected between 35 kDa and 48 kDa. Figure 6A shows that the band for IMR-32 was slightly lower than in the human PBMCs. As for Figure 6B, it seems that the bands for IMR-32 and the human PBMCs were detected at around 35 kDa. Therefore, with the second primary antibody, the band in the human PBMCs and in IMR-32 were at around the same molecular weight. Altogether, it seems that ChAT of a much lower molecular weight than the theoretical molecular weight was expressed within human PBMCs.

Since AChE and ChT play a role in ACh function and will be pharmacologically inhibited in downstream experiments, we assessed their expression at the protein level by western blot. Therefore, the expression of AChE proteins was first assessed via western blots in the murine thymus, murine spleen, murine BM, and human PBMCs (Figure 7). The

theoretical molecular weight of AChE is 68 kDa according to the protein sequence of murine and human AChE (mouse UniProt accession number: P21836, human UniProt accession number: P22303). As shown in Figure 7A, a 75 kDa band was detected in the murine brain (positive control), thymus, spleen, and BM, which is near the theoretical molecular weight of 68 kDa. This suggests that these tissues express AChE. In the murine spleen and thymus, there was also an additional band detected at 180 kDa. For the murine BM, there was an additional band detected slightly above the 75 kDa band. In human PBMCs (Figure 7B), we detected a band for AChE in human PBMCs at around 100 kDa which is much higher than the predicted molecular weight of 68 kDa. No bands were detected in the positive control IMR-32, a human neuronal cell line. Therefore, it seems that AChE was expressed in the murine thymus, spleen, BM, and human PBMCs.

Then, the expression of ChT proteins was assessed in the murine thymus, murine spleen, murine BM, and human PBMCs (Figure 8). The theoretical molecular weight of ChT is approximately 63 kDa according to the sequence of murine and human ChT (mouse UniProt accession number: Q8BGY9, human UniProt accession number: Q9GZV3). The arrows in Figure 8 depicts the approximate location of the theoretical molecular weight. When comparing the bands for the thymus pool sample with the brain sample (Figure 8A), the band detected at approximately 63 kDa was missing. However, the bands at around 75 kDa as well as between 35 KDa and 25 kDa were detected in both the thymus pool sample in conjunction with the brain sample. Figure 8C contains the western blot results for the murine spleen. This figure shows similar results as Figure 8A. Yet, Figure 8C suggests that the spleen did detect that additional band at approximately 63 kDa, the theoretical molecular weight of ChT. In figure 8B and 8D, the western blot results for the human PBMCs and

murine BM are shown respectively. Overall, it seems that human PBMCS and murine BM cells did not express ChT as there were no bands in these samples. However, Figure 8B and 8D do have positive controls with band(s) detected at around 75 kDa for IMR-32, and at 75 kDa, 63kDa, as well as between 25 to 35 kDa for the murine brain. Therefore, it seems that the murine spleen and thymus expressed ChT while human PBMCs and murine BM did not express ChT.

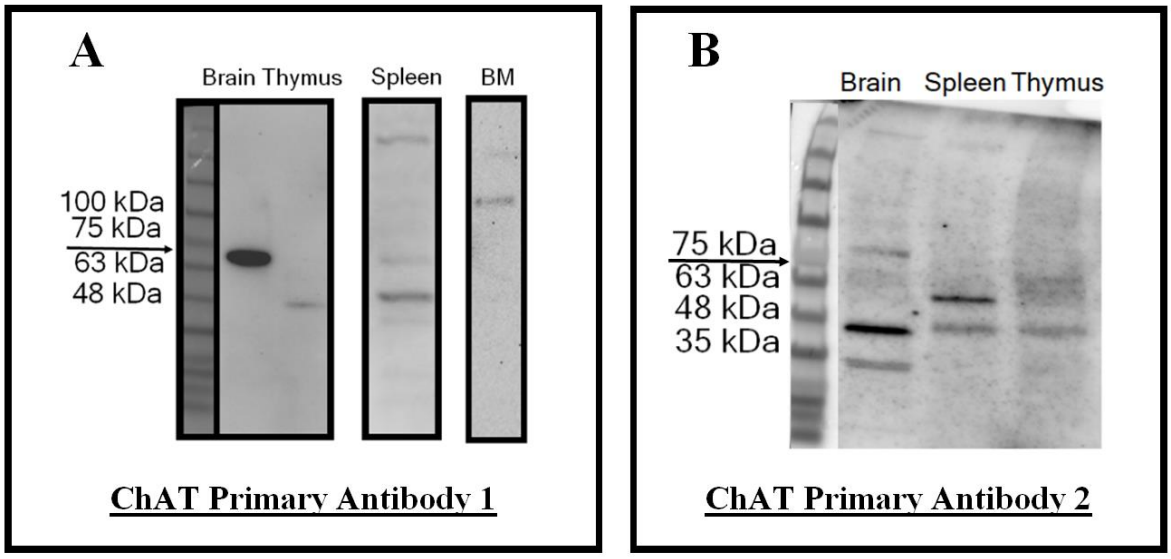

Figure 5: Protein Expression of ChAT in Murine Tissues

The expression of ChAT in protein lysates from the murine spleen, BM, and thymus was assessed by western blots. Each immune tissue lysate shown in this figure consists of a pooled sample from 6 mice. Tissue lysates were added at an equal quantity (15 μg for Figure 5A and 20 μg for Figure 5B). The murine brain was used as a positive control for ChAT. The arrows indicate the location of the theoretical molecular weight on the blot at 72 kDa. These western blot results were auto exposed on the Bio-Rad's ChemiDoc MP Imaging System using chemiluminescence. Taken together, the results in Figure 5 suggest that ChAT of a different molecular weight than the positive control and expected molecular weight was expressed in the murine thymus, spleen, and BM.

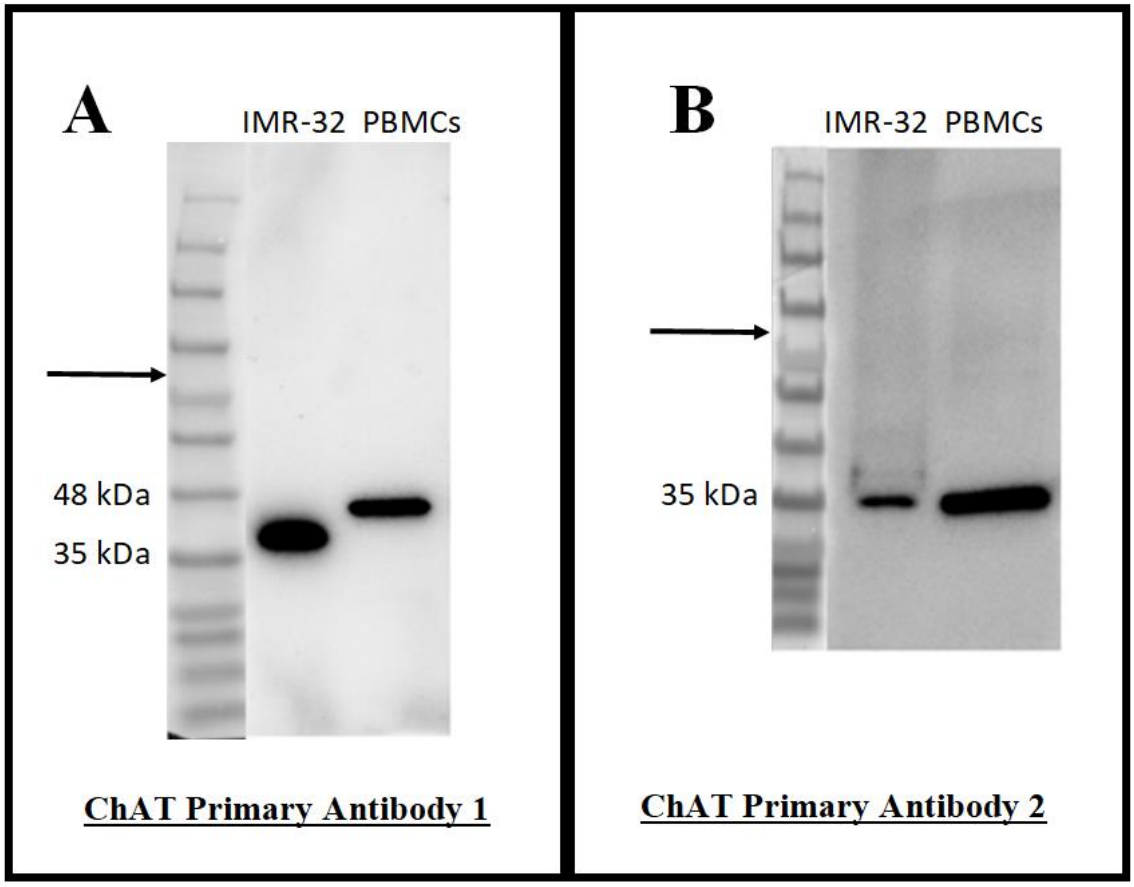

Figure 6: Protein Expression of ChAT in Human PBMCs

The expression of ChAT in protein lysates from human PBMCs was assessed by western blots. Each immune tissue lysate shown in this figure consists of a pooled sample from 6 healthy human participants. Tissue lysates were added at an equal quantity (15 μg for Figure 6A and 20 μg for Figure 6B). A lysate from IMR-32, a human neuronal cell line, was used as a positive control. The arrows indicate the location of the theoretical molecular weight on the blot at 82.5 kDa. The images in Figure 6 were exposed on the ChemiDoc MP Imaging System using chemiluminescence and an auto exposure. Altogether, it seems that the ChAT protein of a different molecular weight than the predicted molecular weight was expressed in human PBMCs.

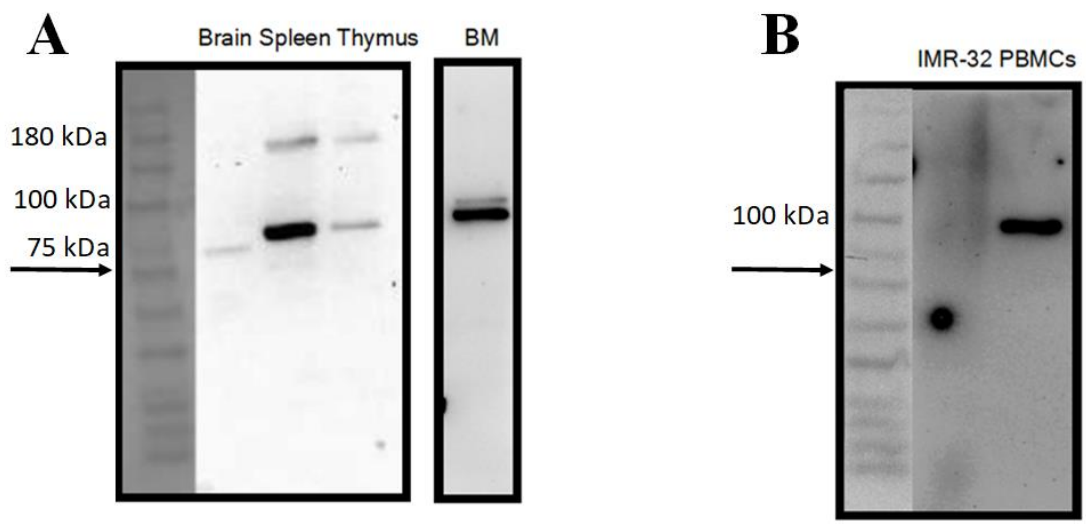

Figure 7: Protein Expression of AChE in Immune Tissues

The expression AChE in protein lysates from the murine thymus, spleen, BM, and human PBMCs was assessed by western blots. Each immune tissue lysate shown in this figure consists of a pooled sample from 6 mice or healthy human participants. Tissue lysates were added at an equal quantity (10 μg). A murine brain lysate was used as a positive control for murine immune tissues and a lysate from IMR-32, a human neuronal cell line, was used as a positive control for human PBMCs. The western blot results (A and B) determines the presence of AChE proteins in the murine and human immune tissues. The arrows indicate the location of the theoretical molecular weight on the blot at 68 kDa. The images in Figure 7 were exposed on the ChemiDoc MP Imaging System using chemiluminescence and an auto exposure. Altogether, it seems that the AChE protein of a different molecular weight than the predicted molecular weight was expressed in murine spleen, thymus, BM, and human PBMCs; yet, for murine immune tissues, AChE of a similar molecular weight than the positive control was expressed.

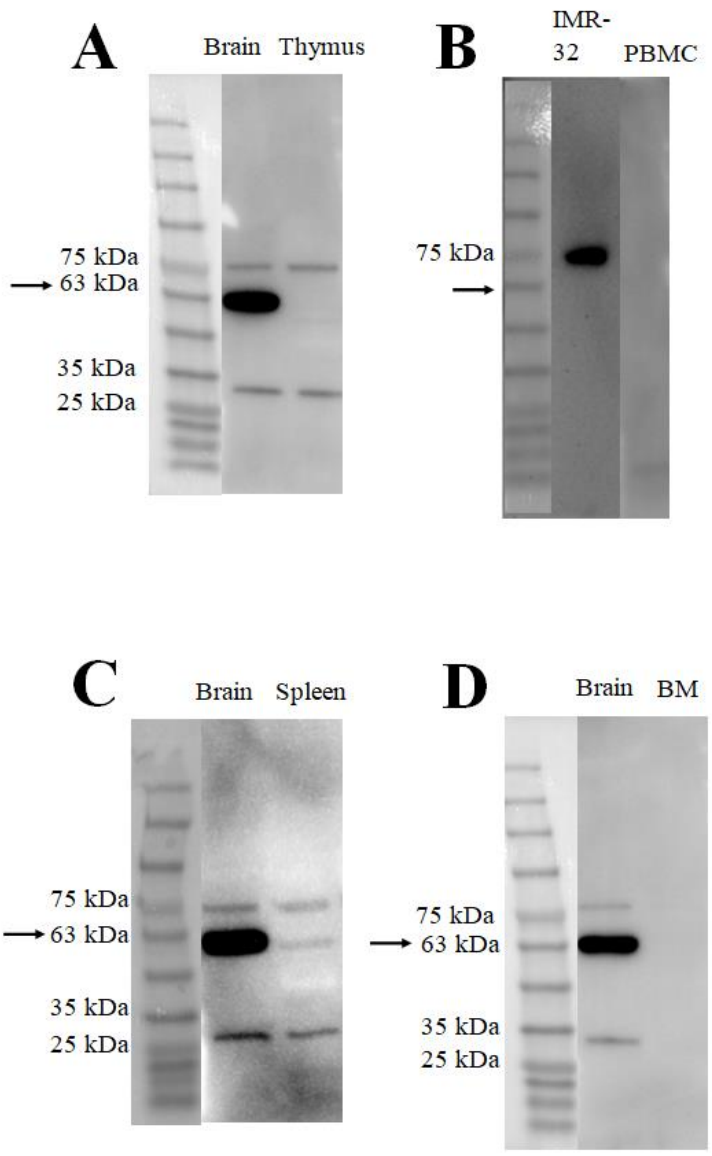

Figure 8: Protein Expression of ChT in Immune Tissues

The expression of ChT in protein lysates from the murine thymus, spleen, BM, and human PBMCs was assessed by western blots. Each immune tissue lysate shown in this figure consists of a pooled sample from 6 mice or healthy human participants. Tissue lysates were added at a maximum amount of immune tissue lysate which did not exceed 50 μg. A murine brain lysate was used as a positive control for murine immune tissues and a lysate from IMR-32, a human neuronal cell line, was used as a positive control for human PBMCs. The arrows show the location of the theoretical molecular weight of 63 kDa. The images of the blots were captured on the ChemiDoc MP using chemiluminescence and the optimal auto-exposure setting. Altogether, it seems that ChT was expressed in the murine thymus and spleen but not in the human PBMCs and murine BM.

3.2 Expression of ChAT in Immune Cells within Immune Tissues

Since our data suggest that ChAT, AChE, ChT are expressed in most immune tissues studied, we then set forth to identify which cell types express ChAT proteins within the spleen, BM and human PBMCs). Therefore, ICC experiments were completed to assess the expression of ChAT within immune cells of the immune tissues (namely the spleen, BM, and human PBMCs).

The expression of ChAT was investigated in killer T cells, helper T cells, B cells and macrophages of the murine spleen in Figures 9, 10, 11 and 12, respectively. According to Figure 9A, we detected strong fluorescence signal in some killer T cells within murine splenocytes, indicating that they expressed ChAT. According to Figure 9B, it seems that between 10-30% of killer T cells in the spleen expressed ChAT. In addition, Figure 10A suggests that a subset of helper T cells within murine splenocytes expressed ChAT. According to Figure 10B, it seems that less than 20% of helper T cells in the spleen expressed ChAT. Furthermore, Figure 11A suggests that a subset of macrophages within murine splenocytes expressed ChAT. According to Figure 11B, it seems that less than 50% of macrophages in the spleen expressed ChAT (Figure 11C). Moreover, it seems that some B cells within the murine splenocytes expressed ChAT (Figure 12A). Figure 12B, shows that less than 20% of B cells in the spleen expressed ChAT. To summarize, it thus seems that subsets of T helper cells, killer T cells, B cells, and macrophages within the murine spleen express ChAT.

Accordingly, the expression of ChAT was investigated in CD105+ cells, monocytes, and B cells of the murine BM in Figures 13, 14, and 15, respectively. CD105 is a marker that targets activated monocytes, endothelial cells, and MSCs.[101,102] Some CD105+ cells within murine BM seemingly expressed ChAT (Figure 13A). It seems that 70-80% of CD105+ expressed ChAT as shown in Figure 13B whereas less than 15% of total BM cells expressed ChAT and CD105 in Figure 13C. Therefore, unlike other immune cells, most CD105+ cells expressed ChAT. According to Figure 14A, some monocytes within murine BM seemed to express ChAT. The trend regarding the percentage of monocytes expressing ChAT was like most immune cells whereby a smaller percentage of monocytes expressed ChAT. In fact, in Figure 14B, it seems that less than 20% of monocytes in the BM expressed ChAT whereas less than 10% of total BM cells expressed ChAT and CD11b (Figure 14C). Hence, less than 20% of monocytes within the BM expressed ChAT. Since CD11b is a cell surface marker for all monocytes and CD105 is mostly for activated monocytes, an activated monocyte would thus be CD11b+and CD105+. Therefore, by comparing the total percentages in Figures 13C and 14C for each corresponding BM sample, it seems that only BM sample 2 likely expressed MSCs expressing ChAT. In addition, by examining Figures 13B and 14B, it seems that most monocytes expressing ChAT were activated. These results will be further discussed in the discussion section. Moreover, in Figure 15A, it seems that some B cells within murine BM expressed ChAT. In Figure 15B, it seems that less than 30% of B cells in the BM expressed ChAT. Therefore, there were less B cells in the murine BM expressing ChAT than B cells that did not express ChAT. Altogether, it seems that B cells and monocytes (mostly those who are activated) seem to express ChAT whereas the expression of ChAT within MSCs remains unclear.

The expression of ChAT was investigated in B cells, monocytes, helper T cells, and killer T cells within human PBMCs in Figures 16, 17, 18 and 19, respectively. As for B cells, some of these cells in human PBMCs seemed to express ChAT (Figure 16A). According to Figure 16B, it seems that less than 40% of B cells in the PBMCs expressed ChAT. These findings suggest that less B cells within human PBMCs expressed ChAT than those that did not express ChAT. Furthermore, it seems that some monocytes within human PBMCs expressed ChAT in Figure 17A. In Figure 17B, it seems that less than 40% of monocytes in the PBMCs expressed ChAT. In other words, only a small percentage of monocytes in human PBMCs expressed ChAT. Moreover, from the 40X images in Figure 18A, it seems that some helper T cells within human PBMCs expressed ChAT. According to Figure 18B, the data was highly variable between the two n values. For one of the n values, the percentage of colocalization was higher than the helper T cells that did not express ChAT while for the other n, the trend was opposite. Altogether, it seems that helper T cells within human PBMCs expressed ChAT. However, the percentage of helper T cells expressing ChAT was highly variable between the two n values which renders the percentages of ChAT protein expression within these T cells unclear. Finally, according to the 40X images in Figure 19A, it seems that some killer T cells within human PBMCs expressed ChAT. Regarding Figure 19B, the data was highly variable between the two n values. For one of the n values, the percentage of colocalization was higher than the killer T cells that did not express ChAT while for the other n, the trend was opposite. Overall, it thus seems that killer T cells within human PBMCs expressed ChAT. On the other hand, akin to helper T cells of human PBMCs, the percentage of killer T cells expressing ChAT was highly variable between the two n values which makes the percentages of ChAT protein

expression within these T cells unclear. In conclusion, some B cells, monocytes, helper T cells, and killer T cells expressed ChAT within human PBMCs.

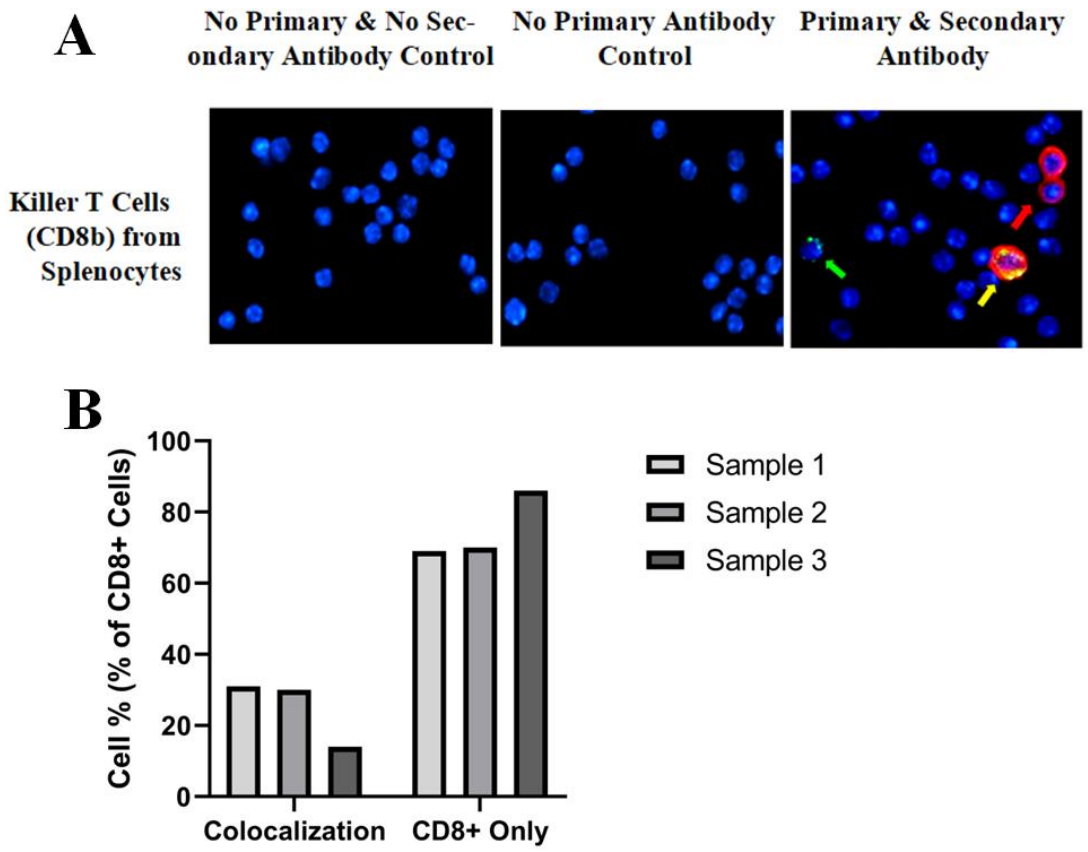

Figure 9: Expression of ChAT within Killer T Cells of Murine Splenocytes

The expression of ChAT proteins was assessed in Killer T Cells derived from murine splenocytes by ICC. Figure 9 illustrates the results for ICC experiments in murine splenocytes in which ChAT and CD8 (cell surface marker from killer T cells) were stained. In Figure 9A, green fluorescence indicates the expression of ChAT, blue fluorescence indicates the nucleus, and red fluorescence indicates the presence of CD8. The green arrow points to cells only expressing ChAT, the red arrow points to cells only expressing CD8, and the yellow arrow points to cells expressing both CD8 as well as ChAT. Altogether, from the 40X images in Figure 9A, it seems that some killer T cells within murine splenocytes expressed ChAT. According to Figure 9B, 10-30% of killer T cells in the spleen expressed ChAT. An n value of 3 was used and the BioTek Cytation 5 imager was used to gather the data in this figure. Altogether, it seems that less than 30% of killer T cells from the spleen expressed ChAT.

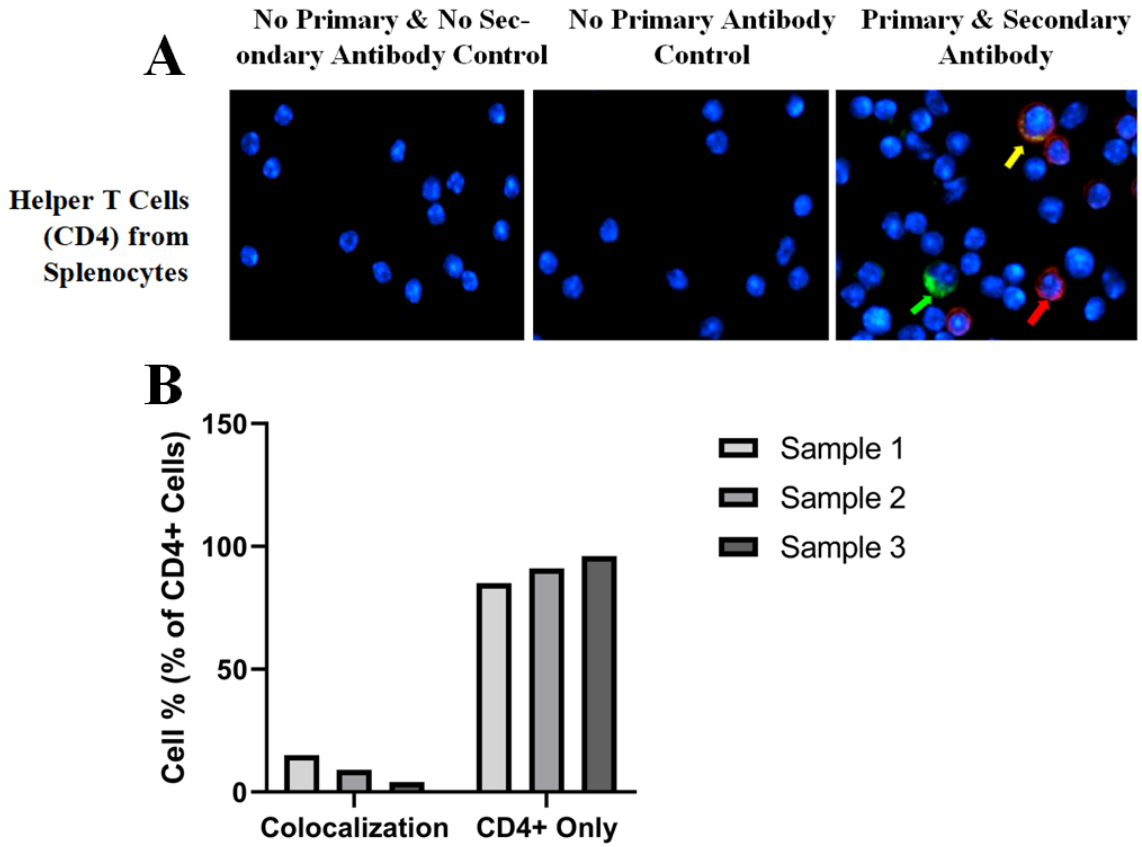

Figure 10: Expression of ChAT within Helper T Cells of Murine Splenocytes

The expression of ChAT proteins was assessed in Helper T Cells derived from murine splenocytes by ICC. Figure 10 shows data for ICC experiments in murine splenocytes in which ChAT and CD4 (cell surface marker from helper T cells) were stained. In Figure 10A, green fluorescence indicates the expression of ChAT, blue fluorescence indicates the nucleus, and red fluorescence suggests the presence of CD4. The green arrow points to cells only expressing ChAT, the red arrow points to cells only expressing CD4, and the yellow arrow points to cells expressing CD4 as well as ChAT. Altogether, from the 40X images in Figure 10A, it seems that a subset of helper T cells within murine splenocytes expressed ChAT. According to Figure 10B, it seems that less than 20% of helper T cells in the spleen expressed ChAT w. An n value of 3 was used and the BioTek Cytation 5 imager was used to gather the data in this figure. Altogether, it seems that less than 20% of helper T cells from the spleen expressed ChAT.

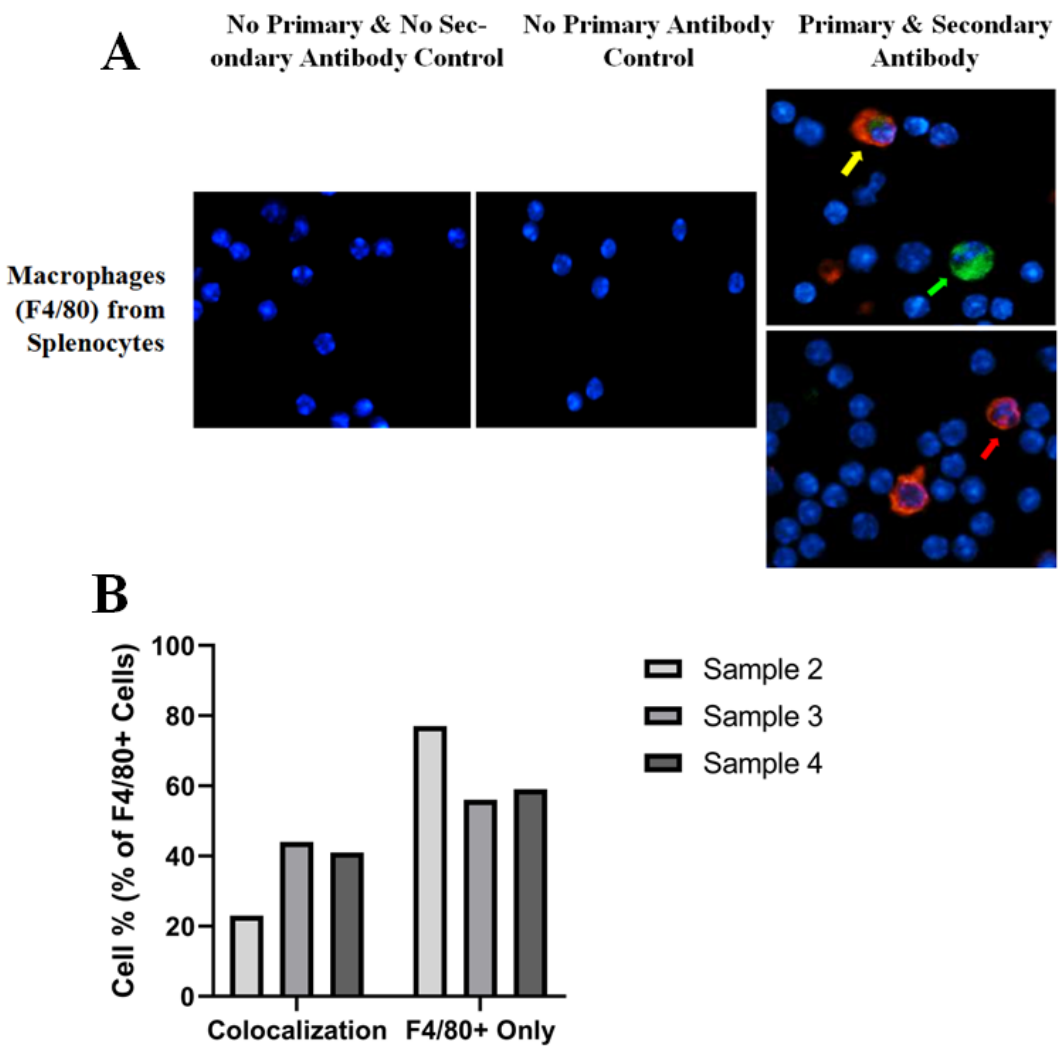

Figure 11: Expression of ChAT within Macrophages of Murine Splenocytes

The expression of ChAT proteins was assessed in macrophages from murine splenocytes by ICC. Figure 11 contains data for ICC experiments in murine splenocytes in which ChAT and F4/80 (cell surface marker from macrophages) were stained. In Figure 11A, green fluorescence indicates the expression of ChAT, blue fluorescence indicates the nucleus, and red fluorescence suggests the presence of F4/80. The green arrow points to cells only expressing ChAT, the red arrow points to cells only expressing F4/80, and the yellow arrow points to cells expressing F4/80 as well as ChAT. Altogether, from the 40X images in Figure 11A, it seems that some macrophages within murine splenocytes expressed ChAT. According to Figure 11B, it seems that less than 50% of macrophages in the spleen expressed ChAT. An n value of 3 was used and the BioTek Cytation 5 imager was used to gather the data in this figure. Altogether, it seems that less than 50% of macrophages from the spleen expressed ChAT.

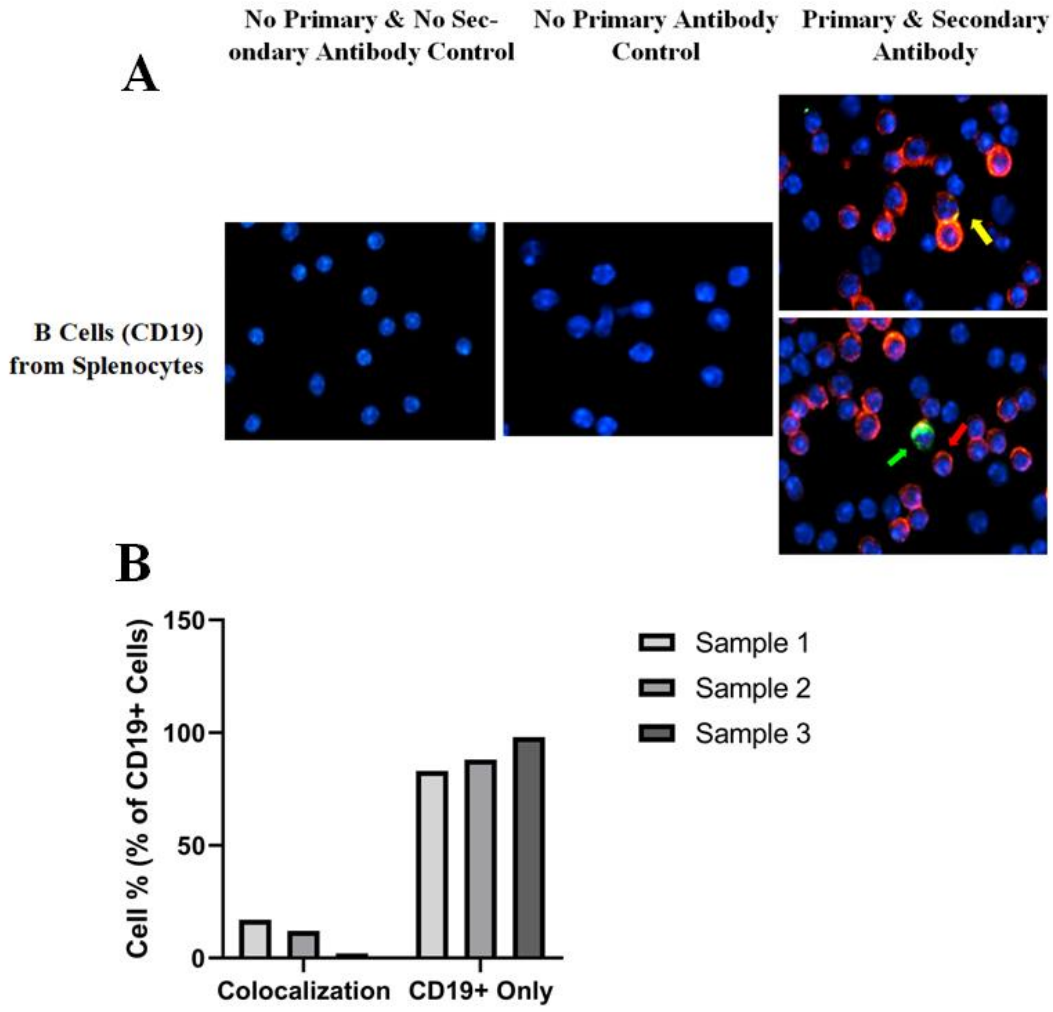

Figure 12: Expression of ChAT within B Cells of Murine Splenocytes

The expression of ChAT proteins was assessed in B cells from murine splenocytes by ICC. Figure 12 illustrates data of ICC experiments in murine splenocytes in which ChAT and CD19 (cell surface marker for B cells) were stained. In Figure 12A, green fluorescence indicates the expression of ChAT, blue fluorescence indicates the nucleus, and red fluorescence suggests the presence of CD19. The green arrow points to cells only expressing ChAT, the red arrow points to cells only expressing CD19, and the yellow arrow points to cells expressing CD19 as well as ChAT. Altogether, from the 40X images in Figure 12A, it seems that some B cells within murine splenocytes expressed ChAT. According to Figure 12B, it seems that less than 20% of B cells in the spleen expressed ChAT. An n value of 3 was used and the BioTek Cytation 5 imager was used to gather the data in this figure. Altogether, it seems that less than 20% of B cells from the spleen expressed ChAT.

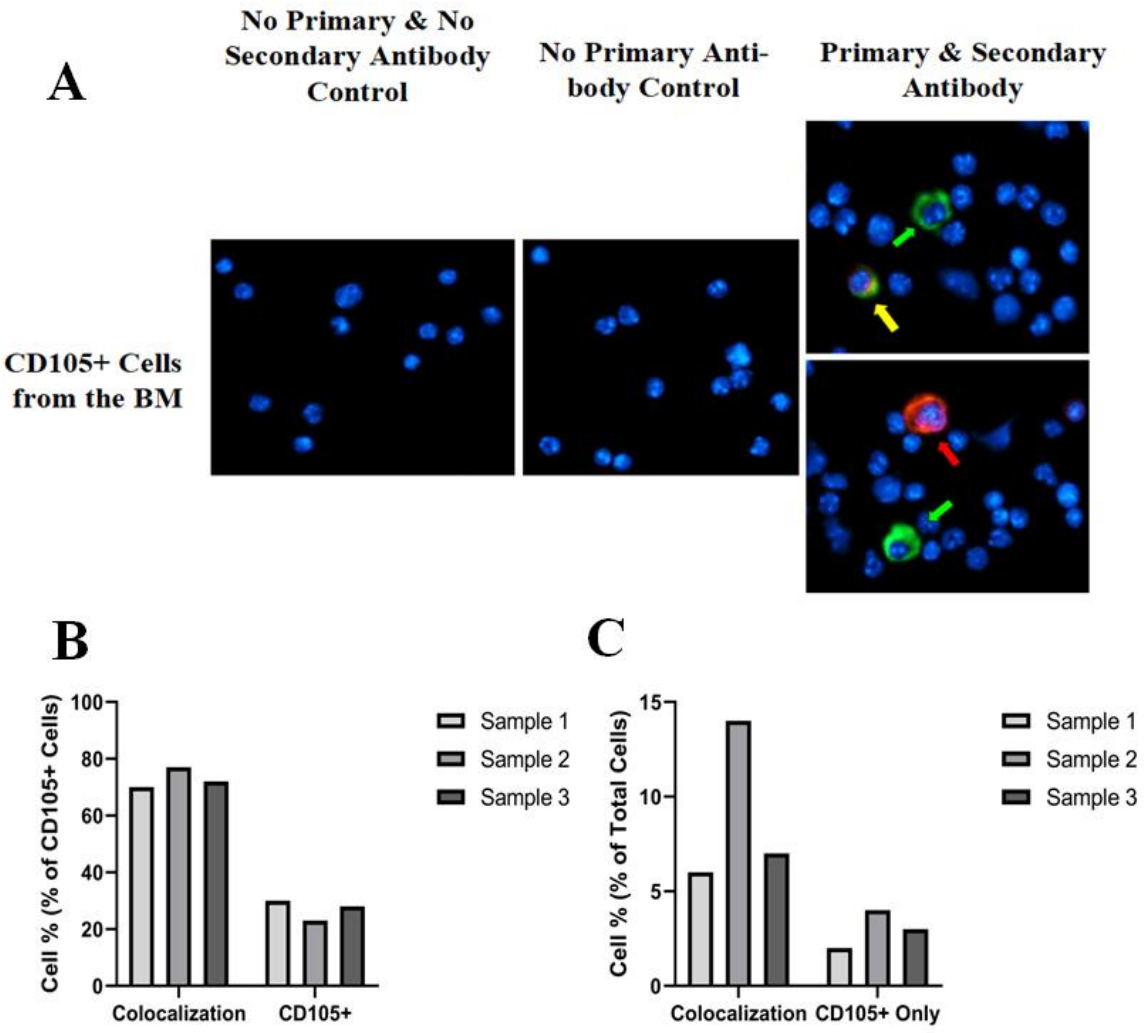

Figure 13: Expression of ChAT within CD105+ of Murine BM

The expression of ChAT proteins was assessed in CD105+ cells from murine BM by ICC. Figure 13 demonstrates the data from ICC experiments in murine BM in which ChAT and CD105 (cell surface marker for mesenchymal stem cells) were stained. In Figure 13A, green fluorescence indicates the expression of ChAT, blue fluorescence indicates the nucleus, and red fluorescence suggests the presence of CD105. The green arrow points to cells only expressing ChAT, the red arrow points to cells only expressing CD105, and the yellow arrow points to cells expressing CD105 as well as ChAT. Altogether, from the 40X images in Figure 13A, it seems that some CD105+ cells within murine BM expressed ChAT. According to Figure 13B, it seems that less than 80% of CD105+ cells in the BM expressed ChAT whereas less than 15% of total BM cells expressed ChAT and CD105 (Figure 13C). An n value of 3 was used and the BioTek Cytation 5 imager was used to gather the data in this figure. Altogether, it seems that less than 80% of CD105+ cells from the BM expressed ChAT.

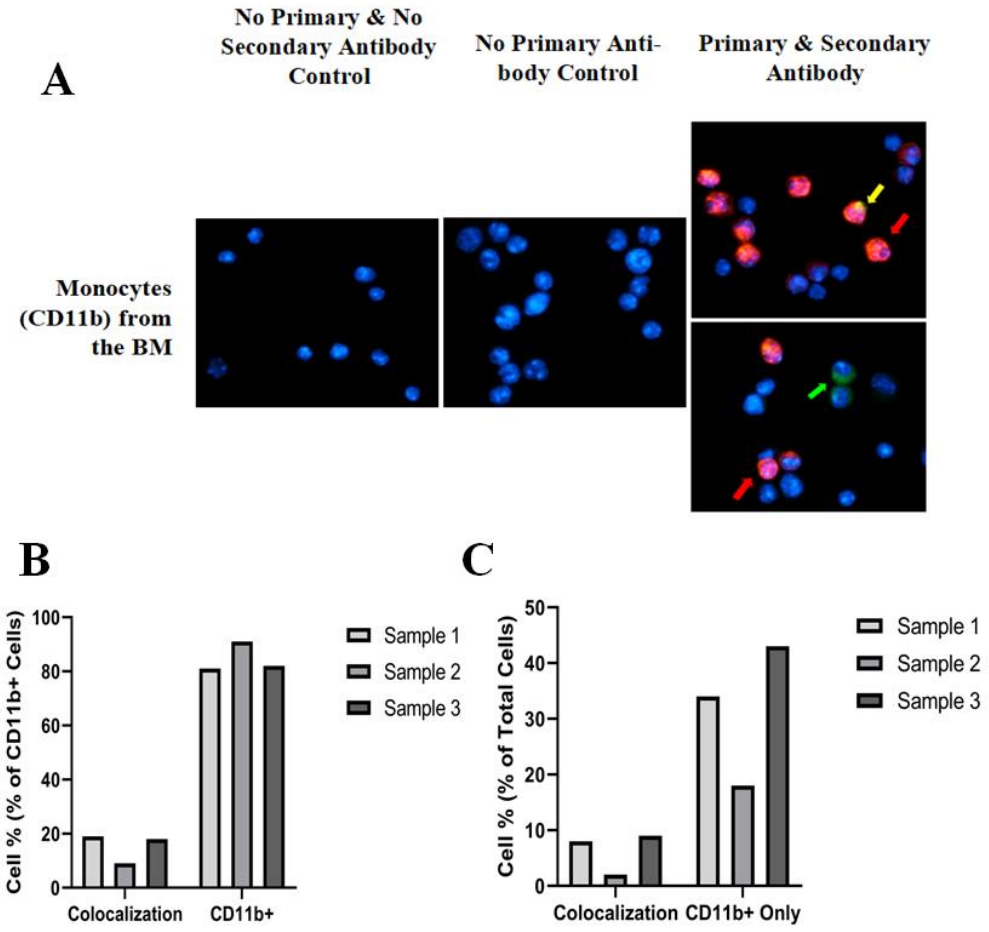

Figure 14: Expression of ChAT within Monocytes of Murine BM

The expression of ChAT proteins was assessed in monocytes from murine BM by ICC. Figure 14 demonstrates the data from ICC experiments in murine BM in which ChAT and CD11b (cell surface marker for monocytes) were stained. In Figure 14A, green fluorescence indicates the expression of ChAT, blue fluorescence indicates the nucleus, and red fluorescence suggests the presence of CD11b. The green arrow points to cells only expressing ChAT, the red arrow points to cells only expressing CD11b, and the yellow arrow points to cells expressing CD11b as well as ChAT. Altogether, from the 40X images in Figure 14A, it seems that some monocytes within murine BM expressed ChAT. According to Figure 14B, it seems that less than 20% of monocytes in the BM expressed ChAT whereas less than 10% of total BM cells expressed ChAT and CD11b (Figure 14C). An n value of 3 was used and the BioTek Cytation 5 imager was used to gather the data in this figure. Altogether, it seems that less than 20% of monocytes from the BM expressed ChAT.

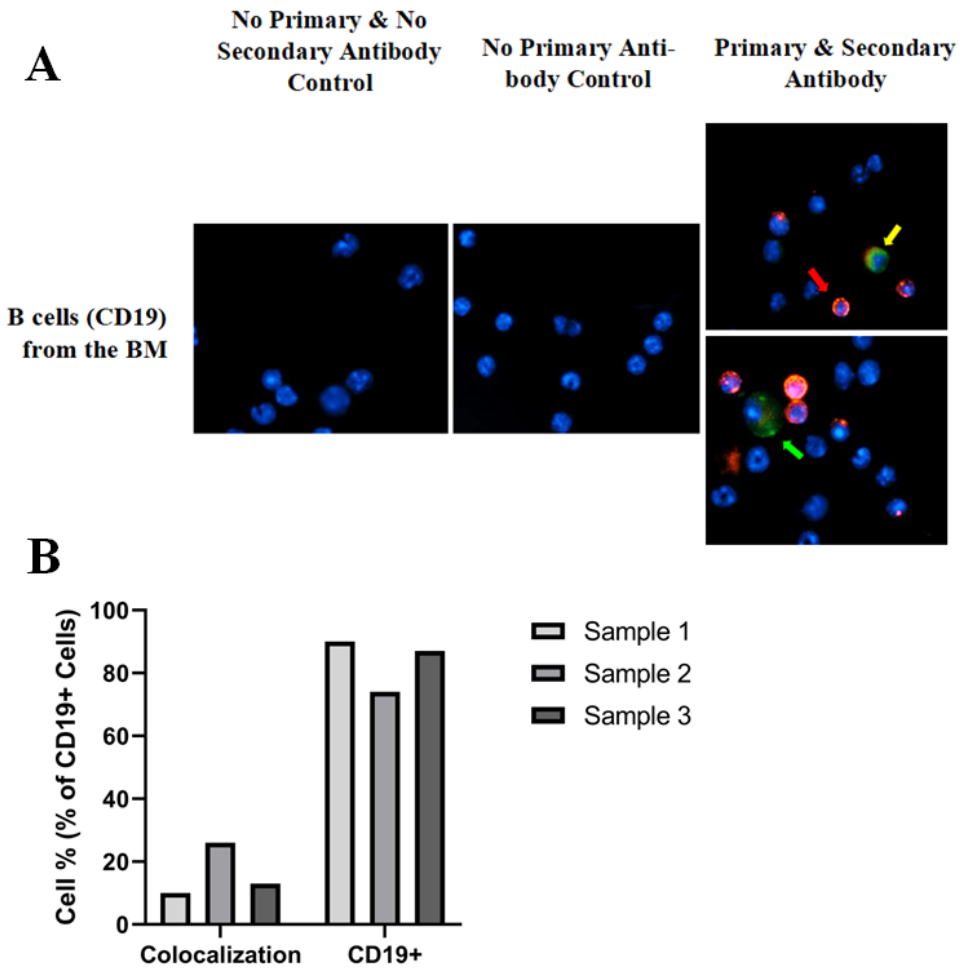

Figure 15: Expression of ChAT within B Cells of Murine BM

The expression of ChAT proteins was assessed in B cells from murine BM by ICC. Figure 15 demonstrates the data from ICC experiments in murine BM in which ChAT and CD19 (cell surface marker for B cells) were stained. In Figure 15A, green fluorescence indicates the expression of ChAT, blue fluorescence indicates the nucleus, and red fluorescence suggests the presence of CD19. The green arrow points to cells only expressing ChAT, the red arrow points to cells only expressing CD19, and the yellow arrow points to cells expressing CD19 as well as ChAT. Altogether, from the 40X images in Figure 15A, it seems that some B cells within murine BM expressed ChAT. According to Figure 15B, it seems that less than 30% of B cells in the BM expressed ChAT. An n value of 3 was used and the BioTek Cytation 5 imager was used to gather the data in this figure. Altogether, it seems that less than 10% of B cells from the BM expressed ChAT.

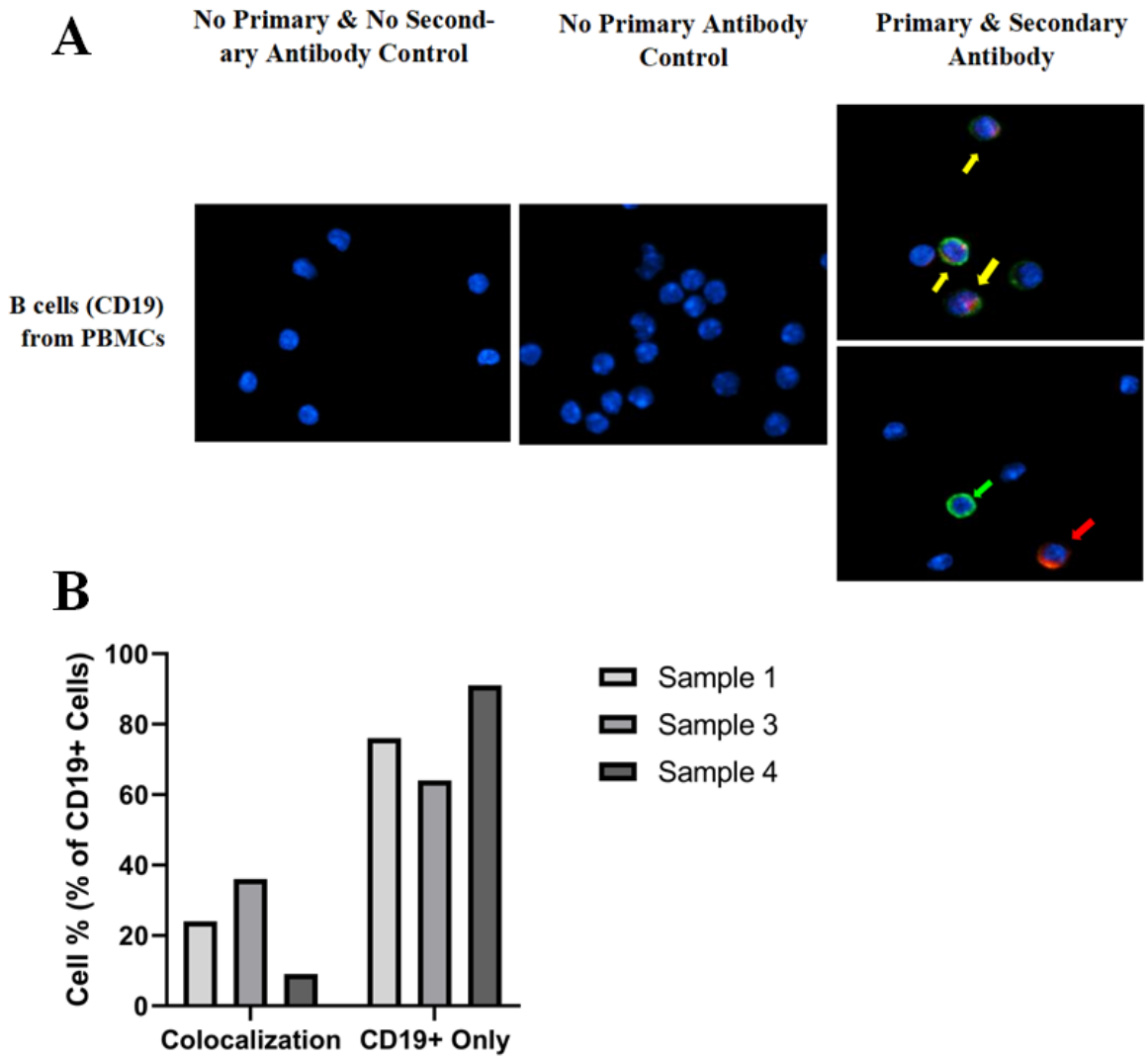

Figure 16: Expression of ChAT within B Cells of Human PBMCs

The expression of ChAT proteins was assessed in B cells from human PBMCs by ICC. Figure 16 demonstrates the data from ICC experiments in human PBMCs in which ChAT and CD19 (cell surface marker for B cells) were stained. In Figure 16A, green fluorescence indicates the expression of ChAT, blue fluorescence indicates the nucleus, and red fluorescence suggests the presence of CD19. The green arrow points to cells only expressing ChAT, the red arrow points to cells only expressing CD19, and the yellow arrow points to cells expressing CD19 as well as ChAT. Altogether, from the 40X images in Figure 16A, it seems that some B cells within human PBMCs expressed ChAT. According to Figure 16B, it seems that less than 40% of B cells in the PBMCs expressed ChAT. An n value of 3 was used and the BioTek Cytation 5 imager was used to gather the data in this figure. Altogether, it seems that less than 40% of B cells from human PBMCs expressed ChAT.

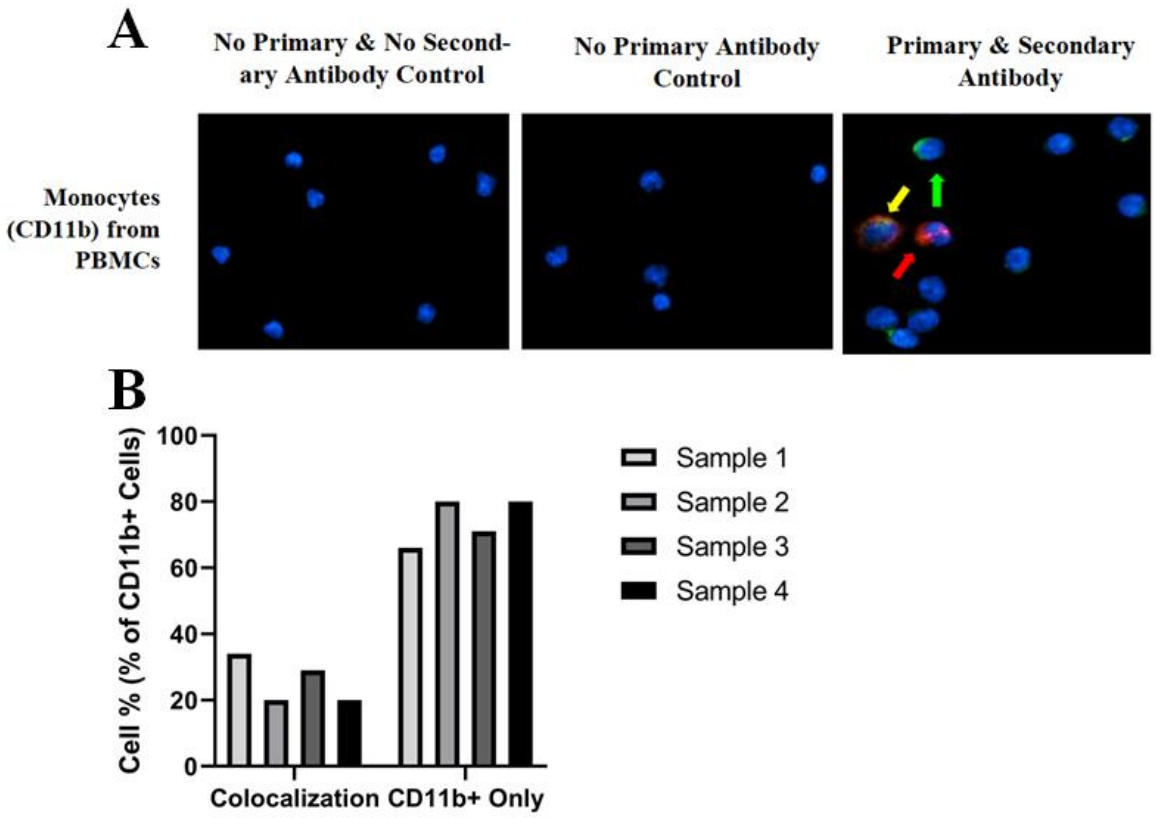

Figure 17: Expression of ChAT within Monocytes of Human PBMCs

The expression of ChAT proteins was assessed in monocytes from human PBMCs by ICC. Figure 17 contains the data from ICC experiments in human PBMCs in which ChAT and CD11b (cell surface marker for monocytes) were stained. In Figure 17A, green fluorescence indicates the expression of ChAT, blue fluorescence indicates the nucleus, and red fluorescence suggests the presence of CD11b. The green arrow points to cells only expressing ChAT, the red arrow points to cells only expressing CD11b, and the yellow arrow points to cells expressing CD11b as well as ChAT. Altogether, from the 40X images in Figure 17A, it seems that some monocytes within human PBMCs expressed ChAT. According to Figure 17B, it seems that less than 40% of monocytes in the PBMCs expressed ChAT. An n value of 4 was used and the BioTek Cytation 5 imager was used to gather the data in this figure. Altogether, it seems that less than 40% of monocytes from human PBMCs expressed ChAT.

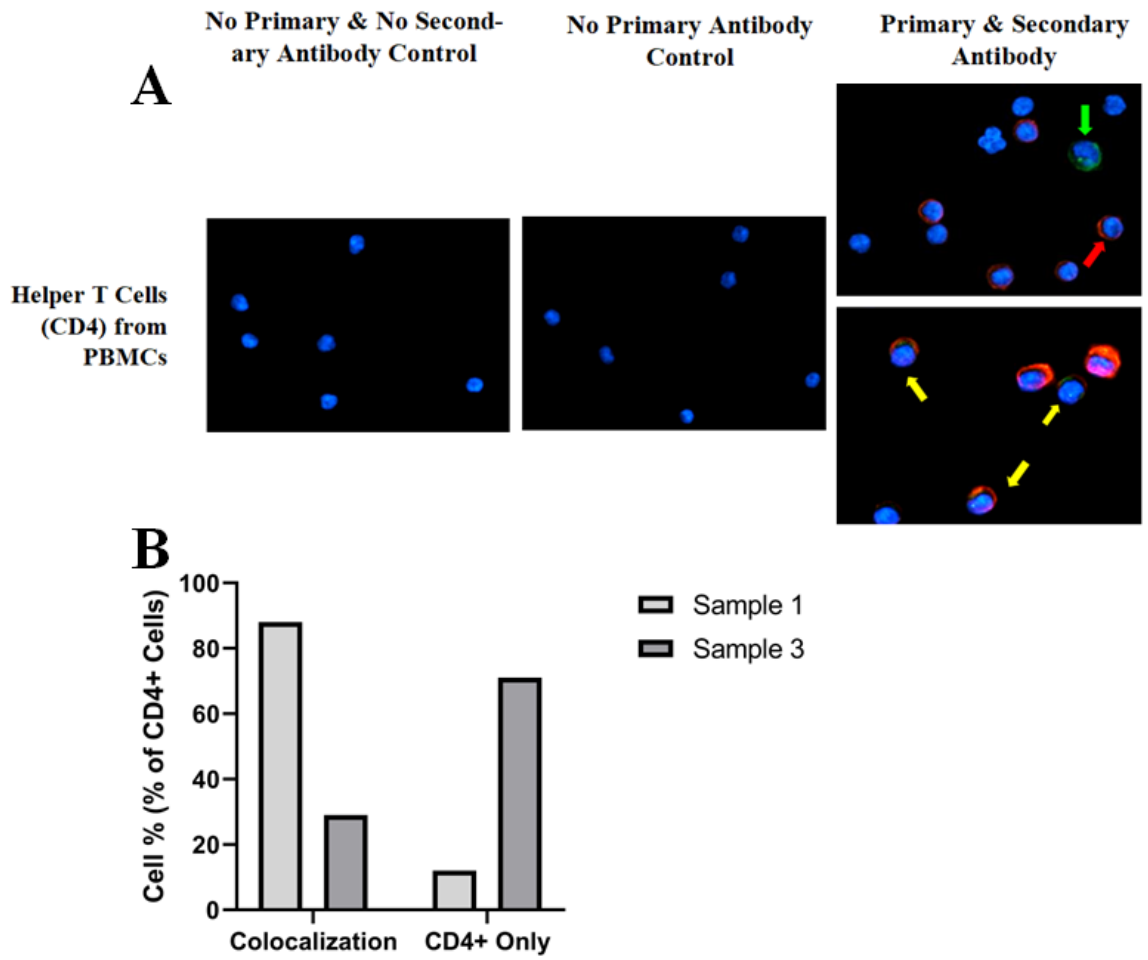

Figure 18: Expression of ChAT within CD4+ T Cells of Human PBMCs

The expression of ChAT proteins was assessed in helper T cells from human PBMCs by ICC. Figure 18 shows the data from the ICC experiments in human PBMCs in which ChAT and CD4 (cell surface marker for helper T cells) were stained. In Figure 18A, green fluorescence indicates the expression of ChAT, blue fluorescence indicates the nucleus, and red fluorescence suggests the presence of CD4. The green arrow points to cells only expressing ChAT, the red arrow points to cells only expressing CD4, and the yellow arrow points to cells expressing CD4 as well as ChAT. Altogether, from the 40X images in Figure 18A, it seems that some helper T cells within human PBMCs expressed ChAT. According to Figure 18B and 18C, the data was highly variable between the two n values. The BioTek Cytation 5 imager was used to gather the data in this figure. Altogether, it seems that helper T cells within human PBMCs expressed ChAT. However, the percentage of helper T cells expressing ChAT highly variable between the two n values.

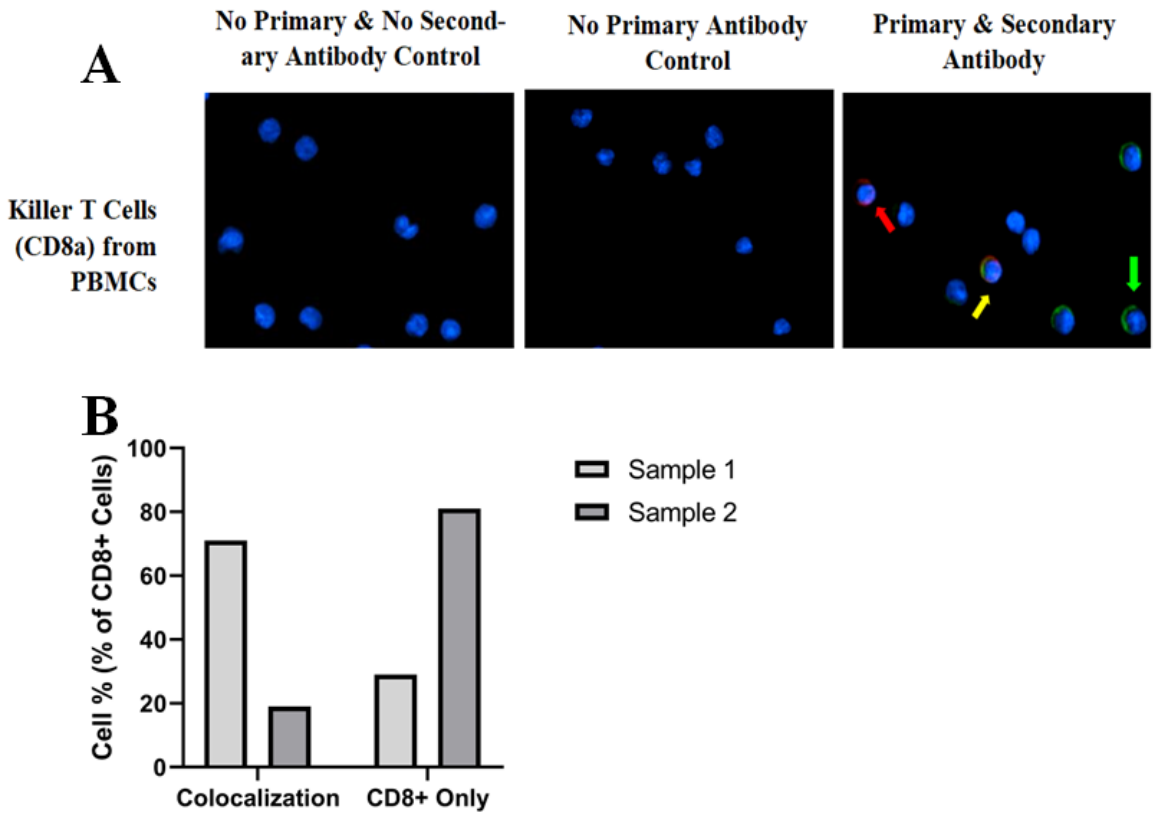

Figure 19: Expression of ChAT within CD8+ T Cells of Human PBMCs

The expression of ChAT proteins was assessed in cytolytic T cells from human PBMCs by ICC. Figure 19 illustrates the data from ICC experiments in human PBMCs in which ChAT and CD8 (cell surface marker for cytolytic T cells) were stained. In Figure 19A, green fluorescence indicates the expression of ChAT, blue fluorescence indicates the nucleus, and red fluorescence suggests the presence of CD8. The green arrow points to cells only expressing ChAT, the red arrow points to cells only expressing CD8, and the yellow arrow points to cells expressing CD4 as well as ChAT. Altogether, from the 40X images in Figure 19A, it seems that some cytolytic T cells within human PBMCs expressed ChAT. According to Figure 19B, the data was highly variable between the two n values. The BioTek Cytation 5 imager was used to gather the data in this figure. Altogether, it seems that cytolytic T cells within human PBMCs expressed ChAT. However, like with helper T cells of human PBMCs, the percentage of cytolytic T cells expressing ChAT was highly variable between the two n values.

3.3 Expression of ACh in Immune Tissues

The expression of ACh was assessed by UPLC coupled with triple quadrupole MS. Peak areas extrapolated from chromatograms obtained from MRM were used to determine the presence of ACh. Figure 2 shows the results for ACh expression within the murine spleen and thymus. Acetonitrile was used as a negative control and an ACh standard at 10 ppb was used as a positive control. Therefore, the peak area of a given sample (indicated on the y axis of Figure 20) must be higher than the peak area of acetonitrile for positive expression of ACh. For the spleen samples, only half of the eight spleen samples seemed to express ACh. As for the thymus samples, it seems like all thymus samples expressed ACh. Therefore, the murine thymus seemed to express ACh and so did the spleen but at much lower levels.

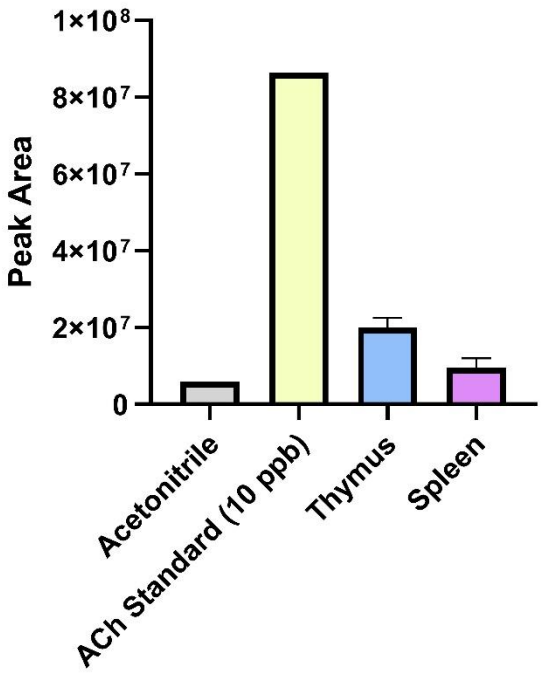

Figure 20: Expression of ACh in the Murine Spleen and Thymus

The expression of ACh was assessed by UPLC coupled with triple quadrupole MS. Figure 20 illustrates the results from the triple-quadrupole MS experiments coupled with UPLC. Acetonitrile was used as a negative control and an ACh standard at 10 ppb was used as a positive control. Therefore, the peak area of a given sample must be higher than the peak area of acetonitrile for positive expression of ACh. An n of 10 was used for the thymus and an n of 8 was used for the spleen. The error bars in this figure represent the SEM. Half of the spleen samples expressed ACh whereas for the thymus, all thymuses seemed to express ACh. Hence, it seems that the murine thymus expressed ACh whereas half of the spleens expressed ACh.

3.4 Cytokine Profile from BMDM Pharmacological Studies

Our data indicate that all immune tissues and cell types included in this study express cholinergic genes and proteins, and that ACh was detected in the spleen and thymus. We therefore next assessed whether pharmacological inhibition would affect the viability and functions of immune cells. Our lab previously demonstrated that nAChR ligands significantly modulates cytokine production by BMDMs, and therefore chose to begin with studying this model.[103] The supernatant resulting from the 6-day BMDM culture was collected to assess cytokine levels via CBAs. The cytokine levels were monitored in BMDMs that were polarized into M1 or M2. At the sixth day of culture, the cells were treated as depicted in Table 6. Figure 21-25 shows the results from the CBA assays. These results can be used to determine the effect of cholinergic agonists and inhibitors on cytokine release in M1 or M2 polarized BMDM cultures. Such pharmacological results can be utilized to assess the functional role of cholinergic markers within an immune environment such as BMDMs. It is important to first mention that outlier samples from the LDH assay (see section 3.5) were also removed from the CBA analysis which is why depending on the condition, the n value differed. Since the n value was generally low, there was not enough power to do a one-way ANOVA for most figures in this section. A power analysis demonstrated that a sample size of 9 was the minimum necessary for statistical analysis and therefore, our aim was to reach that sample size. However, we encountered severe ordering delays on CBA kits due to some new very restrictive ordering protocols established at Laurentian university and we unfortunately did not have enough CBA kits left to complete the intended sample size of anywhere from 2 to 5. Therefore, no statistical significance ($P \leq 0.05$) can be derived from Figures 21-25 but the trend will be commented herein.

In M1 polarized BMDMs, the levels of IL-10 were assessed for each condition (Figure 21). When comparing with the LPS Only condition, IL-10 levels seemed to decrease for the LPS + BrACh and LPS + α-Neta conditions. No differences were observed for IL-10 levels of the LPS + Ch, LPS + ACh, LPS + ML352, LPS + ACh + Galantamine, and the LPS + Galantamine conditions when considering the SEM. Altogether, most treatment conditions did not seem to have an effect on IL-10 levels except for conditions containing a ChAT inhibitor.

For M1 polarized BMDMs, the levels of IL-6 were measured for each condition (Figure 22). This figure can be used to determine the concentrations of IL-6 for different culture conditions of M1 polarized BMDMs. When comparing with the LPS Only condition, IL-6 levels seemed to decrease for the LPS + BrACh and the LPS + α-Neta conditions. No change in IL-6 levels was observed for the LPS + Ch, LPS + ACh, LPS + ML352, LPS + ACh + Galantamine, and the LPS + Galantamine conditions. Overall, most conditions did not seem to change levels of IL-6 except for conditions containing a ChAT inhibitor.

Similar to IL-6 levels assessed from the supernatant of M1 BMDMs, TNF levels were measured for each condition (Figure 23). In terms of trend, it seems that TNF levels increased for the LPS + ACh and LPS + ML352 treatment groups compared to the LPS Only condition. Upon comparison with the LPS Only condition, there does not seem to be much change in TNF levels for the LPS + Ch treatment groups. Yet, it seems that TNF levels decreased for the LPS + ACh + galantamine, LPS + galantamine, LPS + BrACh, and the LPS + α-Neta conditions when comparing to the LPS Only condition. Therefore, in terms of trend, inhibition of ChAT and AChE seemed to reduce levels of TNF yet ACh and inhibition of ChT seemed to increase levels of TNF in M1 polarized BMDMs with LPS.

For M2 polarized BMDMs, IL-6 levels were measured in each condition (Figure 24). When comparing with the LPS Only condition, IL-6 levels seemed to decrease for the LPS + ACh + Galantamine, LPS + Galantamine, LPS + BrACh and the LPS + α-Neta conditions. No change in IL-6 levels was observed when considering the SEM for the LPS +Ch, LPS + ACh, and the LPS + ML352 conditions. Hence, compared to the LPS Only condition and without statistical significance, the IL-6 levels seem to be decreased upon AChE and ChAT inhibition in the presence of LPS.

Moreover, TNF levels were also measured in M2 polarized BMDMs (Figure 25). The results in terms of the trend was essentially the same for Figure 25 as Figure 24. Therefore, compared to the LPS Only condition and without statistical significance, the TNF levels seem to be decreased upon AChE and ChAT inhibition in the presence of LPS.

Altogether, while trends can be examined herein, no conclusions can be made since no analysis was able to take place regarding statistical significance because of a lack in statistical power. However, the sample size for IL-10 measured from the supernatant of M1 BMDMs was large enough to allow for statistical analysis. For these IL-10 results, it seems that none of the treatment conditions caused a statistically significant change in IL-10. Although, inhibition of ChAT in the presence of LPS decreased IL-10 levels but in a non-statistically significant manner.

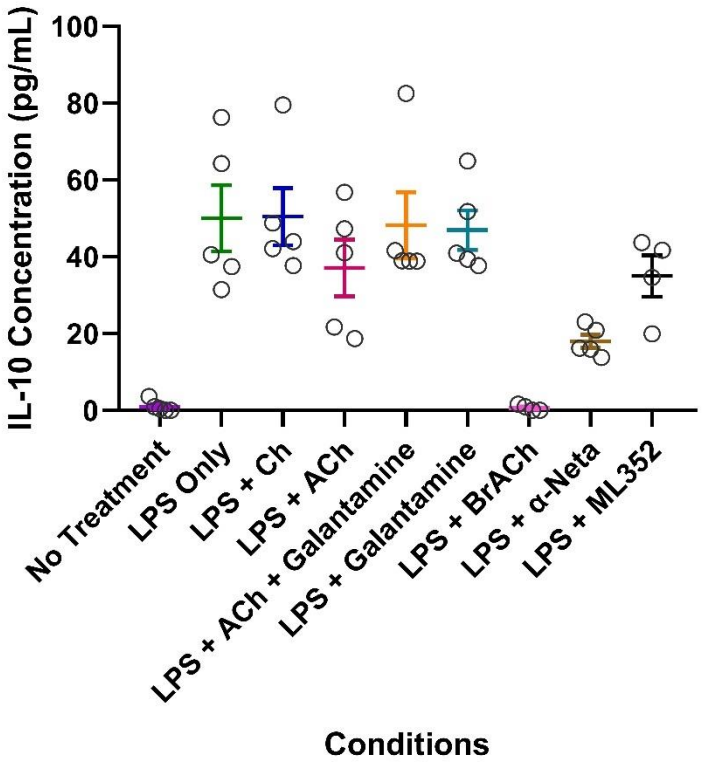

Figure 21: IL-10 Expression in M1 Polarized BMDMs Pharmacologically Treated with Cholinergic Inhibitors

The supernatant from each M1 BMDM culture condition outlined in Table 6 was harvested and used to assess IL-10 levels in M1 BMDMs by CBAs. The data from the CBAs was captured by using the BD FACSCanto II flow cytometer. Figure 21 shows the data from the CBAs of M1 polarized BMDMs for IL-10. This figure can be used to extrapolate the concentrations of IL-10 for different culture conditions of M1 polarized BMDMs. The error bars indicate the SEM. No conclusions can be derived from this figure because the sample size was too small (n = 4-5) to perform a one-way ANOVA. Altogether, most treatment conditions did not seem to significantly change IL-10 levels except for the inhibition of ChAT in the presence of LPS which decreased IL-10 levels in a nearly statistically significant fashion

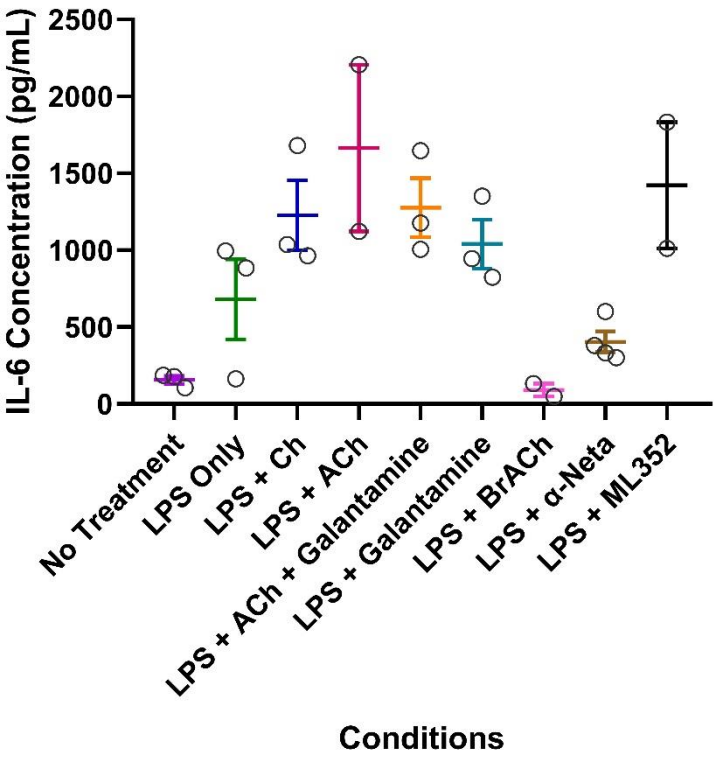

Figure 22: IL-6 Expression in M1 Polarized BMDMs Pharmacologically Treated with Cholinergic Inhibitors

The supernatant from each M1 BMDM culture condition outlined in Table 6 was harvested and used to assess IL-6 levels in M1 BMDMs by CBAs. The data from the CBAs was captured by using the BD FACSCanto II flow cytometer. Figure 22 contains the data from the CBAs of M1 polarized BMDMs for IL-6. This figure can be used to extrapolate the concentrations of IL-6 for different culture conditions of M1 polarized BMDMs. The error bars indicate the SEM. No conclusions can be derived from this figure because the sample size was too small (n = 2-4) to perform a one-way ANOVA. Taken together, in terms of trend, most conditions did not seem to change levels of IL-6 except for conditions containing a ChAT inhibitor whereby IL-6 levels seemed to decrease in the presence of LPS but without statistical significance.

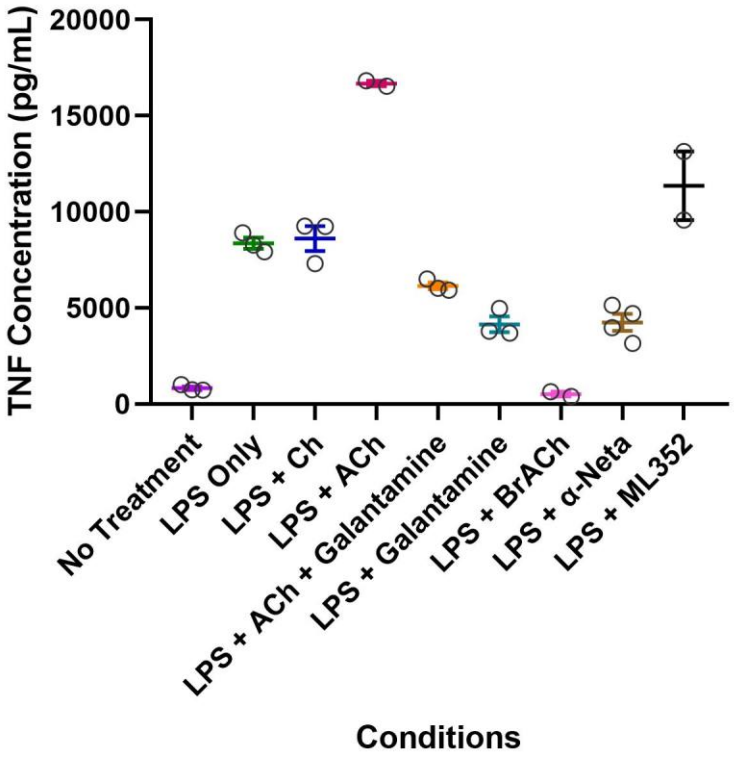

Figure 23: TNF Expression in M1 Polarized BMDMs Pharmacologically Treated with Cholinergic Inhibitors

The supernatant from each M1 BMDM culture condition outlined in Table 6 was harvested and used to assess TNF levels in M1 BMDMs by CBAs. The data from the CBAs was captured by using the BD FACSCanto II flow cytometer. Figure 23 shows the average concentration of TNF in the supernatant of M1 polarized BMDMs after treatment with cholinergic inhibitors. These concentrations were determined by conducting CBA assays. The error bars indicate the SEM. No conclusions can be derived from this figure because the sample size was too small (n = 2-4) to perform a one-way ANOVA. Hence, in terms of trend, inhibition of ChAT and AChE seemed to reduce levels of TNF yet ACh and inhibition of ChT seemed to increase levels of TNF in M1 polarized BMDMs with LPS.

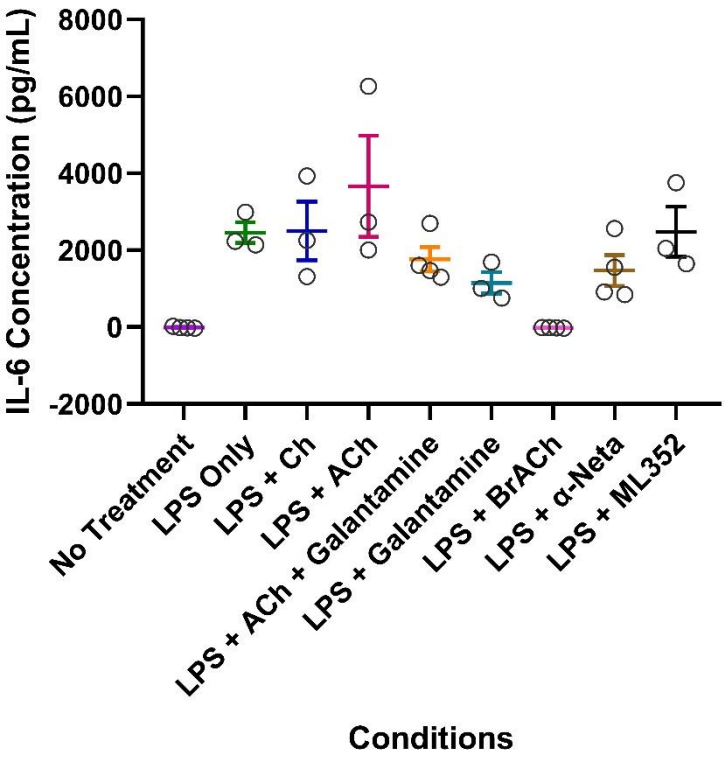

Figure 24: IL-6 Expression in M2 Polarized BMDMs Pharmacologically Treated with Cholinergic Inhibitors

The supernatant from each M2 BMDM culture condition outlined in Table 6 was harvested and used to assess IL-6 levels in M2 BMDMs by CBAs. The data from the CBAs was captured by using the BD FACSCanto II flow cytometer. Figure 24 illustrates the data from the CBAs of M2 polarized BMDMs for IL-6. This figure can be used to extrapolate the concentrations of IL-6 for different culture conditions of M2 polarized BMDMs. The error bars indicate the SEM. No conclusions can be derived from this figure because the sample size was too small (n = 2-4) to perform a one-way ANOVA. Overall, compared to the LPS Only condition and without statistical significance, the IL-6 levels seem to be decreased upon AChE and ChAT inhibition in the presence of LPS.

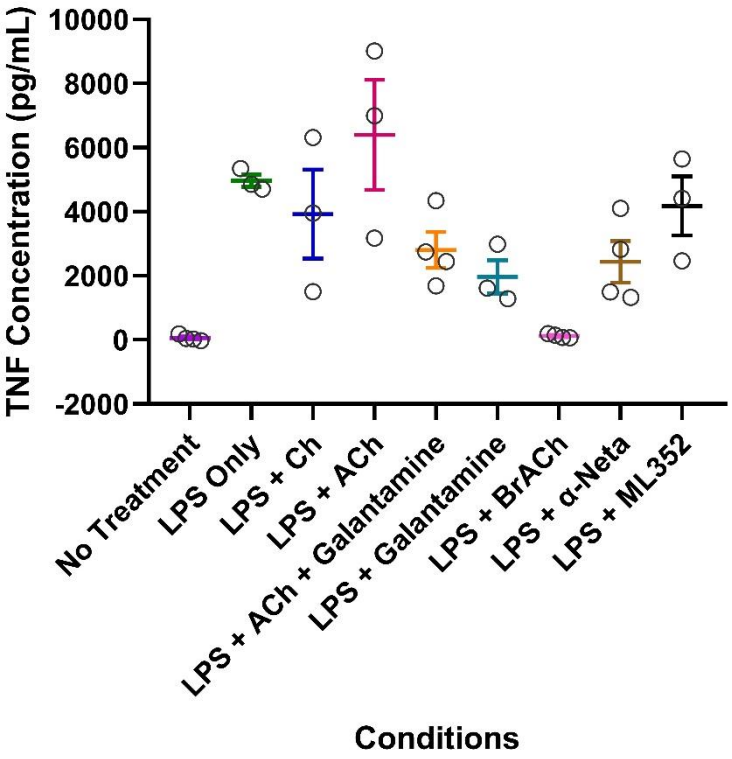

Figure 25: TNF Expression in M2 Polarized BMDMs Pharmacologically Treated with Cholinergic Inhibitors

The supernatant from each M2 BMDM culture condition outlined in Table 6 was harvested and used to assess TNF levels in M2 BMDMs by CBAs. The data from the CBAs was captured by using the BD FACSCanto II flow cytometer. Figure 25 determines the concentration of TNF in the supernatant of M2 polarized BMDMs after treatment with cholinergic inhibitors. The concentration was determined by doing a CBA assay. The error bars indicate the SEM. No conclusions can be derived from this figure because the sample size was too small (n = 2-4) to perform a one-way ANOVA. Taken together, compared to the LPS Only condition and without statistical significance, the TNF levels seem to be decreased upon AChE and ChAT inhibition in the presence of LPS.

3.5 Cell Death from BMDM Pharmacological Studies

Cell viability was assessed with the supernatant of each condition (Table 6) obtained after the 6th day of BMDM culture by using a Fluorescent LDH kit. The quantity of LDH (an enzyme that is released from the cytosol when cells die) was measured to assess cell death. As a blank, complete media supplemented with cytokines for M1 or M2 polarization was used. For a positive control, polarized BMDMs that were not treated and purposely lysed through a freeze/thaw cycle were used. With the fluorescence acquired by each condition in addition to the fluorescence acquired from the controls, the % Cell Death values displayed in Figures 26 and 27 were calculated.

Figure 26 and Figure 27 contain the calculated % Cell Death values of M1 and M2 BMDMs, respectively. An outlier test was performed on Microsoft Excel for each condition and outliers were removed from the data set. Removing outliers was the reason why the sample size for the % Cell Death in M1 BMDMs (Figure 26) was n = 7-9 and the sample size for the % Cell Death in M2 BMDMs (Figure 27) was n= 8-9. A repeated measures one-way ANOVA against the LPS Only control was performed on GraphPad prism using Dunnett's multiple comparisons test, but no statistical significance was shown in M2 BMDMs (Figure 27). However, for M1 BMDMs (Figure 26), LPS + BrACh as well as the LPS + α-Neta had a statistically higher amount of cell death ($P \leq 0.05$) compared to the LPS Only control. According to Figure 27, it does not seem like any of the conditions caused cell death in M2 polarized BMDMs in a statistically significant manner. Although, by examining the trend in Figure 27, in the presence of LPS, it does seem that BrACh, α-Neta, and ML-352 might have caused cell death in M2 polarized BMDMs but not in a statistically significant fashion. Taken together, in M1 BMDMs, ChAT inhibitors in the presence of LPS

seem to have caused cell death in a statistically significant fashion yet in M2 BMDMs ChAT and ChT inhibitors in the presence of LPS seem to have caused cell death in a non-statistically significant fashion.

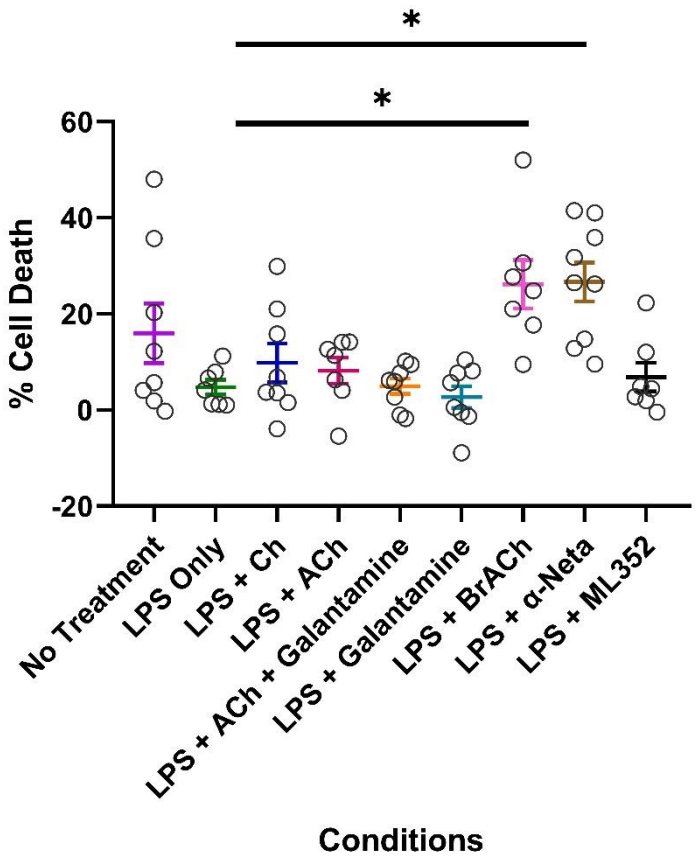

Figure 26: Data from LDH Tests Assessing Cell Death from Pharmacological Treatments of M1 Polarized BMDMs

The supernatant was harvested and used to assess the percentage of cell death in each M1 BMDM culture condition (Table 6) through a fluorescent LDH assay. In Figure 26, there is data from the fluorescent LDH assay whereby the percentage of cell death was calculated by using the fluorescent signals acquired from the Cytation 5. Cell culture media was used as a negative control and a total release control (which is the same as a no treatment condition except that the cells were lysed through a freeze/thaw cycle) was used as a positive control. An outlier test was conducted on Microsoft Excel for each condition and outliers were removed from the data set. The sample size for each condition was n=7-9. The error bars represent the SEM and a repeated measures one-way ANOVA with Dunnett's multiple comparisons test was performed against the LPS Only control. The LPS + BrACh as well as the LPS + α-Neta had a statistically higher amount of cell death compared to the LPS Only condition (*: $P \leq 0.05$). Overall, ChAT inhibitors in the presence of LPS seem to cause cell death in a statistically significant fashion.

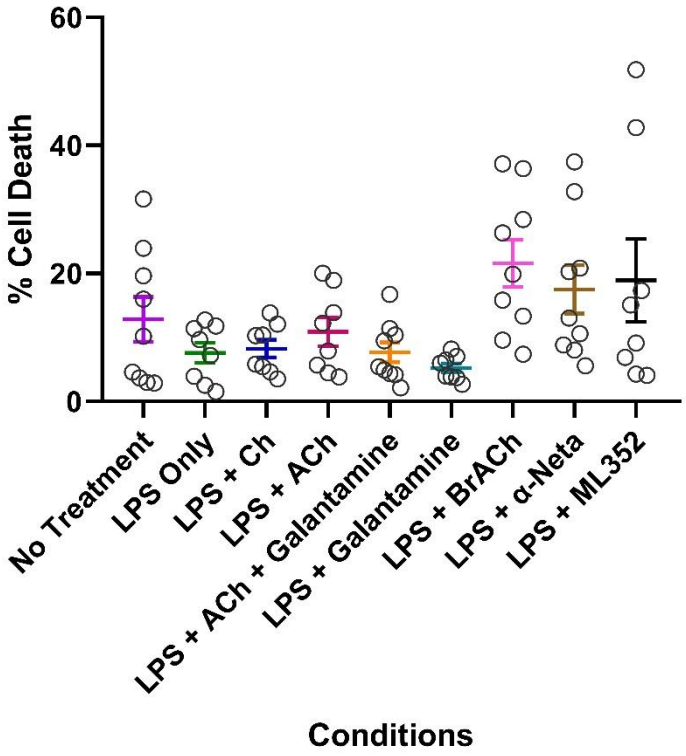

Figure 27: Data from LDH Tests Assessing Cell Death from Pharmacological Treatments of M2 Polarized BMDMs

The supernatant was harvested and used to assess the percentage of cell death in each M2 BMDM culture condition (Table 6) through a fluorescent LDH assay. In Figure 27, there is data from the fluorescent LDH assay whereby the percentage of cell death was calculated by using the fluorescent signals acquired from the Cytation 5. Cell culture media was used as a negative control and a total release control (which is the same as a no treatment condition except that the cells were lysed through a freeze/thaw cycle) was used as a positive control. An outlier test was conducted for each condition and outliers were removed from the data set. The samples size for each condition was n=8-9. The error bars represent the SEM and a one-way ANOVA was performed against the LPS Only control with Dunnett's multiple comparisons test. However, there was no statistical significance ($p \leq 0.05$). Overall, in terms of trend, it seems that treatment with BrACh, α-Neta, and ML352 in the presence of LPS led to more cell death whereas the other pharmacological agents did not seem to cause cell death.

Discussion

In this study, the production of ACh and its function was assessed within immune cells. First, the presence of the cholinergic markers (AChE, CTL2, OCTN1, ChAT, BChE, VAChT, and ChT) was assessed in the WT murine BM, thymus, spleen, and human PBMCs at the transcript level through PCRs. To determine whether these transcripts were translated, the expression of ChAT, AChE, and ChT was assessed at the protein level via western blot. Subsequently, the presence of ACh was assessed in the murine spleen and thymus by UPLC coupled with triple-quadrupole MS. To investigate which immune cells within each immune tissue expressed ChAT, ICC was used with antibodies against ChAT and immune cell-specific surface markers. Finally, to test the functional implications of the cholinergic system within BMDMs, the cytokine profile and the percentage of cell death was assessed after pharmacological treatment.

To begin, the expression of all cholinergic genes was assessed through PCRs that were run on a qPCR thermal cycler. According to the Cq values in Figure 4, it seems that most cholinergic genes were expressed by our tissues and cells of interest. However, even though the melt curve indicated that only one PCR product was amplified, the specificity of the PCR product was further assessed by running the PCR product on an agarose gel for each primer set. When running the PCR product on a gel, one representative sample of each tissue was used whereby the size of the band on the gel confirmed the specificity of the PCR product.

As for the PCRs of human PBMCs (Figure 4F), only one band of the appropriate size was detected for ChT, VAChT, CTL2, and OCTN1. This finding suggests that human

primers against ChT, VAChT, CTL2, and OCTN1 were specific. Although no band was detected for ChAT in human PBMCs (Figure 4F), the presence of a single predicted–sized band for ChAT in human U937 cells (Figure 4B), suggests that the human ChAT primers were also specific. Human primers against AChE and BChE also failed to generate a single clear band in human PBMCs (Figure 4F) but due to a lack of a positive control for these genes, we were unable to conclude whether these primers were specific. In the future, it would be useful to add this control to determine the specificity of our human primers against AChE and BChE. Taken together, human primers against ChT, VAChT, CTL2, OCTN1, and ChAT seem to be specific but the specificity of human AChE and BChE would require further confirmation.

In terms of mRNA expression, we found that ChT, VAChT, CTL2 and OCTN1 are expressed in human PBMCs. Our data also suggest that ChAT appears to be either below the limit of detection (LOD) or not expressed. As discussed earlier, we cannot draw conclusions regarding AChE and BChE. Much of the data corroborates with the previously created Database of Immune Cell Expression (DICE), where RNA sequencing was used to generate RNA expression profiles in immune cells (multiple T cell, B cell and monocyte subsets) isolated from human PBMCs by Fluorescence-activated cell sorting (FACS).[104] According to this database, OCTN1 and CTL2 are present in human PBMCs, while very low levels of ChAT mRNA are present in these cells.[104] Our data therefore confirm these findings. Conversely, ChT and VAChT were not detected in the DICE study, while our data show these mRNA were present in our samples.[104] Finally, the DICE showed that all immune cells analyzed expressed low levels of AChE, but little to no BChE, which we were unable to confirm due to the questionable specificity of our primers.[104] Altogether, our results in

conjunction with previous findings from DICE suggest that most of the cholinergic genes studied are expressed in human PBMCs, but some of these transcripts seem to have very low expression levels for which qPCR and next-generation sequencing have limited ability to accurately quantify.

As for mRNA quantification, qPCR is generally only reliable when Cq values are below 30 cycles. Some of the cholinergic genes assessed in this study were detected at Cq values above 30. This not only suggests that PBMCs have low expression levels for these genes, but also puts into question the reliability of the results. To further confirm and accurately measure the expression of weakly expressed genes, Droplet Digital PCR would be a more reliable technique. In fact, when a sample contains low levels of nucleic acids for a particular target ($Cq \geq 29$), Droplet Digital PCR technology produces more precise, reproducible, and statistically significant data.[105] Therefore, in the future, for cholinergic genes with Cq values above 29 cycles, their expression could be more reliably assessed through Droplet Digital PCR to circumvent the limitations of qPCRs.

Furthermore, we assessed the presence of one specific band at the predicted band size for each murine primer set within the mouse brain (Figure 4A), which served as the positive control. We were thus able to conclude that each murine primer set used herein were specifically targeting each cholinergic gene of interest. However, we obtained higher Cq values and observed faint or smeared bands in murine immune tissues (Figure 4C-E) for ChAT, VAChT and ChT. This leads us to interpret that these genes are either not expressed in immune tissues or their expression levels are so low that it falls below the LOD of PCRs. Therefore, we might similarly need to use a more sensitive technique such as Droplet Digital

PCR to detect the presence of ChAT, VAChT, and ChT within murine immune tissues at the transcript level.

In regard to validating the PCR results, sequencing the PCR product would be the best way to confirm that the observed band actually reflects the amplification of the gene of interest. This technique would thus be a great way to validate the results in Figure 4 as running the PCR product on a gel has its limitations. For instance, running a gel with the PCR product would not differentiate between different transcripts whose bands have either the same or very similar band sizes. Also, sequencing the PCR product would allow to identify different transcript variants of a particular gene that are similar in band sizes. Sequencing would thus be useful for genes like ChAT and AChE who have multiple variants. It would be interesting to investigate which variants of ChAT and AChE are expressed in immune tissues/cells. Also, assessing how their downstream proteins affect cellular function would be fascinating. Hence, sequencing the PCR product would be the most robust way to ensure that the PCR product of interest was indeed being amplified and to identify transcript variants.

ChAT has many different splice variants which include R-, N- and M-type.[106,107] These splice variants are generated from the coding gene region of the cholinergic gene locus and they produced a PCR product of the same band size with the primers used for Figure 4.[106,107] In fact, the M-type mRNA can translate into a large (82 kDa) and a small (69 kDa) isoform in human. [106,107] The isoforms of the ChAT protein made from these splice variants are more commonly known as common ChAT (cChAT) and peripheral ChAT (pChAT).[106,108] cChAT is predominantly found in the CNS whereas pChAT is preferentially expressed in peripheral neurons and has an expected molecular weight of 50 kDa. [106,108] The

isoform pChAT also does not contain the exons 6-9.[108] The evidence on cChAT and pChAT isoforms were found in the rat pterygopalatine ganglion.[108] It has also been shown that another mRNA splice variant in the human brain is translated into a 27 kDa ChAT protein.[106,108,109] This isoform does not have catalytic activity but may have a regulatory role on the activity of the larger forms of ChAT. [106,108,109] Hence, there are many different ChAT isoforms that exist and that translate into many different isoforms which could potentially differ in terms of function.

In fact, in our study we assessed the expression of ChAT proteins in immune tissues via western blots. According to Figure 5, it seems that ChAT was expressed at the protein level in murine immune tissues. However, since the band for immune tissues was detected at a different molecular weight than in the brain, it is likely that ChAT within immune tissues is a different isoform than the one found in neuronal tissues. Essentially, it seems that the band detected at around 48 kDa in the murine thymus and spleen was likely pChAT, especially since its band was confirmed with another pair of primary and secondary antibodies (Figure 5B). However, it is important to acknowledge that much of the research on pChAT and cChAT took place in rat tissues meaning that there might be some species-specific differences regarding ChAT isoforms. In addition, the second primary antibody against murine ChAT proteins was polyclonal and seemed to potentially detect all ChAT isoforms whereas the first primary antibody used was a monoclonal antibody binding to only one unspecified epitope. Indeed, there was an additional band detected at around 60 kDa in the spleen (Figure 5B) which was not detected with the monoclonal primary antibody. Moreover, the murine brain also detected additional bands at 75 kDa, 35 kDa, and 48 kDa with the polyclonal primary antibody (Figure 5B). These findings are not surprising given

the clonality of each murine ChAT antibody. Hence, additional bands might represent other isoforms of ChAT that were not previously detected with the first antibody or it could be a non-specific band. Additional bands would thus need to be confirmed with other primary antibody against ChAT or by using tissues from ChAT conditional knockout mice. Although the identity of these additional band(s) in the murine spleen and brain would require further investigation (Figure 5B), our data suggest that the murine thymus and spleen express pChAT.

In the murine BM, although the band was detected at a different molecular weight than the band for the murine brain, it seems that the BM might also expresses an isoform of ChAT. The molecular weight of the band detected in the murine BM was approximately 100 kDa. Hence, it is unlikely for pChAT to be the isoform expressed in the murine BM. Instead, it is possible for this band to represent cChAT with some post-translational modifications, which in turn may increase its molecular weight.

In fact, in a study examining different forms of ChAT in cerebral spinal fluid (CSF) and the plasma, the authors decided to label ChAT as G_1, G_2, and G_4 since ChAT is present as different molecular forms with distinct molecular weights. [106] The authors of this study used an analogous naming system for the molecular forms of ChAT to the naming system used for AChE and BChE who are often named based on the assembly of their globular subunits (G_n).[106] The authors observed some G_2 ChAT which had a molecular weight of 100-140 kDa.[106] Since G_1 ChAT had a molecular weight of 50-70 kDa, they believed that G_2 ChAT was made of two G_1 ChAT subunits.[106] Interestingly, G_2 ChAT was actually the most common complexed form of ChAT in CSF of human participants with AD.[106] Altogether, given what was shown in this sturdy, perhaps the murine BM expressed an

isoform similar to the G_2 form of ChAT (Figure 5A). Of course, this interpretation would only be suitable if such forms of ChAT are also present in the mouse. Unfortunately, no evidence of this form of ChAT in the mouse was found in the literature but it would be possible for ChAT in the BM to be in an isoform similar to the G_2 form of ChAT.

It is also possible that the band for the BM in Figure 5A to be due to non-specific binding, especially since we were unable to confirm its expression with another set of primary/secondary antibodies. The reason we were unable to confirm the BM findings was mostly due to limitations in terms of BM protein concentration and lack of sample. Therefore, although it seems more likely that ChAT was expressed in the BM, the lack of confirmation with a second primary antibody warrants further studies to validate these findings.

Furthermore, the expression of ChAT proteins was also assessed in human PBMCs. According to Figure 6, ChAT in human PBMCs was not expressed at 72 kDa. Rather, it seems that ChAT was detected at a molecular weight between 35 and 48 kDa in human PBMCs. The results were confirmed by using two separate antibodies targeting ChAT and the molecular weight was very similar to the positive control IMR-32. The ChAT in human PBMCs was likely a different isoform than cChAT. Perhaps, it was a variant of the pChAT expressed in human PBMCs, or rather it is possible for the pChAT expressed in human tissues to have a different post-translational modification than the pChAT in murine tissues. It could also be the previously mentioned 27 kDa isoform of human ChAT with some additional post-translational modifications.[106,108,109] Moreover, as previously mentioned, the two primary antibodies used against human tissues were polyclonal which makes this

antibody more likely to detect different isoforms. Taken together, it seems that ChAT was indeed expressed in human PBMCs but as a different isoform than IMR-32.

Overall, our findings suggest that the ChAT protein is expressed in the murine spleen, the murine thymus, and in human PBMCs. Even though it seems that the murine BM expresses ChAT, unfortunately it was not confirmed with another primary antibody. It is worth noting that although using a different primary antibody to confirm western blot results was used herein, it does not confirm the findings in an absolute fashion. The best way to confirm the findings would have been to compare the findings in Figures 5 and 6 with western blots on tissues from conditional ChAT knockout mice. Indeed, using such knockout animals would have also been useful in confirming the specificity of the primers used in Figure 4. However, we were unable to do this kind of confirmation due to the lack of available conditional knockout animals for cholinergic genes within immune tissues/cells. Nevertheless, our data suggest that isoforms of ChAT are expressed in the murine spleen, the murine thymus, the murine BM, and in human PBMCs.

As previously mentioned, AChE also has several splice variants. Splice variants for AChE include AChE-E, AChE-S, and AChE-R. [110–112] These splice variants differ in terms of solubility and subcellular localization.[110–112] All of these splice variants produced a PCR product of the same band size with the primers used for Figure 4. These different splice variants could translate into different isoforms. According to Figure 7, the murine thymus, the murine spleen, the murine BM, and the human PBMCs seemed to express AChE of a slightly higher molecular weight than the theoretical molecular weight and the band observed in the brain (positive control). Perhaps AChE had some post-translational modifications in immune tissues; especially when looking at the bands in the BM where

they may have differed due to post translational modifications. It is also possible that differences in molecular weights from the theoretical molecular weight and the molecular weight of the positive control may have been due to differences in isoforms or even non-specific binding. Generally, previous studies have shown that the band for AChE is anywhere between 55 and 78 kDa.[113–115] In fact, in one study comparing expression levels of AChE isoforms present in healthy human plasma and the plasma of individuals likely to have AD, they showed the expression of more than one band (both in the healthy and AD plasma samples), suggesting the presence of multiple AChE isoforms.[113] Overall, the bands observed in Figure 7 were detected within the range of AChE bands documented in the literature (with the exception of the band at 180 kDa), further suggesting that the thymus, the spleen, the BM, and the PBMCs expressed AChE. Collectively, our data suggest that AChE proteins are expressed in all immune tissues as different isoforms or as with different post-translational modifications but it is important to acknowledge that the results were not validated with tissues from conditional knockouts nor with another AChE primary antibody. Therefore, confirming AChE western blot results would be good future step.

Interestingly, IMR-32, a neuronal cell line was supposed to act as a human positive control for AChE. However, there was no band which could suggest that either IMR-32 did not express AChE or that it expressed an isoform not targeted by the primary antibody used herein. Also, not all neurons express AChE and the physiology within cell lines are often different from the physiology within primary cells. Therefore, the absence of a band in IMR-32 does not necessarily negate the band detected in human PBMCs (Figure 7B). Hence, AChE antibody validation warrants further investigation.

In addition, the expression of ChT proteins was assessed via western blots in the various immune tissues (Figure 8). Overall, the brain (which was used as a positive control) detected 3 bands, one at the predicted molecular weight (63 kDa), one at 75 kDa, and one at 25-35 kDa. Overall, it seems that the murine spleen and thymus expressed ChT but the murine BM and human PBMCs did not seem to express ChT as no bands were detected. In the literature, it has been well documented that ChT is expressed at around 60-75 kDa.[116–118] These variations in the latter reported molecular weight were likely due to differences in post-translational modifications. Therefore, it seems that the bands detected at 63 kDa and 75 kDa suggest the expression of ChT where there are differences in post-translational modifications. As for the band detected at 25-35 kDa, according to the literature, there is no evidence of a band at this size in previous studies so it is likely a result of nonspecific binding. ChT is commonly known to mostly be expressed in the nervous system where other transporter proteins such as CTL2 would mediate the transport of choline in non-neuronal cells.[79] Therefore, it is not surprising that the ChT transcript was barely expressed in the immune tissues of Figure 4 and that the murine BM in conjunction with the human PBMCs did not express ChT in Figure 8. Altogether, it seems that only the murine thymus and spleen expressed ChT proteins but in the future, the bands observed herein should be confirmed by either using tissues from conditional ChT knockouts or by using another primary antibody targeting ChT.

Once the expression of ChAT proteins was assessed in immune tissues via western blots, its expression was then assessed in immune cell subsets within the immune tissues. According to Figures 9-19, all immune cells assessed, except for MSCs, seemed to express ChAT. More specifically, within the spleen (Figures 9-12), T cells, B cells, and

macrophages stained positive for ChAT, however fewer than 50% of each immune cell type expressed the protein. In human PBMCs (Figures 16-19), T cells, B cells, and monocytes have been shown to express ChAT. Regarding the BM (Figures 13-15), less than 40% of B cells and monocytes seemed to express ChAT but the expression of ChAT in MSCs of the BM calls for further research.

Firstly, for Figure 13, it is important to acknowledge that the cell surface marker used for MSCs was CD105 which can also be used to identify endothelial cells and activated monocytes.[101,102] Staining for CD34, an endothelial cell marker was attempted but the staining was unsuccessful. Hence, either CD34 was not expressed in the BM or the antibody did not work properly despite all efforts. Regarding activated monocytes, CD11b stains all monocytes regardless of their activation state, whereas CD105 specifically stains the activated monocytes. Thus, it is possible that cells showing fluorescence for CD105 and CD11b represent an activated monocyte population. Therefore, by examining the data in Figures 13 and 14, it is possible that CD105+ChAT+ cells were mostly activated monocytes rather than MSCs. Regardless, it is important to acknowledge that the expression of ChAT proteins within BM derived MSCs warrants further investigation as it would be necessary to stain for more than one cell surface marker in addition to ChAT through flow cytometry or ICC to truly reveal the identity of the cells who colocalize ChAT with CD105. Even though we were not able confirm the presence of ChAT in BM derived MSCs, previous studies have shown that MSCs express ChAT and utilize its ACh to modulate inflammation through α7nAChR binding.[78] In fact, the mere addition of MSCs have been shown to reduce lymphocyte proliferation, IFNγ levels, and TNFα levels.[78] Therefore, given what has been

shown in the literature, it seems likely for MSCs to express ChAT but further research must occur to confirm the previous findings including its role in immunity.

Within human PBMCs (Figures 16-19), B cells, T cells, and monocytes expressed ChAT. Less than 40% of B cells and monocytes expressed ChAT but the results for T cells were conflicting. For T cells of human PBMCs (Figures 18-19), one sample had most of their T cells expressing ChAT while the other showed the opposite trend. Nonetheless, it is important to realize that Figures 18-19 only had an n of 2 so it is important to be cautious while interpreting these results. In the future, it would be important to study ChAT expression in a greater number of PBMC samples. In spite of this limitation, it seems that less than half of B cells and monocytes within human PBMCs expressed ChAT yet the percentage of its T cells expressing ChAT had a trend was that differed for the two samples, suggesting immune differences between these two human PBMC samples that were assessed.

Intriguingly, human PBMC Sample 1 in Figures 18-19 came from a participant with asthma. In fact, it has been shown that the cholinergic system plays a key role in the pathophysiology of asthma.[119] More specifically, in individuals with asthma, too much ACh binds to mAChRs.[119] Therefore, patients with asthma sometimes take anticholinergic drugs which act as antagonists to mAChRs.[119] Moreover, ACh levels have been shown to be elevated in skin biopsies from patients with atopic dermatitis which is usually related with bronchial asthma.[120,121] Also, patients with asthma have been shown to have an increased vagal tone.[122] It is quite possible for this increase in vagal tone to elevate the expression levels of ChAT within immune cells, leading ACh to bind to other cells in an autocrine or paracrine fashion. All these pieces of evidence in the literature might thus partially explain

why there are more T cells expressing ChAT in human PBMC Sample 1 (Figures 18 and 19). In closing, it would be interesting to conduct a study to assess differences in expression levels of cholinergic markers in human PBMCs from participants with asthma versus those who are healthy as it seems likely that the higher levels of ChAT in human PBMC Sample 1 was due to their asthma.

Among the ICC observed, as shown in Figures 9-12 and Figures 14-19, ChAT was detected in all immune cells within the murine BM, spleen, and human PBMCs. However, less than half of the cells from each immune cell type stained positive for ChAT, suggesting a regulated expression of this protein. Since the cells used for ICC experiments were not immunologically stimulated, this finding is in line with what would be expected as ChAT and ACh are reportedly not highly expressed without immunological stimulation.[63,83] Also, the ICC results especially seem to be valid for the murine spleen and human PBMCs since the ChAT primary antibodies that were used for these ICCs were the same as those validated in the western blots of immune tissues in Figures 5 and 6, respectively. Furthermore, the T cells of the spleen expressed ChAT, which is well known from the literature as it is a key component of the CAP.[9,10] Hence, the results for the immune cells derived from splenocytes (Figures 9-12) are further validated as they are in line with previous findings from the literature. Assessing the functional role of the cholinergic system present in each of the immune cells derived from each immune tissue would be intriguing as it has not been studied extensively. Taken together, less than half of B cells, T cells, and monocytes/macrophages within the murine spleen, BM, and human PBMCs seem to express ChAT but its function within each immune cell goes beyond the scope of this study.

Once the cholinergic markers were assessed in immune tissues and/or immune cells, the production of ACh was then assessed via UPLC coupled with triple quadrupole mass spectrometry in the murine spleen and thymus. Figure 20 shows the mass spectrometry results to assess ACh production in the murine spleen and thymus. According to these results, ACh was detectable in approximately half of the spleen and all thymus samples. In the literature, the thymic epithelial cell line named TE750 has been shown to express alpha-3, alpha-5 and beta-4 AChR as well as ChAT, suggesting that ACh can be produced by the thymic parenchyma.[123] Hence, our findings that ACh was produced in the thymus is in line with this finding from the literature. According to previous studies, ACh is produced in the spleen and is a key component of the CAP.[9,10] Therefore, ACh is expected to be detected in the spleen. The lack of expression in half of the spleen samples could be due to prolonged storage of those samples leading to ACh degradation or due to the age of the mice from which the spleens were harvested. Indeed, evidence has shown that aging decreases the synthesis of ACh in the brain and cardiomyocytes.[124] Therefore, it is likely that a similar effect would be observed in the spleen making it possible that the ACh levels were not detectable because of the age of these mice. Further, the expression of ACh in the murine BM and human PBMCs should have been assessed as well but many limitations encountered prevented us from extending our study to these immune tissues. Finally, it would have also be a good idea to isolate individual immune cells through FACS or magnetic-activated cell sorting from immune tissues and assess their endogenous ACh levels. Nonetheless, it seems that ACh is produced in the murine thymus and spleen, but it would be important to gather fresh spleen samples from younger adult mice to confirm the interpretations regarding the spleen tissue.

To evaluate the function of cholinergic markers in BMDMs, a pharmacological approach with different treatment conditions (Table 6) was used. After culturing and stimulating the M1/M2 BMDMs, the supernatant of each condition was harvested to assess the cytokine levels via CBAs. Before discussing the results in Figures 21-25, it is important to first acknowledge that the sample size was not sufficiently large for statistical analysis due to severe order delays of the CBA kits used herein. Therefore, only the trend can be discussed for these results (see section 3.4 for more information).

For conditions containing ChAT inhibitors, it is worth noting that when comparing to the LPS Only group, the levels of IL-10, IL-6, and TNF were lower in terms of trend for the LPS + BrACh and the LPS + α-Neta condition of M1/M2 polarized BMDMs. Therefore, there was a potential slight reduction in these cytokines for the LPS + BrACh and the LPS + α-Neta conditions in M1/M2 BMDMs. Studies show that ACh has anti-apoptotic properties in keratocytes and cardiomyocytes.[125–127] Hence, it is likely that this property is maintained in the ACh found within BMDMs. In addition, in sepsis, it has been shown that administering apoptotic cells reduce the levels of cytokines in their environment.[128] Although IL-10 is commonly known as an anti-inflammatory cytokine, the levels of IL-10 have been shown to be significantly higher in patients with severe sepsis.[129–131] Therefore, the attenuation of the cytokine storm by administrating apoptotic cells would include the reduction in levels of IL-10, not only proinflammatory cytokines. Regarding our study, these findings in the literature would suggest that perhaps ChAT inhibitors reduced cytokine levels by increasing apoptosis.

Correspondingly, in this study, the supernatant from each condition (Table 6) of the M1/M2 BMDMs was used to assess the percentage of cell death through a fluorescent LDH

assay. LDH levels may be used to measure cytotoxicity and apoptosis.[132] Upon examining the LDH results in M1 and M2 polarized BMDMs (Figures 26 and 27, respectively), the addition of ChAT inhibitors seemingly increased the percentage of cell death in a non-statistically significant fashion for M2 BMDMs and in a statistically significant manner for M1 BMDMs. These results from the LDH assay further suggest that supplementation of ChAT inhibitors like BrACh and α-Neta lead to an increase in apoptosis by preventing ACh synthesis, which in turn, might lead to more apoptosis. Consequently, this surge in apoptosis would reduce IL-10, IL-6, and TNF levels while increasing LDH levels (Figures 21-27). In future studies, it would be interesting to measure levels of caspase-3 or use an apoptosis assay after treating with LPS + BrACh and LPS + α-Neta to confirm whether this observation was due to apoptosis rather than necrosis or cytotoxicity. Such experiments would also clarify the role of ACh regarding apoptosis in an immune environment.

As for treatment conditions that did not involve ChAT inhibition, the percentage of cell death depicted in Figure 26 suggests that all other conditions did not seem to cause cell death in M1 polarized BMDMs. Therefore, the latter results suggest that the cytokine effects observed in Figures 21- 23 for the other conditions (which do not involve inhibition of ChAT), were not likely due to apoptosis, necrosis, nor cytotoxicity. The results for the % cell death in M1 polarized BMDMs (Figure 26) were similar to those for the % cell death in M2 polarized BMDMs (Figure 27). However, in Figure 27, there was no statistical significance and the level of % cell death for the LPS +ML352 seemed slightly more elevated in terms of trend for M2 polarized BMDMs. The results from Figure 27 thus suggest that changes in cytokine levels in M2 polarized BMDMs (Figures 24 and 25) were not likely due to apoptosis, necrosis, nor cytotoxicity for the conditions that do not involve

ChAT or ChT inhibition. Altogether, among M1 BMDMs the only conditions that seem to cause cell death involves the inhibition of ChAT whereas among M2 BMDMs the only conditions that seem to potentially cause cell death involved the inhibition of ChAT and ChT.

For treatment conditions that did not contain ChAT inhibitors, IL-10 levels did not seem to change within M1 BMDMs (Figure 21). These results are not surprising since ACh reportedly does not change IL-10 levels.[6,133,134] In reality, ACh displays its anti-inflammatory effect primarily by reducing levels of proinflammatory cytokines such as IL-6 and TNF. [6,10,134] Whether these effects hold true outside of the CAP induced by VNS has not been clarified. For that reason, it was important to assess the functional role of the cholinergic system within M1/M2 BMDMs by measuring levels of proinflammatory cytokines such as TNF and IL-6. The following paragraphs will thus discuss the effect of Ch, ACh, galantamine, and ML352 in the presence of LPS on IL-6 and TNF levels.

A condition containing Ch and LPS was added to assess Ch's effect on inflammation. In Figures 22-25, Ch did not seem to have much of an effect when considering the averages and its SEM. This finding was not expected since Ch has been shown to have an anti-inflammatory effect in numerous studies.[135–137] However, the treatments used herein were added in an acute fashion (the BMDMs were treated for 5 hours), whereas the studies suggesting that Ch has an anti-inflammatory effect, treated with Ch for 24 hours to a few days.[135,137] Therefore, perhaps the reason why Ch did not seem to have much of an anti-inflammatory effect (by reducing levels of TNF and IL-6 in Figures 22-25) was because of the shorter stimulation/treatment time used herein. In addition, in a paper by Parrish et al., Ch did not seem to have a statistically significant effect on reducing

inflammation at a concentration of 100 μM in RAW 264.7 cells, a monocyte/macrophage murine cell line.[68] In fact, Ch at a concentration of 50 mM had the most significant anti-inflammatory effect by significantly reducing TNF and nuclear NF-κB levels.[68] Going forward, it would thus be a good idea to test different incubation times and see if Ch has more of an effect after 24 hours of treatment time. It would also be a good idea to assess higher Ch concentrations. Nonetheless, in the study herein, Ch did not seem to have much of an effect on inflammation and further optimization would have to take place to truly see whether Ch would prevent inflammation in BMDMs.

Furthermore, a treatment condition with ACh and LPS was added to assess ACh's effect as an agonist to AChRs. The LPS + ACh condition in Figures 22-25, seemed to cause anywhere from no changes to a slight increase in proinflammatory cytokine levels. As previously mentioned, in an immune context, ACh is more commonly known for its anti-inflammatory role. For instance, when ACh binds to α7nAChRs, it has been shown to induce an anti-inflammatory immune response mainly by preventing the release of proinflammatory cytokines.[6,10,39,44,48,68,83,138] However, when ACh binds to some mAChRs, it can induce a proinflammatory immune response.[139,140] Collectively, it seems that ACh's effect on inflammation might differ depending on the receptor it interacts with.

In regards to mAChRs, one study suggested that in cigarette smoke-induced inflammation, the M3 mAChRs of the airway parenchymal cells played a key role in the proinflammatory effects of ACh.[139,140] It has also been reported that Tiotropium, a long acting muscarinic antagonist which has a higher selectivity to M3 muscarinic receptors, reduced pulmonary inflammation in a mouse COPD model induced by cigarette smoke.[140,141] Moreover, M1 mAChRs , M5 mAChRs , and M3 mAChRs can all directly

activate phospholipase C which activates protein kinase C downstream.[140,141] The activation of protein kinase C can in turn activate pathways leading to inflammation such as the Mitogen-activated protein kinase pathway and NF-κB.[140,141] In contrast to ACh's ability to bind to nAChRs and mAChRs, agonists such as nicotine interact with α7nAChRs but not mAChRs, and as such, nicotine is relatively well known to induce anti-inflammatory effects.[142–145] Interestingly, nicotine has been shown to be an antagonist of the α9nAChRs and the α9α10nAChRs.[146–148] Perhaps the findings observed in Figures 22-25 reflect the net change in IL-6 and TNF levels as it binds to both nAChRs and mAChR amongst BMDMs. Unfortunately, there is a lack of evidence in the literature regarding the relative expression of mAChRs and nAChRs in BMDMs and differences in ACh affinity to mAChRs and nAChRs. In future studies, it would thus be interesting to assess the effects of adding mAChRs antagonists and muscarine, an agonist specific to mAChRs. In general, it seems possible that the effect of ACh on BMDMs in terms of inflammation relies on a net effect between the proinflammatory immune response resulting from its binding to certain mAChR subtypes and the anti-inflammatory immune resulting from its binding to certain nAChR subtypes.

In addition, treatment conditions containing galantamine, an AChE inhibitor, were used to assess the functional role of AChE in BMDMs. Among the CBAs, there were two conditions containing galantamine: LPS + ACh + Galantamine and LPS + Galantamine. More specifically, the LPS + ACh + Galantamine condition assessed the effect that ACh would have in conjunction with galantamine's effect as an AChE inhibitor within BMDMs. Overall, in Figures 23-25, the addition of galantamine seemed to reduce the amount of proinflammatory cytokines released in non-statistically significant fashion. Although AChE

was expressed in the BM according to Figures 4C and 7A, given that ACh seems to have more of a proinflammatory effect herein, it does not seem likely for galantamine's somewhat anti-inflammatory effect to be due to its inhibition of AChE because if ACh caused a net proinflammatory effect and the degradation of ACh was inhibited, then theoretically a more pronounced proinflammatory effect would take place as there would be an increase in ACh levels. Rather, in numerous studies, galantamine has been shown to act as a positive allosteric modulator (PAM) of nAChRs; meaning that it alters the confirmation of these receptors to help agonists bind to them.[149,150] However, another study showed different results where galantamine did not seem to act as a PAM.[151] The authors have shown that galantamine's ability to inhibit ACh degradation increased approximately eight-fold near nAChRs.[151] Therefore, it seems that galantamine's somewhat anti-inflammatory effect was either because it acted as a PAM of nAChRs or because of galantamine's ability to inhibit ACh's degradation increases near nAChRs, thus theoretically increasing the amount ACh nearby nAChRs. However, it currently does not seem to be known if that increase in AChE inhibition would also take place near mAChRs. In summary, galantamine seemed to have an anti-inflammatory effect in BMDMs but the reason for its effect while considering the other findings herein remains unclear.

Given what has previously been discussed regarding the treatment of ACh with LPS, it makes sense that the levels of TNF for the LPS + ACh + galantamine condition was somewhat slightly higher than the LPS + galantamine condition (Figures 23 and 25). However, further research would have to take place to assess why galantamine caused somewhat of an overall anti-inflammatory effect.

Unlike TNF, adding galantamine did not seem to have much of an effect on IL-6 in M1 polarized BMDMs (Figure 22). Moreover, given the larger error bars in Figure 24, one can argue that galantamine does not have much of an effect on IL-6 in M2 polarized BMDMs as well. Perhaps this is due to using acute treatment conditions which only provided enough time for TNF secretion, one of the most prominent and early proinflammatory cytokines, to have an observable effect at the 5 hour timepoint used in this study.[152] Regardless, as current circumstances made us settle for an inadequate sample size, it is reasonable to believe that the data in Figure 22 and Figure 24 would have shown more of a trend with the intended sample size. Hence, it seems that the lack of effect that galantamine had on IL-6 in BMDMs might be a matter of timing.

As for the next treatment condition, a pharmacological condition containing ML352 was initially added to assess ChT's inflammatory role in BMDMs. In Figures 22, 24, and 25, it seems that ML-352 did not have any significant effect on cytokine release. However, even though none of the data in Figures 22-25 were statistically significant, it seems that in M1 BMDMs, TNF release was slightly increased (Figure 23). Since Figure 8D suggests that ChT proteins were not expressed in the BM, it seems unlikely for the potential increase in TNF levels (Figure 23) to be due to the inhibition of ChT. Also, according to Figure 4, it seems much more likely for Ch to be transported through CTL2 rather than ChT; especially since ChT was shown to only be expressed in the nervous system while CTL2 was shown to be a more suitable candidate for Ch transport in immune cells.[79] It is also worth noting that ML352 is a specific inhibitor of ChT.[100] In other words, it does not reportedly inhibit CTL2. Therefore, in BMDMs, ML352's effect does not seem to be due to its ability to inhibit ChT.

Indeed, it is more likely for the potential effect on TNF levels in M1 polarized BMDMs (Figure 23) to be due to some off-target effect of ML352. In fact, ML352 was shown to inhibit the β2-Adrenergic receptors with 43% inhibition and nAChRs at 13% inhibition.[100] ML352 was also shown to partially inhibit histamine receptors (7-37% inhibition) but these receptors have not been shown to be widely expressed in the BM. It thus seems that the potentially elevated levels of TNF with the addition of ML352 in M1 BMDMs (Figure 23) to be due to the inhibition of other receptors such as the β2-Adrenergic receptors.

According to the literature, β2-Adrenergic receptors seem to be expressed in BMDMs in conjunction with immune cells and they have been shown to play an important role in preventing inflammation through reducing the levels of TNF-α while increasing the levels of IL-10 by using a β2-Adrenergic receptor knock out animal.[153] Moreover, it is quite possible that the same potential effect would have been observed on TNF levels in Figure 25 if the % cell death was lower. In other words, it seems that the higher % cell death of the M2 polarized BMDMs treated with LPS + ML352 (Figure 27) might be the reason for the lack of this effect on TNF in Figure 25. In addition, this condition did not seem to influence IL-6 (Figures 22 and 24). In the literature, it was shown that the stimulation of β2-Adrenergic receptors induced the differentiation of macrophages into an M2 polarization and increased the release of cytokines, such as IL-6 and TGFβ, while reducing the production of proinflammatory cytokines such as TNF-α.[154,155] Therefore, without cell death, it would be possible for ML352 to have the opposite effect on IL-6. Furthermore, another potential reason for this finding might be because, as previously discussed, an acute treatment condition was used which only provided enough time for TNF, one of the most important

proinflammatory cytokines to have an effect.[152] In the future, it would be interesting to see the effects of adding ML352 with an antagonist of β2-Adrenergic receptors. Overall, it seems more probable that ML352's effects in BMDMs are off-target.

Polarization into M1 or M2 BMDMs seemed to have little to no effect on how the BMDMs responded to the treatments (at the exception of what has been previously mentioned). As expected, in general, the amount of TNF secreted from M1 BMDMs was higher than the quantity of TNF secreted from M2 BMDMs (Figures 22 and 24). In contrast, there was generally more IL-6 released from M2 polarized BMDMs than IL-6 secreted from M1 polarized BMDMs (Figures 23 and 25). It has been shown in murine BMDMs that IL-6 is actually a cytokine that is released when cells are treated in vitro with IL-4; which was one of the cytokines that were used herein for macrophage M2 polarization.[156] It has also been shown that IL-6 might play a pleiotropic role whereby it can act as a cytokine that increases inflammation but it can also help with the differentiation of M2 polarized macrophages in mouse and human cells.[157] Interestingly, in one study, IL-6 seemed to act as a cytokine released from Th2 cells (alternatively activated T cells) which in turn stimulated M2 polarization in macrophages of adipose tissue from obese mice.[158] In addition, the reason there was no Figure for IL-10 in M2 BMDMs was because the levels were below the LOD. Perhaps this was because IL-10 was only expressed in conditions whereby it is needed to counterbalance significant proinflammatory environments such as those found in M1 BMDMs. In general, the effects of the treatment conditions assessed herein did not seem to change in M1 and M2 polarized BMDMs for IL-6 and TNF however, the concentrations of IL-6 and TNF changed in a way that reflected their roles in the immune system.

In closing, it would be necessary to acquire the CBA data for the full sample size to confirm the current trends resulting from pharmacological treatments in BMDMs. In addition, it would be interesting to extend this study to human PBMCs. Subsequently, it would be valuable to assess the phenotype of macrophages within BMDMs and PBMCs after pharmacological treatment. Given the pharmacological limitations experiences herein, if there were no financial limitations, it would have been better to isolate BM cells from conditional knock-out animals. Lastly, further research is necessary to determine the functional importance of the cholinergic system in immune tissues which could provide novel targets for inflammatory and autoimmune diseases as they are caused by mis regulation of inflammation and of the immune response, respectively. Despite the limitations experienced herein, our findings provided novel insights on the cholinergic system within immune cells and tissues which serves as a fundamental step in fully understanding the cholinergic system's role in immunity.

Conclusion

Taken together, our data show that ChAT and AChE are expressed in the murine thymus, murine spleen, murine BM, and human PBMCs. Also, ChT seems to be expressed in the spleen and thymus but not in the BM and PBMCs. All the immune cells of interest (T cells, B cells, and monocytes/macrophages) express ChAT within the spleen, BM, and human PBMCs at a low cell percentage. On the contrary, ChAT within BM derived MSCs is still unclear. Moreover, ACh seems to be produced in the murine thymus as well as in the murine spleen. Altogether, the cholinergic machinery required for ACh synthesis seems to be expressed within immune cells derived from immune tissues.

Some of the data from the pharmacological studies disagree with the original hypothesis, unraveling another potential role for the cholinergic system in immune function. First, the addition of ChAT inhibitors seems to significantly cause cell death in M1 BMDMs but to not significantly cause cell death in M2 BMDMs, leading to low cytokine levels. Ch does not seem to have an effect on acute inflammation, ACh seems to have a potential proinflammatory effect, galantamine seems to reduce inflammation, and ML352 seems to promote inflammation in M1 BMDMs. However, the pharmacological effects of galantamine and ML352 in BMDMs seem to potentially be due to off target effects rather than through inhibition of AChE and ChT, respectively. It is also important to acknowledge that these effects are only discussed in relation to the trend and not statistical significance due to the limited sample size.

The data herein provides progress towards revealing the functional role of cholinergic markers within immune cells. More specifically, the evidence in this thesis

might be the first step in discovering another role for the cholinergic system within immune cells/tissues, resulting in a more complete understanding on its role in immunity. This research is thus a necessary step in the search of novel targets for drugs against autoimmune and inflammatory diseases.

References

1. Tiwari, P., Dwivedi, S., Singh, M. P., Mishra, R. & Chandy, A. Basic and modern concepts on cholinergic receptor: A review. *Asian Pac. J. Trop. Dis.* **3,** 413–420 (2013).
2. Horiuchi, Y., Kimura, R., Kato, N., Fujii, T., Seki, M., Endo, T., Kato, T. & Kawashima, K. Evolutional study on acetylcholine expression. *Life Sci.* **72,** 1745–56 (2003).
3. Kenney, M. J. & Ganta, C. K. Autonomic nervous system and immune system interactions. *Compr. Physiol.* **4,** 1177–1200 (2014).
4. Abbas, A., Lichtman, A. & Pillai, S. *Cellular and Molecular Immunology*. (Elsevier, 2017).
5. Meregnani, J., Clarençon, D., Vivier, M., Peinnequin, A., Mouret, C., Sinniger, V., Picq, C., Job, A., Canini, F., Jacquier-Sarlin, M. & Bonaz, B. Anti-inflammatory effect of vagus nerve stimulation in a rat model of inflammatory bowel disease. *Auton. Neurosci. Basic Clin.* **160,** 82–89 (2011).
6. Borovikova, L. V., Ivanova, S., Zhang, M., Yang, H., Botchkina, G. I., Watkins, L. R., Wang, H., Abumrad, N., Eaton, J. W. & Tracey, K. J. Vagus nerve stimulation attenuates the systemic inflammatory response to endotoxin. *Nature* **405,** 458–462 (2000).
7. Cox, M. A., Bassi, C., Saunders, M. E., Nechanitzky, R., Morgado-Palacin, I., Zheng, C. & Mak, T. W. Beyond neurotransmission: acetylcholine in immunity and inflammation. *J. Intern. Med.* **287,** 120–133 (2020).

8. Kawashima, K., Fujii, T., Misawa, H., Yamada, S., Tajima, S., Suzuki, T., Fujimoto, K. & Kasahara, T. in *Neurochem. Cell. Mol. Clin. Asp.* (eds. Teelken, A. & Korf, J.) 813–819 (Springer US, 1997). doi:10.1007/978-1-4615-5405-9_134
9. Reardon, C., Duncan, G. S., Brüstle, A., Brenner, D., Tusche, M. W., Olofsson, P. S., Olofsson, P., Rosas-Ballina, M., Tracey, K. J. & Mak, T. W. Lymphocyte-derived ACh regulates local innate but not adaptive immunity. *Proc. Natl. Acad. Sci. U. S. A.* **110,** 1410–1415 (2013).
10. Rosas-Ballina, M., Olofsson, P. S., Ochani, M., Valdés-Ferrer, S. I., Levine, Y. A., Reardon, C., Tusche, M. W., Pavlov, V. A., Andersson, U., Chavan, S., Mak, T. W. & Tracey, K. J. Acetylcholine-synthesizing T cells relay neural signals in a vagus nerve circuit. *Science* **334,** 98–101 (2011).
11. Wang, L., Wang, F.-S. & Gershwin, M. E. Human autoimmune diseases: a comprehensive update. *J. Intern. Med.* **278,** 369–395 (2015).
12. Podbielska, M., Banik, N. L., Kurowska, E. & Hogan, E. L. Myelin Recovery in Multiple Sclerosis: The Challenge of Remyelination. *Brain Sci.* **3,** 1282–1324 (2013).
13. de Castro, B. M., De Jaeger, X., Martins-Silva, C., Lima, R. D. F., Amaral, E., Menezes, C., Lima, P., Neves, C. M. L., Pires, R. G., Gould, T. W., Welch, I., Kushmerick, C., Guatimosim, C., Izquierdo, I., Cammarota, M., Rylett, R. J., Gomez, M. V., Caron, M. G., Oppenheim, R. W., Prado, M. A. M. & Prado, V. F. The Vesicular Acetylcholine Transporter Is Required for Neuromuscular Development and Function. *Mol. Cell. Biol.* **29,** 5238–5250 (2009).
14. Choline transporters. *Br. J. Pharmacol.* **158,** S187 (2009).
15. Rand, J. Acetylcholine. *WormBook* (2007). doi:10.1895/wormbook.1.131.1

16. Fujii, T., Mashimo, M., Moriwaki, Y., Misawa, H., Ono, S., Horiguchi, K. & Kawashima, K. Physiological functions of the cholinergic system in immune cells. *J. Pharmacol. Sci.* **134,** 1–21 (2017).
17. Gabay, C. Interleukin-6 and chronic inflammation. *Arthritis Res. Ther.* **8,** S3 (2006).
18. Tanaka, T., Narazaki, M. & Kishimoto, T. IL-6 in Inflammation, Immunity, and Disease. *Cold Spring Harb. Perspect. Biol.* **6,** (2014).
19. Tie, R., Li, H., Cai, S., Liang, Z., Shan, W., Wang, B., Tan, Y., Zheng, W. & Huang, H. Interleukin-6 signaling regulates hematopoietic stem cell emergence. *Exp. Mol. Med.* **51,** 1–12 (2019).
20. Su, H., Lei, C.-T. & Zhang, C. Interleukin-6 Signaling Pathway and Its Role in Kidney Disease: An Update. *Front. Immunol.* **8,** (2017).
21. Luo, Y. & Zheng, S. G. Hall of Fame among Pro-inflammatory Cytokines: Interleukin-6 Gene and Its Transcriptional Regulation Mechanisms. *Front. Immunol.* **7,** (2016).
22. Parameswaran, N. & Patial, S. Tumor Necrosis Factor-α Signaling in Macrophages. *Crit. Rev. Eukaryot. Gene Expr.* **20,** 87–103 (2010).
23. Iyer, S. S. & Cheng, G. Role of Interleukin 10 Transcriptional Regulation in Inflammation and Autoimmune Disease. *Crit. Rev. Immunol.* **32,** 23–63 (2012).
24. Wills-Karp, M., Nathan, A., Page, K. & Karp, C. L. New insights into innate immune mechanisms underlying allergenicity. *Mucosal Immunol.* **3,** 104–110 (2010).
25. Delgado-Vélez, M. & Lasalde-Dominicci, J. A. The Cholinergic Anti-Inflammatory Response and the Role of Macrophages in HIV-Induced Inflammation. *Int. J. Mol. Sci.* **19,** (2018).

26. Chu, H. X., Arumugam, T. V., Gelderblom, M., Magnus, T., Drummond, G. R. & Sobey, C. G. Role of CCR2 in inflammatory conditions of the central nervous system. *J. Cereb. Blood Flow Metab.* **34,** 1425–1429 (2014).
27. Lee, P. Y., Wang, J.-X., Parisini, E., Dascher, C. C. & Nigrovic, P. A. Ly6 family proteins in neutrophil biology. *J. Leukoc. Biol.* **94,** 585–594 (2013).
28. Auffray, C., Sieweke, M. H. & Geissmann, F. Blood Monocytes: Development, Heterogeneity, and Relationship with Dendritic Cells. *Annu. Rev. Immunol.* **27,** 669–692 (2009).
29. Laffer, B., Bauer, D., Wasmuth, S., Busch, M., Jalilvand, T. V., Thanos, S., Meyer zu Hörste, G., Loser, K., Langmann, T., Heiligenhaus, A. & Kasper, M. Loss of IL-10 Promotes Differentiation of Microglia to a M1 Phenotype. *Front. Cell. Neurosci.* **13,** (2019).
30. Rőszer, T. Understanding the Mysterious M2 Macrophage through Activation Markers and Effector Mechanisms. *Mediators Inflamm.* **2015,** (2015).
31. Ben-Mordechai, T., Lawrence, Y., Symon, Z., Shimoni-Sebag, A., Appel, S. & Amit, U. CX3CR1 Expressing Macrophages Infiltrate the Tumor Microenvironment and Promote Radiation Resistance in a Mouse Model of Lung Cancer. *Int. J. Radiat. Oncol. • Biol. • Phys.* **105,** S125–S126 (2019).
32. Burgess, M., Wicks, K., Gardasevic, M. & Mace, K. A. Cx3CR1 Expression Identifies Distinct Macrophage Populations That Contribute Differentially to Inflammation and Repair. *ImmunoHorizons* **3,** 262–273 (2019).

33. Bandeira-Melo, C., Cordeiro, R. S., Silva, P. M. & Martins, M. A. Modulatory role of eosinophils in allergic inflammation: new evidence for a rather outdated concept. *Mem. Inst. Oswaldo Cruz* **92,** 37–43 (1997).
34. Eosinophils in allergy: role in disease, degranulation, and cytokines - PubMed. at <https://pubmed.ncbi.nlm.nih.gov/8620088/>
35. Dale, H. H. & Dudley, H. W. The presence of histamine and acetylcholine in the spleen of the ox and the horse. *J. Physiol.* **68,** 97–123 (1929).
36. Chang, H. C. & Gaddum, J. H. Choline esters in tissue extracts. *J. Physiol.* **79,** 255–285 (1933).
37. Tracey, K. J. Physiology and immunology of the cholinergic antiinflammatory pathway. *J. Clin. Invest.* **117,** 289–96 (2007).
38. *Heart Failure Management: The Neural Pathways*. (Springer International Publishing, 2016). at <https://www.springer.com/gp/book/9783319249919>
39. Pavlov, V. A. & Tracey, K. J. The vagus nerve and the inflammatory reflex—linking immunity and metabolism. *Nat. Rev. Endocrinol.* **8,** 743–754 (2012).
40. Johnson, R. L. & Wilson, C. G. A review of vagus nerve stimulation as a therapeutic intervention. *J. Inflamm. Res.* **Volume 11,** 203–213 (2018).
41. Bonaz, B., Picq, C., Sinniger, V., Mayol, J. F. & Clarençon, D. Vagus nerve stimulation: from epilepsy to the cholinergic anti-inflammatory pathway. *Neurogastroenterol. Motil. Off. J. Eur. Gastrointest. Motil. Soc.* **25,** 208–221 (2013).
42. Yu, Z. J., Weller, R. A., Sandidge, K. & Weller, E. B. Vagus nerve stimulation: can it be used in adolescents or children with treatment-resistant depression? *Curr. Psychiatry Rep.* **10,** 116–122 (2008).

43. Bonaz, B., Sinniger, V., Hoffmann, D., Clarençon, D., Mathieu, N., Dantzer, C., Vercueil, L., Picq, C., Trocmé, C., Faure, P., Cracowski, J.-L. & Pellissier, S. Chronic vagus nerve stimulation in Crohn's disease: a 6-month follow-up pilot study. *Neurogastroenterol. Motil. Off. J. Eur. Gastrointest. Motil. Soc.* **28,** 948–953 (2016).
44. Bonaz, B., Sinniger, V. & Pellissier, S. Anti-inflammatory properties of the vagus nerve: potential therapeutic implications of vagus nerve stimulation. *J. Physiol.* **594,** 5781–5790 (2016).
45. Yin, J., Ji, F., Gharibani, P. & Chen, J. D. Vagal Nerve Stimulation for Glycemic Control in a Rodent Model of Type 2 Diabetes. *Obes. Surg.* **29,** 2869–2877 (2019).
46. Al-Dwairi, A., Alqudah, T. E., Al-Shboul, O., Alqudah, M., Mustafa, A. G. & Alfaqih, M. A. Glucagon-like peptide-1 exerts anti-inflammatory effects on mouse colon smooth muscle cells through the cyclic adenosine monophosphate/nuclear factor-κB pathway in vitro. *J. Inflamm. Res.* **11,** 95–109 (2018).
47. Insuela, D. B. R. & Carvalho, V. F. Glucagon and glucagon-like peptide-1 as novel anti-inflammatory and immunomodulatory compounds. *Eur. J. Pharmacol.* **812,** 64–72 (2017).
48. Koopman, F. A., Chavan, S. S., Miljko, S., Grazio, S., Sokolovic, S., Schuurman, P. R., Mehta, A. D., Levine, Y. A., Faltys, M., Zitnik, R., Tracey, K. J. & Tak, P. P. Vagus nerve stimulation inhibits cytokine production and attenuates disease severity in rheumatoid arthritis. *Proc. Natl. Acad. Sci. U. S. A.* **113,** 8284–8289 (2016).
49. van Maanen, M. A., Lebre, M. C., van der Poll, T., LaRosa, G. J., Elbaum, D., Vervoordeldonk, M. J. & Tak, P. P. Stimulation of nicotinic acetylcholine receptors attenuates collagen-induced arthritis in mice. *Arthritis Rheum.* **60,** 114–122 (2009).

50. van Maanen, M. A., Stoof, S. P., Larosa, G. J., Vervoordeldonk, M. J. & Tak, P. P. Role of the cholinergic nervous system in rheumatoid arthritis: aggravation of arthritis in nicotinic acetylcholine receptor α7 subunit gene knockout mice. *Ann. Rheum. Dis.* **69,** 1717–1723 (2010).
51. Pellissier, S., Dantzer, C., Canini, F., Mathieu, N. & Bonaz, B. Psychological adjustment and autonomic disturbances in inflammatory bowel diseases and irritable bowel syndrome. *Psychoneuroendocrinology* **35,** 653–662 (2010).
52. Pellissier, S., Dantzer, C., Mondillon, L., Trocme, C., Gauchez, A.-S., Ducros, V., Mathieu, N., Toussaint, B., Fournier, A., Canini, F. & Bonaz, B. Relationship between vagal tone, cortisol, TNF-alpha, epinephrine and negative affects in Crohn's disease and irritable bowel syndrome. *PloS One* **9,** e105328 (2014).
53. Bansal, V., Ryu, S. Y., Lopez, N., Allexan, S., Krzyzaniak, M., Eliceiri, B., Baird, A. & Coimbra, R. Vagal stimulation modulates inflammation through a ghrelin mediated mechanism in traumatic brain injury. *Inflammation* **35,** 214–220 (2012).
54. dos Santos, C. C. dos, Shan, Y., Akram, A., Slutsky, A. S. & Haitsma, J. J. Neuroimmune regulation of ventilator-induced lung injury. *Am. J. Respir. Crit. Care Med.* **183,** 471–482 (2011).
55. Slade, E., Tamber, P. S. & Vincent, J.-L. The Surviving Sepsis Campaign: raising awareness to reduce mortality. *Crit. Care Lond. Engl.* **7,** 1–2 (2003).
56. Wang, D.-W., Yin, Y.-M. & Yao, Y.-M. Vagal Modulation of the Inflammatory Response in Sepsis. *Int. Rev. Immunol.* **35,** 415–433 (2016).
57. Klapproth, H., Reinheimer, T., Metzen, J., Münch, M., Bittinger, F., Kirkpatrick, C. J., Höhle, K.-D., Schemann, M., Racké, K. & Wessler, I. Non-neuronal acetylcholine, a

signalling molecule synthezised by surface cells of rat and man. *Naunyn. Schmiedebergs Arch. Pharmacol.* **355,** 515–523 (1997).

58. Wessler, I., Kirkpatrick, C. J. & Racké, K. Non-neuronal acetylcholine, a locally acting molecule, widely distributed in biological systems: Expression and function in humans. *Pharmacol. Ther.* **77,** 59–79 (1998).
59. Yamada, T., Fujii, T., Kanai, T., Amo, T., Imanaka, T., Nishimasu, H., Wakagi, T., Shoun, H., Kamekura, M., Kamagata, Y., Kato, T. & Kawashima, K. Expression of acetylcholine (ACh) and ACh-synthesizing activity in Archaea. *Life Sci.* **77,** 1935–1944 (2005).
60. Fujii, T., Mashimo, M., Moriwaki, Y., Misawa, H., Ono, S., Horiguchi, K. & Kawashima, K. Expression and Function of the Cholinergic System in Immune Cells. *Front. Immunol.* **8,** (2017).
61. Ogawa, H., Fujii, T., Watanabe, Y. & Kawashima, K. Expression of multiple mRNA species for choline acetyltransferase in human T-lymphocytes. *Life Sci.* **72,** 2127–2130 (2003).
62. Kawashima, K. & Fujii, T. Extraneuronal cholinergic system in lymphocytes. *Pharmacol. Ther.* **86,** 29–48 (2000).
63. Kawashima, K., Yoshikawa, K., Fujii, Y. X., Moriwaki, Y. & Misawa, H. Expression and function of genes encoding cholinergic components in murine immune cells. *Life Sci.* **80,** 2314–2319 (2007).
64. Jiang, W., Li, D., Han, R., Zhang, C., Jin, W.-N., Wood, K., Liu, Q., Shi, F.-D. & Hao, J. Acetylcholine-producing NK cells attenuate CNS inflammation via modulation of infiltrating monocytes/macrophages. *Proc. Natl. Acad. Sci.* **114,** E6202–E6211 (2017).

65. St-Pierre, S., Jiang, W., Roy, P., Champigny, C., LeBlanc, É., Morley, B. J., Hao, J. & Simard, A. R. Nicotinic Acetylcholine Receptors Modulate Bone Marrow-Derived Pro-Inflammatory Monocyte Production and Survival. *PLOS ONE* **11,** e0150230 (2016).
66. Hao, J., Simard, A. R., Turner, G. H., Wu, J., Whiteaker, P., Lukas, R. J. & Shi, F.-D. Attenuation of CNS inflammatory responses by nicotine involves α7 and non-α7 nicotinic receptors. *Exp. Neurol.* **227,** 110–119 (2011).
67. Li, Q., Zhou, X.-D., Kolosov, V. P. & Perelman, J. M. Nicotine reduces TNF-α expression through a α7 nAChR/MyD88/NF-κB pathway in HBE16 airway epithelial cells. *Cell. Physiol. Biochem. Int. J. Exp. Cell. Physiol. Biochem. Pharmacol.* **27,** 605–612 (2011).
68. Parrish, W. R., Rosas-Ballina, M., Gallowitsch-Puerta, M., Ochani, M., Ochani, K., Yang, L.-H., Hudson, L., Lin, X., Patel, N., Johnson, S. M., Chavan, S., Goldstein, R. S., Czura, C. J., Miller, E. J., Al-Abed, Y., Tracey, K. J. & Pavlov, V. A. Modulation of TNF release by choline requires alpha7 subunit nicotinic acetylcholine receptor-mediated signaling. *Mol. Med. Camb. Mass* **14,** 567–574 (2008).
69. Gao, F., Chiu, S. M., Motan, D. a. L., Zhang, Z., Chen, L., Ji, H.-L., Tse, H.-F., Fu, Q.-L. & Lian, Q. Mesenchymal stem cells and immunomodulation: current status and future prospects. *Cell Death Dis.* **7,** e2062–e2062 (2016).
70. Puissant, B., Barreau, C., Bourin, P., Clavel, C., Corre, J., Bousquet, C., Taureau, C., Cousin, B., Abbal, M., Laharrague, P., Penicaud, L., Casteilla, L. & Blancher, A. Immunomodulatory effect of human adipose tissue-derived adult stem cells: comparison with bone marrow mesenchymal stem cells. *Br. J. Haematol.* **129,** 118–129 (2005).

71. Yañez, R., Lamana, M. L., García-Castro, J., Colmenero, I., Ramírez, M. & Bueren, J. A. Adipose tissue-derived mesenchymal stem cells have in vivo immunosuppressive properties applicable for the control of the graft-versus-host disease. *Stem Cells Dayt. Ohio* **24,** 2582–2591 (2006).

72. Glennie, S., Soeiro, I., Dyson, P. J., Lam, E. W.-F. & Dazzi, F. Bone marrow mesenchymal stem cells induce division arrest anergy of activated T cells. *Blood* **105,** 2821–2827 (2005).

73. Selmani, Z., Naji, A., Zidi, I., Favier, B., Gaiffe, E., Obert, L., Borg, C., Saas, P., Tiberghien, P., Rouas-Freiss, N., Carosella, E. D. & Deschaseaux, F. Human Leukocyte Antigen-G5 Secretion by Human Mesenchymal Stem Cells Is Required to Suppress T Lymphocyte and Natural Killer Function and to Induce CD4+CD25highFOXP3+ Regulatory T Cells. *STEM CELLS* **26,** 212–222 (2008).

74. Corcione, A., Benvenuto, F., Ferretti, E., Giunti, D., Cappiello, V., Cazzanti, F., Risso, M., Gualandi, F., Mancardi, G. L., Pistoia, V. & Uccelli, A. Human mesenchymal stem cells modulate B-cell functions. *Blood* **107,** 367–372 (2006).

75. Ramasamy, R., Fazekasova, H., Lam, E. W.-F., Soeiro, I., Lombardi, G. & Dazzi, F. Mesenchymal stem cells inhibit dendritic cell differentiation and function by preventing entry into the cell cycle. *Transplantation* **83,** 71–76 (2007).

76. Burchell, J. T., Strickland, D. H. & Stumbles, P. A. The role of dendritic cells and regulatory T cells in the regulation of allergic asthma. *Pharmacol. Ther.* **125,** 1–10 (2010).

77. Spaggiari, G. M., Capobianco, A., Becchetti, S., Mingari, M. C. & Moretta, L. Mesenchymal stem cell-natural killer cell interactions: evidence that activated NK cells

are capable of killing MSCs, whereas MSCs can inhibit IL-2-induced NK-cell proliferation. *Blood* **107,** 1484–1490 (2006).

78. Yi, T.-G., Cho, Y.-K., Lee, H.-J., Kim, J., Jeon, M.-S., Ham, D.-S., Kim, W. C. & Song, S. U. A Novel Immunomodulatory Mechanism Dependent on Acetylcholine Secreted by Human Bone Marrow-derived Mesenchymal Stem Cells. *Int. J. Stem Cells* **12,** 315–330 (2019).
79. Inazu, M. Choline transporter-like proteins CTLs/SLC44 family as a novel molecular target for cancer therapy. *Biopharm. Drug Dispos.* (2014). doi:10.1002/bdd.1892
80. Traiffort, E., O'Regan, S. & Ruat, M. The choline transporter-like family SLC44: properties and roles in human diseases. *Mol. Aspects Med.* **34,** 646–654 (2013).
81. Di Bari, M., Reale, M., Di Nicola, M., Orlando, V., Galizia, S., Porfilio, I., Costantini, E., D'Angelo, C., Ruggieri, S., Biagioni, S., Gasperini, C. & Tata, A. M. Dysregulated Homeostasis of Acetylcholine Levels in Immune Cells of RR-Multiple Sclerosis Patients. *Int. J. Mol. Sci.* **17,** (2016).
82. Fujii, T., Takada-Takatori, Y., Horiguchi, K. & Kawashima, K. Mediatophore regulates acetylcholine release from T cells. *J. Neuroimmunol.* **244,** 16–22 (2012).
83. Fujii, T., Takada-Takatori, Y. & Kawashima, K. Regulatory mechanisms of acetylcholine synthesis and release by T cells. *Life Sci.* **91,** 981–985 (2012).
84. Pochini, L., Scalise, M., Galluccio, M. & Indiveri, C. Regulation by physiological cations of acetylcholine transport mediated by human OCTN1 (SLC22A4). Implications in the non-neuronal cholinergic system. *Life Sci.* **91,** 1013–1016 (2012).
85. Cox, M. A., Duncan, G. S., Lin, G. H. Y., Steinberg, B. E., Yu, L. X., Brenner, D., Buckler, L. N., Elia, A. J., Wakeham, A. C., Nieman, B., Dominguez-Brauer, C., Elford,

A. R., Gill, K. T., Kubli, S. P., Haight, J., Berger, T., Ohashi, P. S., Tracey, K. J., Olofsson, P. S. & Mak, T. W. Choline acetyltransferase-expressing T cells are required to control chronic viral infection. *Science* **363,** 639–644 (2019).

86. Rasheed, M. A. U., Latner, D. R., Aubert, R. D., Gourley, T., Spolski, R., Davis, C. W., Langley, W. A., Ha, S.-J., Ye, L., Sarkar, S., Kalia, V., Konieczny, B. T., Leonard, W. J. & Ahmed, R. Interleukin-21 Is a Critical Cytokine for the Generation of Virus-Specific Long-Lived Plasma Cells. *J. Virol.* **87,** 7737–7746 (2013).
87. Di Pinto, G., Di Bari, M., Martin-Alvarez, R., Sperduti, S., Serrano-Acedo, S., Gatta, V., Tata, A. M. & Mengod, G. Comparative study of the expression of cholinergic system components in the CNS of experimental autoimmune encephalomyelitis mice: Acute vs remitting phase. *Eur. J. Neurosci.* **48,** 2165–2181 (2018).
88. Zhang, C., Xia, Y., Jiang, W., Wang, C., Han, B. & Hao, J. Determination of non-neuronal acetylcholine in human peripheral blood mononuclear cells by use of hydrophilic interaction ultra-performance liquid chromatography-tandem mass spectrometry. *J. Chromatogr. B Analyt. Technol. Biomed. Life. Sci.* **1022,** 265–273 (2016).
89. Wang, Y., Wang, T., Shi, X., Wan, D., Zhang, P., He, X., Gao, P., Yang, S., Gu, J. & Xu, G. Analysis of acetylcholine, choline and butyrobetaine in human liver tissues by hydrophilic interaction liquid chromatography-tandem mass spectrometry. *J. Pharm. Biomed. Anal.* **47,** 870–875 (2008).
90. Alkondon, M., Pereira, E. F., Cortes, W. S., Maelicke, A. & Albuquerque, E. X. Choline is a selective agonist of alpha7 nicotinic acetylcholine receptors in the rat brain neurons. *Eur. J. Neurosci.* **9,** 2734–2742 (1997).

91. Richter, K., Mathes, V., Fronius, M., Althaus, M., Hecker, A., Krasteva-Christ, G., Padberg, W., Hone, A. J., McIntosh, J. M., Zakrzewicz, A. & Grau, V. Phosphocholine – an agonist of metabotropic but not of ionotropic functions of α9-containing nicotinic acetylcholine receptors. *Sci. Rep.* **6,** 28660 (2016).
92. Marks, M. J., Whiteaker, P., Calcaterra, J., Stitzel, J. A., Bullock, A. E., Grady, S. R., Picciotto, M. R., Changeux, J. P. & Collins, A. C. Two pharmacologically distinct components of nicotinic receptor-mediated rubidium efflux in mouse brain require the beta2 subunit. *J. Pharmacol. Exp. Ther.* **289,** 1090–1103 (1999).
93. Hsu, K. S. Modulation of the nicotinic acetylcholine receptor channels by spermine in Xenopus muscle cell culture. *Neurosci. Lett.* **182,** 99–103 (1994).
94. Huo, S., Zhong, X., Wu, X. & Li, Y. Effects of Norepinephrine and Acetylcholine on the Development of Cultured Leydig Cells in Mice. *J. Biomed. Biotechnol.* **2012,** e503093 (2012).
95. Stokes, C. & Papke, R. L. Use of an α3-β4 nicotinic acetylcholine receptor subunit concatamer to characterize ganglionic receptor subtypes with specific subunit composition reveals species-specific pharmacologic properties. *Neuropharmacology* **63,** 538–546 (2012).
96. Nassar-Gentina, V., Catalán, L. & Luxoro, M. Nicotonic and muscarinic components in acetylcholine stimulation of porcine adrenal medullary cells. *Mol. Cell. Biochem.* **169,** 107–113 (1997).
97. Woodruff-Pak, D. S., Lander, C. & Geerts, H. Nicotinic Cholinergic Modulation: Galantamine as a Prototype. *CNS Drug Rev.* **8,** 405–426 (2002).

98. Choline Acetyltransferase and the Synthesis of Acetylcholine | SpringerLink. at <https://link.springer.com/chapter/10.1007/978-3-642-73220-1_7>

99. Sastry, B., Jaiswal, N., Owens, L., Janson, V. & Moore, R. 2-(alpha-Naphthoyl)ethyltrimethylammonium iodide and its beta-isomer: new selective, stable and fluorescent inhibitors of choline acetyltransferase. *J. Pharmacol. Exp. Ther.* (1988).

100. Ennis, E. A., Wright, J., Retzlaff, C. L., McManus, O. B., Lin, Z., Huang, X., Wu, M., Li, M., Daniels, J. S., Lindsley, C. W., Hopkins, C. R. & Blakely, R. D. Identification and Characterization of ML352: A Novel, Noncompetitive Inhibitor of the Presynaptic Choline Transporter. *ACS Chem. Neurosci.* **6,** 417–427 (2015).

101. Chakhachiro, Z. I., Zuo, Z., Aladily, T. N., Kantarjian, H. M., Cortes, J. E., Alayed, K., Nguyen, M. H., Medeiros, L. J. & Bueso-Ramos, C. CD105 (Endoglin) Is Highly Overexpressed in a Subset of Cases of Acute Myeloid Leukemias. *Am. J. Clin. Pathol.* **140,** 370–378 (2013).

102. Czapla, J., Matuszczak, S., Wiśniewska, E., Jarosz-Biej, M., Smolarczyk, R., Cichoń, T., Głowala-Kosińska, M., Śliwka, J., Garbacz, M., Szczypior, M., Jaźwiec, T., Langrzyk, A., Zembala, M. & Szala, S. Human Cardiac Mesenchymal Stromal Cells with CD105+CD34- Phenotype Enhance the Function of Post-Infarction Heart in Mice. *PLoS ONE* **11,** (2016).

103. Godin, J.-R., Roy, P., Quadri, M., Bagdas, D., Toma, W., Narendrula-Kotha, R., Kishta, O. A., Damaj, M. I., Horenstein, N. A., Papke, R. L. & Simard, A. R. A silent agonist of α7 nicotinic acetylcholine receptors modulates inflammation ex vivo and attenuates EAE. *Brain. Behav. Immun.* **87,** 286–300 (2020).

104. Schmiedel, B. J., Singh, D., Madrigal, A., Valdovino-Gonzalez, A. G., White, B. M., Zapardiel-Gonzalo, J., Ha, B., Altay, G., Greenbaum, J. A., McVicker, G., Seumois, G., Rao, A., Kronenberg, M., Peters, B. & Vijayanand, P. Impact of Genetic Polymorphisms on Human Immune Cell Gene Expression. *Cell* **175,** 1701-1715.e16 (2018).

105. Taylor, S. C., Laperriere, G. & Germain, H. Droplet Digital PCR versus qPCR for gene expression analysis with low abundant targets: from variable nonsense to publication quality data. *Sci. Rep.* **7,** 2409 (2017).

106. Vijayaraghavan, S., Karami, A., Aeinehband, S., Behbahani, H., Grandien, A., Nilsson, B., Ekdahl, K. N., Lindblom, R. P. F., Piehl, F. & Darreh-Shori, T. Regulated Extracellular Choline Acetyltransferase Activity— The Plausible Missing Link of the Distant Action of Acetylcholine in the Cholinergic Anti-Inflammatory Pathway. *PLoS ONE* **8,** (2013).

107. Oda, Y. Choline acetyltransferase: the structure, distribution and pathologic changes in the central nervous system. *Pathol. Int.* **49,** 921–937 (1999).

108. Tooyama, I. & Kimura, H. A protein encoded by an alternative splice variant of choline acetyltransferase mRNA is localized preferentially in peripheral nerve cells and fibers. *J. Chem. Neuroanat.* **17,** 217–226 (2000).

109. Grosman, D. D., Lorenzi, M. V., Trinidad, A. C. & Strauss, W. L. The human choline acetyltransferase gene encodes two proteins. *J. Neurochem.* **65,** 484–491 (1995).

110. Meshorer, E. & Soreq, H. Virtues and woes of AChE alternative splicing in stress-related neuropathologies. *Trends Neurosci.* **29,** 216–224 (2006).

111. Gilboa-Geffen, A., Lacoste, P. P., Soreq, L., Cizeron-Clairac, G., Le Panse, R., Truffault, F., Shaked, I., Soreq, H. & Berrih-Aknin, S. The thymic theme of acetylcholinesterase splice variants in myasthenia gravis. *Blood* **109,** 4383–4391 (2007).

112. Blohberger, J., Kunz, L., Einwang, D., Berg, U., Berg, D., Ojeda, S. R., Dissen, G. A., Fröhlich, T., Arnold, G. J., Soreq, H., Lara, H. & Mayerhofer, A. Readthrough acetylcholinesterase (AChE-R) and regulated necrosis: pharmacological targets for the regulation of ovarian functions? *Cell Death Dis.* **6,** e1685–e1685 (2015).

113. García-Ayllón, M.-S., Riba-Llena, I., Serra-Basante, C., Alom, J., Boopathy, R. & Sáez-Valero, J. Altered Levels of Acetylcholinesterase in Alzheimer Plasma. *PLoS ONE* **5,** e8701 (2010).

114. Hour, F. Q., Moghadam, A. J., Shakeri-Zadeh, A., Bakhtiyari, M., Shabani, R. & Mehdizadeh, M. Magnetic targeted delivery of the SPIONs-labeled mesenchymal stem cells derived from human Wharton's jelly in Alzheimer's rat models. *J. Controlled Release* **321,** 430–441 (2020).

115. Hoogduijn, M. J., Rakonczay, Z. & Genever, P. G. The effects of anticholinergic insecticides on human mesenchymal stem cells. *Toxicol. Sci. Off. J. Soc. Toxicol.* **94,** 342–350 (2006).

116. Ennis, E. A. & Blakely, R. D. in *Adv. Pharmacol.* (ed. Schwarcz, R.) **76,** 175–213 (Academic Press, 2016).

117. Hartnett, S., Zhang, F., Abitz, A. & Li, Y. Ubiquitin C-terminal hydrolase L1 interacts with choline transporter in cholinergic cells. *Neurosci. Lett.* **564,** 115–119 (2014).

118. Banerjee, M., Arutyunov, D., Brandwein, D., Janetzki-Flatt, C., Kolski, H., Hume, S., Leonard, N. J., Watt, J., Lacson, A., Baradi, M., Leslie, E. M., Cordat, E. & Caluseriu, O. The novel p.Ser263Phe mutation in the human high-affinity choline transporter 1 (CHT1/ *SLC5A7*) causes a lethal form of fetal akinesia syndrome. *Hum. Mutat.* **40,** 1676–1683 (2019).

119. Gosens, R. & Gross, N. The mode of action of anticholinergics in asthma. *Eur. Respir. J.* **52,** 1701247 (2018).

120. Gosens, R., Zaagsma, J., Meurs, H. & Halayko, A. J. Muscarinic receptor signaling in the pathophysiology of asthma and COPD. *Respir. Res.* **7,** 73 (2006).

121. Wessler, I., Reinheimer, T., Kilbinger, H., Bittinger, F., Kirkpatrick, C. J., Saloga, J. & Knop, J. Increased acetylcholine levels in skin biopsies of patients with atopic dermatitis. *Life Sci.* **72,** 2169–2172 (2003).

122. Molfino, N. A. Increased vagal airway tone in fatal asthma. *Med. Hypotheses* **74,** 521–523 (2010).

123. Mihovilovic, M. & Butterworth-Robinette, J. Thymic epithelial cell line expresses transcripts encoding alpha-3, alpha-5 and beta-4 subunits of acetylcholine receptors, responds to cholinergic agents and expresses choline acetyl transferase. An in vitro system to investigate thymic cholinergic mechanisms. *J. Neuroimmunol.* **117,** 58–67 (2001).

124. Gibson, G. E. & Peterson, C. Aging decreases oxidative metabolism and the release and synthesis of acetylcholine. *J. Neurochem.* **37,** 978–984 (1981).

125. Sloniecka, M., Backman, L. J. & Danielson, P. Antiapoptotic Effect of Acetylcholine in Fas-Induced Apoptosis in Human Keratocytes. *Invest. Ophthalmol. Vis. Sci.* **57,** 5892–5902 (2016).

126. Rana, O. R., Schauerte, P., Kluttig, R., Schröder, J. W., Koenen, R. R., Weber, C., Nolte, K. W., Weis, J., Hoffmann, R., Marx, N. & Saygili, E. Acetylcholine as an age-dependent non-neuronal source in the heart. *Auton. Neurosci. Basic Clin.* **156,** 82–89 (2010).

127. Zhao, M., Yang, Y., Bi, X., Yu, X., Jia, H., Fang, H. & Zang, W. Acetylcholine Attenuated TNF-α-Induced Apoptosis in H9c2 Cells: Role of Calpain and the p38-MAPK Pathway. *Cell. Physiol. Biochem.* **36,** 1877–1889 (2015).

128. Karbian, N., Abutbul, A., el-Amore, R., Eliaz, R., Beeri, R., Reicher, B. & Mevorach, D. Apoptotic cell therapy for cytokine storm associated with acute severe sepsis. *Cell Death Dis.* **11,** 1–14 (2020).

129. CHAUDHRY, H., ZHOU, J., ZHONG, Y., ALI, M. M., MCGUIRE, F., NAGARKATTI, P. S. & NAGARKATTI, M. Role of Cytokines as a Double-edged Sword in Sepsis. *Vivo Athens Greece* **27,** 669–684 (2013).

130. Rau, M., Schiller, M., Krienke, S., Heyder, P., Lorenz, H. & Blank, N. Clinical manifestations but not cytokine profiles differentiate adult-onset Still's disease and sepsis. *J. Rheumatol.* **37,** 2369–2376 (2010).

131. Surbatovic, M., Filipovic, N., Radakovic, S., Stankovic, N. & Slavkovic, Z. Immune cytokine response in combat casualties: blast or explosive trauma with or without secondary sepsis. *Mil. Med.* **172,** 190–195 (2007).

132. Kumar, P., Nagarajan, A. & Uchil, P. D. Analysis of Cell Viability by the Lactate Dehydrogenase Assay. *Cold Spring Harb. Protoc.* **2018,** (2018).

133. Tyagi, E., Agrawal, R., Nath, C. & Shukla, R. Inhibitory role of cholinergic system mediated via α7 nicotinic acetylcholine receptor in LPS-induced neuro-inflammation. *Innate Immun.* **16,** 3–13 (2010).

134. Czura, C. J., Friedman, S. G. & Tracey, K. J. Neural inhibition of inflammation: the cholinergic anti-inflammatory pathway. *J. Endotoxin Res.* **9,** 409–413 (2003).

135. Rowley, T. J., McKinstry, A., Greenidge, E., Smith, W. & Flood, P. Antinociceptive and anti-inflammatory effects of choline in a mouse model of postoperative pain. *Br. J. Anaesth.* **105,** 201–207 (2010).

136. Parrish, W. R., Gallowitsch Puerta, M., Ochani, M., Ochani, K., Moskovic, D., Lin, X., Czura, C. J., Miller, E. J., Al-Abed, Y., Tracey, K. J. & Pavlov, V. A. CHOLINE SUPPRESSES INFLAMMATORY RESPONSES. *Shock* **25,** 45 (2006).

137. Liu, L., Lu, Y., Bi, X., Xu, M., Yu, X., Xue, R., He, X. & Zang, W. Choline ameliorates cardiovascular damage by improving vagal activity and inhibiting the inflammatory response in spontaneously hypertensive rats. *Sci. Rep.* **7,** 42553 (2017).

138. Wang, H., Yu, M., Ochani, M., Amella, C. A., Tanovic, M., Susarla, S., Li, J. H., Wang, H., Yang, H., Ulloa, L., Al-Abed, Y., Czura, C. J. & Tracey, K. J. Nicotinic acetylcholine receptor alpha7 subunit is an essential regulator of inflammation. *Nature* **421,** 384–388 (2003).

139. Kistemaker, L. E. M., van Os, R. P., Dethmers-Ausema, A., Bos, I. S. T., Hylkema, M. N., van den Berge, M., Hiemstra, P. S., Wess, J., Meurs, H., Kerstjens, H. A. M. & Gosens, R. Muscarinic M3 receptors on structural cells regulate cigarette smoke-induced

neutrophilic airway inflammation in mice. *Am. J. Physiol. Lung Cell. Mol. Physiol.* **308,** L96-103 (2015).

140. Yamada, M. & Ichinose, M. The Cholinergic Pathways in Inflammation: A Potential Pharmacotherapeutic Target for COPD. *Front. Pharmacol.* **9,** (2018).

141. Bucher, H., Duechs, M. J., Tilp, C., Jung, B. & Erb, K. J. Tiotropium Attenuates Virus-Induced Pulmonary Inflammation in Cigarette Smoke–Exposed Mice. *J. Pharmacol. Exp. Ther.* **357,** 606–618 (2016).

142. Lakhan, S. E. & Kirchgessner, A. Anti-inflammatory effects of nicotine in obesity and ulcerative colitis. *J. Transl. Med.* **9,** 129 (2011).

143. Anti-inflammatory Effects of Nicotine in Parkinson's Disease | Parkinson's Disease. at <https://www.michaeljfox.org/grant/anti-inflammatory-effects-nicotine-parkinsons-disease>

144. Gao, Z., Nissen, J. C., Ji, K. & Tsirka, S. E. The experimental autoimmune encephalomyelitis disease course is modulated by nicotine and other cigarette smoke components. *PloS One* **9,** e107979 (2014).

145. Dratcu, L. & Boland, X. Does Nicotine Prevent Cytokine Storms in COVID-19? *Cureus* **12,**

146. McIntosh, J. M., Absalom, N., Chebib, M., Elgoyhen, A. B. & Vincler, M. Alpha9 nicotinic acetylcholine receptors and the treatment of pain. *Biochem. Pharmacol.* **78,** 693–702 (2009).

147. Elgoyhen, A. B., Johnson, D. S., Boulter, J., Vetter, D. E. & Heinemann, S. Alpha 9: an acetylcholine receptor with novel pharmacological properties expressed in rat cochlear hair cells. *Cell* **79,** 705–715 (1994).

148. Elgoyhen, A. B., Vetter, D. E., Katz, E., Rothlin, C. V., Heinemann, S. F. & Boulter, J. alpha10: a determinant of nicotinic cholinergic receptor function in mammalian vestibular and cochlear mechanosensory hair cells. *Proc. Natl. Acad. Sci. U. S. A.* **98,** 3501–3506 (2001).

149. Hopkins, T. J., Rupprecht, L. E., Hayes, M. R., Blendy, J. A. & Schmidt, H. D. Galantamine, an Acetylcholinesterase Inhibitor and Positive Allosteric Modulator of Nicotinic Acetylcholine Receptors, Attenuates Nicotine Taking and Seeking in Rats. *Neuropsychopharmacology* **37,** 2310–2321 (2012).

150. B, H., Ch, R., M, L., Gi, E. & Efr, P. Evidence for positive allosteric modulation of cognitive-enhancing effects of nicotine by low-dose galantamine in rats. *Pharmacol. Biochem. Behav.* **199,** 173043–173043 (2020).

151. Kowal, N. M., Ahring, P. K., Liao, V. W. Y., Indurti, D. C., Harvey, B. S., O'Connor, S. M., Chebib, M., Olafsdottir, E. S. & Balle, T. Galantamine is not a positive allosteric modulator of human α4β2 or α7 nicotinic acetylcholine receptors. *Br. J. Pharmacol.* **175,** 2911–2925 (2018).

152. Zelová, H. & Hošek, J. TNF-α signalling and inflammation: interactions between old acquaintances. *Inflamm. Res.* **62,** 641–651 (2013).

153. Agac, D., Estrada, L. & Farrar, D. Beta-2 adrenergic receptor signaling prevents hyperinflammation through early release of IL-10. *J. Immunol.* **198,** 221.4-221.4 (2017).

154. Grailer, J. J., Haggadone, M. D., Sarma, J. V., Zetoune, F. S. & Ward, P. A. Induction of M2 regulatory macrophages through the β2-adrenergic receptor with protection during endotoxemia and acute lung injury. *J. Innate Immun.* **6,** 607–618 (2014).

155. Wu, L., Tai, Y., Hu, S., Zhang, M., Wang, R., Zhou, W., Tao, J., Han, Y., Wang, Q. & Wei, W. Bidirectional Role of β2-Adrenergic Receptor in Autoimmune Diseases. *Front. Pharmacol.* **9,** (2018).

156. Casella, G., Garzetti, L., Gatta, A. T., Finardi, A., Maiorino, C., Ruffini, F., Martino, G., Muzio, L. & Furlan, R. IL4 induces IL6-producing M2 macrophages associated to inhibition of neuroinflammation in vitro and in vivo. *J. Neuroinflammation* **13,** 139 (2016).

157. Fernando, M. R., Reyes, J. L., Iannuzzi, J., Leung, G. & McKay, D. M. The Pro-Inflammatory Cytokine, Interleukin-6, Enhances the Polarization of Alternatively Activated Macrophages. *PLOS ONE* **9,** e94188 (2014).

158. Braune, J., Weyer, U., Hobusch, C., Mauer, J., Brüning, J. C., Bechmann, I. & Gericke, M. IL-6 Regulates M2 Polarization and Local Proliferation of Adipose Tissue Macrophages in Obesity. *J. Immunol.* **198,** 2927–2934 (2017).